

**ADAPTIVE CONTROLLER DESIGN FOR NONLINEAR UNCERTAIN
SYSTEMS USING MULTIPLE MODEL BASED TWO LEVEL ADAPTATION
TECHNIQUE**

VINAY KUMAR PANDEY

ADAPTIVE CONTROLLER DESIGN FOR NONLINEAR UNCERTAIN SYSTEMS USING MULTIPLE MODEL BASED TWO LEVEL ADAPTATION TECHNIQUE

A

Thesis Submitted

for the award of the degree of

DOCTOR OF PHILOSOPHY

By

VINAY KUMAR PANDEY



Department of Electronics and Electrical Engineering

Indian Institute of Technology Guwahati

Guwahati - 781039, ASSAM, INDIA.

July, 2018

Certificate

This is to certify that the thesis entitled “**ADAPTIVE CONTROLLER DESIGN FOR NONLINEAR UNCERTAIN SYSTEMS USING MULTIPLE MODEL BASED TWO LEVEL ADAPTATION TECHNIQUE**”, submitted by **Vinay Kumar Pandey** (10610230), a research scholar in the *Department of Electronics and Electrical Engineering, Indian Institute of Technology Guwahati*, for the award of the degree of **Doctor of Philosophy**, is a record of an original research work carried out by him under our supervision and guidance. The thesis has fulfilled all requirements as per the regulations of the Institute and in our opinion has reached the standard needed for submission. The results embodied in this thesis have not been submitted to any other University or Institute for the award of any degree or diploma.

Dated:
Guwahati.

Dr. Indrani Kar
Associate Professor
Dept. of Electronics and Electrical Engg.
Indian Institute of Technology Guwahati
Guwahati - 781039, India.

Dated:
Guwahati.

Prof. Chitralkha Mahanta
Professor
Dept. of Electronics and Electrical Engg.
Indian Institute of Technology Guwahati
Guwahati - 781039, India.

*This thesis is dedicated to my beloved family, specially my
father Mr Bimal Kumar Pandey...*

Acknowledgement

I feel it as a great privilege in expressing my deepest and most sincere gratitude to my supervisors Dr. Indrani Kar and Prof. Chitralkha Mahanta, for their excellent guidance. Their kindness, dedication, friendly accessibility and attention to details have been a great inspiration to me. My heartfelt thanks to my supervisors for the unlimited support and patience shown to me. I would particularly like to thank for all their help in patiently and carefully correcting all my manuscripts.

I am also very thankful to my doctoral committee members Prof. S. Majhi, Dr. P. Tripathy, and Dr. P. Kumar for sparing their precious time to evaluate the progress of my work. Their suggestions have been valuable. I am grateful to all the members of the research and technical staff of the department, specially Mr. S. Sonowal and Mr. Syed S. Mazid, without whose help I could not have completed this thesis.

Thanks go out to all my friends in the Control and Instrumentation Laboratory. They have always been around to provide useful suggestions, companionship and created a peaceful research environment. My friends at IITG made my life joyful and were a constant source of encouragement. Among my friends, I would like to extend my special thanks to Arghya Chakravarty, Atul Kumar, Brijesh Kumbhani, Parveen Malik, Basudeba Behera, Sushant Kundu, Mayank Agarwal and Janak Sethi. My work definitely would not have been possible without their love and care which helped me to enjoy my new life in IITG. Special thanks also go to Shivanshu, Somen, Anandkamal, Kuntal, Ramkumar, Abhijeet, Bajrangbali, Mandar, Madhulika, Mriganka, Ravinder, Sudhir, Sujan, Shivam and Shyam for their help during my stay. My special thanks go to my beloved wife, *Vibha*, for her wholehearted and unfailing support during my final days of thesis writing. My deepest gratitude goes to my family for the continuous love and support showered on me throughout. The opportunities that they have given me and their unlimited sacrifices are the reasons for my being where I am and what I have accomplished so far.

Abstract

Adaptive control technique is a popular and successful control strategy for controlling nonlinear uncertain systems. However, using adaptive control schemes in parametrically uncertain environments often lead to poor transient response and sluggish steady state response. Use of multiple estimation models has been found to be promising in addressing these issues. This thesis proposes an adaptive control method for nonlinear uncertain systems using multiple models based two level adaptation (MMTLA). At the first level, multiple models are used and a single model at the second level is proposed by combining these first level models for controlling different classes of nonlinear uncertain systems. The proposed control method is applied to nonlinear single-input single-output (SISO) systems with linear and nonlinear parameterizations, nonlinear multiple-input multiple-output (MIMO) coupled systems and nonlinear MIMO model following control systems. For all the considered systems, state transformation and feedback linearization method have been used to algebraically transform nonlinear system dynamics to linear ones. The unknown system parameters are assumed to be bounded within a set of compact parameter space. Multiple estimation models are distributed evenly in this region of uncertainty and their unknown parameters are tuned. The tuning laws for estimator parameters have been obtained using Lyapunov stability criterion. Stability analysis using Lyapunov's criterion has been carried out to assess the close loop stability and tracking error convergence of the overall system. The transient and steady state performances using the proposed scheme are evaluated by conducting simulation studies, which confirm superior performance of the proposed control technique over some existing adaptive control methods. The common problems with adaptive control like oscillatory transient response, poor parameter convergence and sluggish response are found to be improved considerably by using the proposed multiple model based two level adaptive controller. In addition to simulation studies, the proposed controller is tested experimentally on real time by applying it to a laboratory set-up of twin rotor MIMO system (TRMS). Experimental studies are performed

on the TRMS model for regulation and tracking using pitch and yaw control. An extended Kalman filter (EKF) has been used to observe the unavailable states of the TRMS. Furthermore, an adaptive model following control of a nonlinear MIMO coupled system with unknown parameters is considered. In this case, the system cannot be decoupled by static state feedback because of the singularity of the decoupling matrix. A dynamic state feedback controller with nonlinear structure algorithm is designed for the system. Simulation and experimental studies show efficacy of the proposed control scheme.

Contents

List of Figures	xi
List of Tables	xiii
List of Acronyms	xiv
List of Symbols	xvi
List of Publications	xviii
1 Introduction	1
1.1 Introduction	2
1.2 Literature Review	3
1.3 Research Motivation	4
1.4 Contributions of the Thesis	5
1.5 Organization of the Thesis	7
2 Preliminary Concepts	8
2.1 Introduction	9
2.2 Change in Operating Environment	9
2.2.1 Assumptions used regarding the environment	9
2.2.2 Switching and tuning among different environments	9
2.3 The Adaptive Control Problem	11
2.4 Multiple Model Adaptive Control (MMAC) with Switching	11
2.4.1 Basic structure of MMAC	11
2.4.2 MMAC for linear systems	12
2.4.3 Single identification model	13
2.4.4 Multiple identification models	16
2.4.5 Various combinations of fixed and adaptive models	17

2.5	Summary	17
3	Adaptive Controller Design for Linearly Parameterized SISO Nonlinear Systems Using Multiple Model Based Two Level Adaptation Technique	18
3.1	Introduction	19
3.2	Adaptive Control of Nonlinear Systems with Linear Parameterization	20
3.2.1	Controller Input	21
3.2.2	Estimation model design at the first level	22
3.2.3	Closed loop error dynamics at the first level	23
3.2.4	Closed loop stability at the first level	25
3.3	Multiple Model based Two Level Adaptation (MMTLA) method	27
3.3.1	First level adaptation	28
3.3.2	Visualization of the parameter space	28
3.3.3	Second level adaptation	29
3.3.4	Overall stability assessment	33
3.4	General Work Flow Chart	36
3.5	Simulation Results	36
3.6	Summary	45
4	Adaptive Controller Design for Nonlinearly Parameterized SISO Nonlinear Systems Using Multiple Model Based Two Level Adaptation Technique	47
4.1	Introduction	48
4.2	Nonlinearly Parameterized Nonlinear System Description	49
4.3	Adaptive Feedback Controller and Estimation Model Design	50
4.3.1	System stability and adaptive law design	51
4.4	Multiple Model Based Two Level Adaptation Technique	54
4.4.1	Complete system stability after two level adaptation	55
4.5	Simulation Results	57
4.6	Summary	66
5	Adaptive Controller Design for Nonlinear Coupled MIMO Systems Using Multiple Model Based Two Level Adaptation Technique	67
5.1	Introduction	68
5.2	System Description	69

5.3	Design of Estimation Model	70
5.4	Controller Design Using Feedback Linearization	70
5.5	Introduction of Multiple Models	75
5.6	Two Level Adaptation for Nonlinear MIMO Systems	75
5.6.1	System stability and tracking error convergence using two level adaptation	77
5.7	Simulation and Experimental Results	81
5.7.1	Case 1: Step input tracking	85
5.7.2	Case 2: Sinusoidal input tracking	90
5.7.3	Case 3: Square input tracking	94
5.8	Summary	98
6	Adaptive Controller Design for Nonlinear MIMO Model Following Control Systems Using Multiple Model Based Two Level Adaptation Technique	99
6.1	Introduction	100
6.2	System Model	101
6.3	Estimation Model Architecture	101
6.4	Model Following Controller Architecture	102
6.5	Controller Design Using MMTLA Method	104
6.6	Simulation Results	105
6.7	Summary	110
7	Conclusions and Scope for Future Work	112
7.1	Conclusions	113
7.2	Scope for Future Work	114
A	Appendix	116
A.1	Definitions	117
A.2	Cezayirli et al.'s method	117
A.3	Ge et al.'s method	118
A.4	Extended Kalman Filter (EKF)	118
A.5	Performance Specifications	119
A.6	Momentum equation for TRMS	120
	References	122

List of Figures

2.1	Multiple models in a system environment	10
2.2	Basic Structure of MMAC	12
3.1	Two level adaptation (TLA)	29
3.2	Control block diagram with second level adaptation (SLA)	33
3.3	General work flow chart	37
3.4	Case 1: Trajectory tracking	38
3.5	Case 1: Parameter convergence and control input	39
3.6	Case 1: Parameter and adaptive weight convergence	39
3.7	Model of 1-link robot arm driven by a brushed DC-motor	41
3.8	Case 2: Trajectory tracking by angular position of robot arm	43
3.9	Case 2: Parameter Convergence	43
3.10	Case 2: Control input	44
3.11	Case 2: First and second level Parameter convergence	44
3.12	Case 2: Adaptive weight convergence	45
4.1	Case 1: Trajectory tracking	59
4.2	Case 1: Parameter Convergence	60
4.3	Case 1: Control Input	60
4.4	Case 1: Adaptive weights	61
4.5	Cart-pendulum system	61
4.6	Case 2: Trajectory tracking	64
4.7	Case 2: Parameter Convergence	65
4.8	Case 2: Control Input	65
4.9	Case 2: Adaptive weights	66

5.1	Noninteracting control	74
5.2	TRMS laboratory model	82
5.3	A schematic description of TRMS	82
5.4	Cross coupled TRMS system	83
5.5	Trajectory tracking for Step input	86
5.6	Tracking error for step input	87
5.7	Observed vs actual pitch angle for step input	87
5.8	Observed vs actual yaw angle for step input	88
5.9	Control input for step trajectory tracking	89
5.10	Trajectory tracking for sinusoidal input	91
5.11	Trajectory tracking error for sinusoidal input	92
5.12	Control input for sinusoidal trajectory tracking	93
5.13	Trajectory tracking for square input	95
5.14	Trajectory tracking error for square input	96
5.15	Control input for square trajectory tracking	97
6.1	3-DOF laboratory helicopter model	106
6.2	Reference trajectory tracking	108
6.3	Tracking error	109
6.4	Control input	109

List of Tables

3.1	Comparison between schemes: Case 1	40
3.2	Electromechanical system constants for single link robot arm.	42
3.3	Comparison between schemes: Case 2	44
4.1	Simulation results: Case 1	59
4.2	Physical system constants of cart-pendulum system	62
4.3	Simulation results: Case 2	64
5.1	Physical parameters of the TRMS	84
5.2	Comparison between single model and MMTLA: Pitch control for step input	85
5.3	Comparison between single model and MMTLA: Yaw control for step input	88
5.4	Comparison between single model and MMTLA: Pitch control for sinusoidal input	90
5.5	Comparison between single model and MMTLA: Yaw control for sinusoidal input	92
5.6	Comparison between single model and MMTLA: Pitch control for square input	94
5.7	Comparison between single model and MMTLA: Yaw control for square input	96
6.1	Physical parameters of the 3 DOF helicopter model	107
6.2	Comparison between single model and MMTLA	110

List of Acronyms

BIBO	Bounded-input bounded-output
BIBS	Bounded-input bounded-state
CE	Control energy
CMMAC	Combined multiple model adaptive control
DC	Direct current
DOF	Degrees of freedom
EKF	Extended Kalman Filter
FAA	Federal aviation administration
IAE	Integral absolute error
ISE	Integral square error
LTI	Linear time invariant
MIMO	Multi-Input Multi-Output
MMAC	Multiple model adaptive control
MRAC	Model reference adaptive control
MMTLA	Multiple model with two level adaptation
PC	Personal computer
PCI	Peripheral component interconnect
PDNN	Parallel dynamic neural networks
PE	Persistently exciting
PSF	Parametric strict feedback
RMSE	Root mean square error
SISO	Single-Input Single-Output
TLA	Two level adaptation
TRMS	Twin rotor MIMO system

TV	Total variation
UAV	unmanned aerial vehicle
UMMAC	Unfalsified multiple model adaptive control
WCLF	Weighted control Lyapunov function

List of Symbols

A	System matrix of continuous time LTI system
\mathfrak{A}	Decoupling matrix
A^{-1}	Inverse of matrix A
A^T	Transpose of matrix A
B	Input matrix of continuous time LTI system
\mathfrak{B}	Input matrix of linearized MIMO system
C	Output matrix
e	Tracking error
e_I	Identification/estimation error
e_{ss}	Steady state error
f, g, h	Smooth vector fields of fitting order
\mathcal{F}, \mathcal{G}	Known smooth functions of fitting order
i	Index for number of inputs/outputs
I	Identity matrix of fitting order
j	Index for number of models
J	Performance index
$L_f h$	Lie derivative of h with respect to f
\mathcal{L}_2	Space of functions having 2-norm
\mathcal{L}_∞	Space of bounded functions
m	Number of inputs/outputs
n	Number of states of an LTI system model
N	Number of estimation models
p	Number of unknown parameters
P	Positive definite matrices

Q	Positive definite diagonal matrix
\mathbb{R}	Set of real numbers
\mathbb{R}^+	Set of strictly positive real numbers, $(0, \infty)$
\mathbb{R}^n	Real vector space of dimension n
$\mathbb{R}^{n \times m}$	Real vector space of dimension $n \times m$
\mathcal{S}	Closed and bounded set in a finite dimensional parameter space
M_p	Maximum overshoot
M_u	Maximum undershoot
t_c	Convergence time
t_s	Settling time
u	Control input
v	Tracking control input
V, V_φ	Lyapunov function
\mathbf{x}	State vector of a system
$\hat{\mathbf{x}}$	Estimate of the state vector
y	Output vector of a system
y_d	Desired trajectory for tracking
J_l	Lumped inertia
L_l	Lumped load
μ, μ_1	Small positive constant
$ \cdot $	Absolute value of a scalar; 1-norm of a vector
$\ \cdot\ $	Euclidean norm for vectors and spectral norm for matrices

List of Publications

Book Chapters/Refereed Journals

1. Vinay Kumar Pandey, Indrani Kar and Chitralkha Mahanta, “Adaptive Control of Nonlinear systems Using Multiple Models with Second Level Adaptation”, *Systems Thinking Approach for Social Problems, Lecture Notes in Electrical Engineering, Springer India*, Vol. 327, pp. 129-141, 2015.
2. Vinay Kumar Pandey, Indrani Kar and Chitralkha Mahanta, “Controller Design for a Class of Nonlinear MIMO Coupled System using Multiple Models and Second Level Adaptation”, *ISA Transactions, Elsevier*, Vol. 69, pp. 256-272, 2017.
3. Vinay Kumar Pandey, Indrani Kar and Chitralkha Mahanta, “Multiple Model Adaptive Control using Second Level Adaptation for Nonlinear Systems with Linear Parameterization,” *International Journal of Dynamics and Control, Springer*, 2017, DOI: <https://doi.org/10.1007/s40435-017-0374-y>.
4. Vinay Kumar Pandey, Indrani Kar and Chitralkha Mahanta, “Multiple models with two level adaptation control for a class of nonlinearly parameterized nonlinear system,” under review in *International Journal of Dynamics and Control, Springer*.

Conference Proceedings

1. D.K.Saroj, I.Kar and Vinay Kumar Pandey, “Sliding mode controller design for Twin Rotor MIMO system with a nonlinear state observer,” *International Multi-Conference on Automation, Computing, Communication, Control and Compressed Sensing (iMac4s)*, Mar 22-23, 2013, Kottayam, Kerala, India.
2. Vinay Kumar Pandey, Indrani Kar and Chitralkha Mahanta, “Multiple Models and Second Level Adaptation for a Class of Nonlinear Systems with Nonlinear Parameterization,” *9th IEEE International Conference on Industrial and Information Systems (ICIIS2014)*, 15-17 Dec 2014, IIITM Gwalior, Madhya Pradesh, India.
3. Vinay Kumar Pandey, Indrani Kar and Chitralkha Mahanta, “Control of twin-rotor mimo system using multiple models with second level adaptation”, *4th International Conference on Advances in Control and Optimization of Dynamical Systems (ACODS 2016)*, Feb 1-5, 2016, Trichy, India.
4. Vinay Kumar Pandey, Indrani Kar and Chitralkha Mahanta, “Controller design for a 3-DOF helicopter using multiple models with second level adaptation”, *4th International Conference on Control (ICC 2017)*, Jan 4-6, 2017, IIT Guwahati, Assam India.

1

Introduction

Contents

1.1	Introduction	2
1.2	Literature Review	3
1.3	Research Motivation	4
1.4	Contributions of the Thesis	5
1.5	Organization of the Thesis	7

1.1 Introduction

In linear time invariant (LTI) control problems it is commonly assumed that the parametric uncertainties inherent in the system under consideration are reasonably small. But due to large variations in operating conditions, failure of system components and changes in subsystem dynamics, this assumption gets often violated. As such, modern control techniques are not able to achieve the desired closed-loop behavior and satisfy required stability conditions in such cases. A variety of areas like biological plants, robotic manipulators, chemical reactors, finance and economics sector, aircraft and automobile industry require mechanisms for identification and control of plants working in widely uncertain environments [1, 2]. Adaptive control [3–13] is a widely popular technique for controlling such systems with unknown or uncertain parameters. Adaptive control methods cope with parametric uncertainty by tuning controller gains in response to estimated changes in the system model. Adaptive control technique provides asymptotic stability in most applications but its transient response may not be satisfactory in case of large parametric uncertainties [14]. It was later realized that using a classical adaptive controller with a single adaptive model yielded slow and oscillatory response. Hence multiple estimation models with switching and tuning were introduced [15]. The concept of multiple models is useful when the system parameters are changing rapidly. Multiple identification models represent the system dynamics in different environments. The control strategy is to determine the best model for the current environment at every instant and activate the corresponding controller. The concept of multiple models was first introduced in 1975 for stochastic control of a F-8C aircraft [15]. Later, Narendra et al. started exploring this area in mid-90s and contributed a good number of theoretical and practical results for adaptive control of linear time invariant (LTI) uncertain systems using multiple models [16–20]. Multiple model adaptive control (MMAC), using multiple identification models with suitable controllers designed offline, provided a better platform to combine the adaptive and modern robust control techniques [21]. However, certain flaws were observed in this emerging technique of multiple models with switching and tuning. One drawback of the MMAC with switching and tuning was the requirement of a large number of models which increased exponentially with increase in dimension of the unknown parameter vector and the system. Use of large number of models made all of them relatively close to each other, which yielded comparable identification errors and hence switching occurred very fast. The discontinuity arising in the control signal due to this rapid switching reduces the performance of the system and may lead to complete system instability. This opens new

directions of research in MMAC, and many methods came up to reduce the fast switching and number of required models, and finally to completely discard the switching among models. One such method proposed by Han et al. for uncertain LTI systems was multiple models with second level adaptation [20]. Unlike the MMAC with switching and tuning in which only one model was selected and used for controller design, in multiple models with two level adaptation (MMTLA), the information from each and every model was used efficiently and all of them contributed simultaneously to control the system. Recently Cezayirli et al. developed multiple model adaptive control (MMAC) for a class of SISO nonlinear systems in uncertain environments [9, 10, 22].

1.2 Literature Review

A well known problem in adaptive control is its poor transient response [16]. A stable strategy was developed by Narendra et al. [16] for improving transient response of a system by developing its multiple identification models. They proposed a general methodology for designing an adaptive control technique using multiple models for the dynamical system operating in a rapidly varying environment. This general methodology was next applied for controlling nonlinear systems with uncertainties [17]. Model reference adaptive control (MRAC) using multiple models for a SISO linear time invariant (LTI) system was later developed by Narendra et al. [18]. Subsequently, Boskovic et al. [23] presented the concept of multiple models, switching and tuning for designing a reconfigurable control strategy for Tailless Advanced Fighter Aircraft (TAFA). The overall control system consisted of multiple parallel identification models, describing different percentages of wing damage and corresponding controllers. Based on a suitably chosen switching mechanism, the system quickly found the model that was closest to the current damage mode and switched to the corresponding controller achieving excellent overall performance. Cezayirli et al. [10] developed a multiple model adaptive control (MMAC) method for SISO nonlinear systems with parametric uncertainties based on input-output linearization method using multiple identification models and switching. Faster convergence of the tracking error and low transients were achieved in this method. A multiple model adaptive control method was proposed by Xudong Ye [14] for nonlinear systems in parametric strict feedback (PSF) form. Kuipers et al. [21] proposed a MMAC architecture based on adaptive mixing control. Chen et al. [24] combined an estimator-based MMAC (EMMAC) and an unfalsified MMAC (UMMAC) yielding combined MMAC (CMMAC) which was capable of monitoring the adequacy of candidate models in terms of their

estimation performances. The CMMAC scheme was designed for a class of nonlinear systems with nonlinear parameterization. Ishitobi et al. [25] developed an adaptive nonlinear model following control for a 3-DOF helicopter which contained high nonlinearity, cross-coupling and large uncertainty. The basic idea of this controller design was linearization of the input-output relationship of the system. Han et al. [20] proposed a MMAC technique with comparatively lesser number of models which cooperated among themselves to yield faster system identification. Chemachema et al. [26] developed an output feedback linearization based controller for a twin rotor MIMO system (TRMS). Cristofaro et al. [27,28] used multiple model adaptive estimation to deal with the changing aircraft shape and parameters due to ice layers on the surface of an aircraft. Tao et al. [29] showed an interesting use of multiple models in model predictive control (MPC) by using the switching strategy among multiple models to improve the tracking performance. Tan et al. [30,31] proposed a MMAC switching scheme for multivariable systems.

1.3 Research Motivation

As discussed above, adaptive controllers started to use multiple identification models when the system was vulnerable to changes in the system environment, input and external disturbances. The multiple identification models were utilized for predicting accurate estimates of the system parameters and then using them for controlling the system. However, when the number of models required was substantial, poor performance and instability were the major issues arising due to fast switching [20]. This opened new directions of research in MMAC. Moreover, the classes of nonlinear systems like nonlinear SISO systems with linear and nonlinear parameterization and nonlinear MIMO coupled systems are very common in many physical systems like cart-pendulum [12], fermentation process [32], [33], adaptive brake control [34], robot manipulators [35], electro-hydraulic system [36], bioreactors [37], helicopters [25], TRMS [26], Unmanned Aerial Vehicles (UAVs) [27], hypersonic vehicles [29]. While designing multiple model based adaptive control (MMAC) methods for such systems, switching among models and optimal number of models to be chosen are vital. Moreover, ensuring fast parameter convergence, speedy and satisfactory transient response, accurate tracking are the primary concerns. Motivated by these facts, this research work attempts to design multiple model based two level adaptation (MMTLA) control schemes for various classes of nonlinear SISO and MIMO uncertain systems with an aim to provide faithful tracking performance with good transient response and fast parameter

convergence.

1.4 Contributions of the Thesis

This work is aimed at designing an adaptive controller for a class of nonlinear systems with large parametric uncertainties. A multiple model based two level adaptation (MMTLA) technique is used in controller which is proposed for nonlinear single-input single-output (SISO) systems with both linear and nonlinear parameterizations. Further, the proposed MMTLA method is utilized in developing an adaptive controller for nonlinear multiple-input multiple-output (MIMO) systems with cross-coupling. The primary contributions of the thesis are outlined below.

(i) **Controller Design for Linearly Parameterized SISO Nonlinear Systems Using Multiple Model Based Two Level Adaptation Technique**

At first, a multiple model based two level adaptation (MMTLA) scheme is used to design a controller for nonlinear systems with linear parameterization. A commonly accepted perception is that the number of models chosen has a direct bearing on the system performance. Hence selection of the least possible number of models is the main concern. Multiple identification models having identical structure and adaptive nature are developed with initial parameters optimally spanning the given compact parameter space. The adaptive laws for identifier parameters are obtained using Lyapunov stability criterion. Since the bounds on the parameters are known, the initial parameters for all the models can be so chosen that the actual parameter lies in the convex hull of those. A theorem then ensures that once the parameter vector is in the convex hull it will always stay in there. Then the right convex combination was found asymptotically using Lyapunov stability analysis. Thus the estimated parameter at the second level is a convex combination of the parameters at the first level. The control input is found by using feedback linearization technique employing the second level estimation. The proposed MMTLA method performs at par with existing switching based multiple model adaptive control methods although using a significantly lesser number of models. Moreover, parameter convergence of the proposed MMTLA method is reasonably fast. Also, the control effort required is reduced in MMTLA based adaptive control.

(ii) **Controller Design for Nonlinearly Parameterized SISO Nonlinear Systems Using Multiple Model Based Two Level Adaptation Technique**

Next, a multiple model based two level adaptation (MMTLA) technique is utilized for designing a controller for nonlinear systems having nonlinear parameterization using similar design methodology as mentioned above. The proposed control technique is best suited for systems where parametric errors are large and convergence of first level models is slow. The proposed MMTLA method offers improvement in transient and steady state performances compared to some existing single model based adaptive control scheme. Moreover, parameter convergence with the proposed MMTLA control method is significantly faster than the existing single model based adaptive control technique.

(iii) **Controller Design for Nonlinear Coupled MIMO Systems Using Multiple Model Based Two Level Adaptation Technique**

A multiple model based two level adaptation (MMTLA) control technique is proposed next for nonlinear coupled MIMO systems. Feedback linearization technique is used to design the control input which also decouples the nonlinear system. The unknown parameters present in the model are estimated using a Kalman filter based observer. Adaptive tuning laws for the unknown parameters are derived using Lyapunov stability criterion. Experimental studies are conducted on a twin rotor MIMO system (TRMS) model for regulation and tracking problem using different reference signals. Experimental results show improvement in transient and steady state performances using the proposed multiple model based two level adaptation (MMTLA) method compared to an existing single model based adaptive control method. The results for pitch and yaw tracking show an improvement in overshoots, settling time, steady state error and root mean square error. Superior tracking response, improved convergence time and smoother control effort with reduction in control energy establish efficacy of the proposed method.

(iv) **Controller Design for Nonlinear MIMO Model Following Control Systems Using Multiple Model Based Two Level Adaptation Technique**

The multiple model based two level adaptation (MMTLA) method is investigated next for the challenging problem of controlling a class of nonlinear MIMO model following control systems. Feedback linearization technique with dynamic state feedback and nonlinear structure algorithm is used to design the control input and to decouple the nonlinear system having a singular decoupling matrix. Superior tracking response, improved convergence time and smoother as

well as lesser control effort are highlights of the proposed method.

1.5 Organization of the Thesis

This thesis includes seven chapters which are briefly introduced below.

- **Chapter 2:** The adaptive control method is briefly discussed and a few preliminary concepts in multiple model adaptive control are introduced in Chapter 2.
- **Chapter 3:** In this chapter, a multiple model based two level adaptation (MMTLA) scheme is designed for linearly parameterized SISO nonlinear systems. Simulation studies are conducted and results are compared with some already existing adaptive control method.
- **Chapter 4:** A nonlinearly parameterized SISO nonlinear system is considered in this chapter and MMTLA technique is used to design its controller. Simulation results are compared with some existing method present in the literature.
- **Chapter 5:** In this chapter, a multiple model based two level adaptation (MMTLA) controller is developed for a cross-coupled MIMO nonlinear system. Feedback linearization method is utilized for linearizing as well as decoupling the system. Real time experiments are performed on a twin rotor MIMO system (TRMS), which is a highly nonlinear cross-coupled MIMO system. Simulation and experimental results are presented.
- **Chapter 6:** In this chapter, an important class of nonlinear MIMO system with cross-couplings between its axes, but having a singular decoupling matrix is considered. After designing the control input using nonlinear adaptive model following control with nonlinear structure algorithm, the MMTLA method is applied. Simulation studies on a 3-DOF tandem rotor model helicopter are presented.
- **Chapter 7:** In this chapter conclusions from the research work are drawn and the scope for future research is outlined.

2

Preliminary Concepts

Contents

2.1	Introduction	9
2.2	Change in Operating Environment	9
2.3	The Adaptive Control Problem	11
2.4	Multiple Model Adaptive Control (MMAC) with Switching	11
2.5	Summary	17

2.1 Introduction

The preliminary concepts discussed here are aimed to provide the background and basics on use of multiple models in adaptive control of systems with uncertain parameters. Before moving to the two level adaptation, the fundamental approach of switching between different models in multiple model adaptive control (MMAC) with switching is elucidated. Furthermore, various combinations of available MMAC techniques like single adaptive model, single fixed model, three fixed and one adaptive model and multiple adaptive model are briefly explained.

2.2 Change in Operating Environment

Changes in values of parameters of system occur due to change in operating environment which can be caused due to [18]

- Faults in system
- Sensor/actuator failure
- External disturbance like varying wind speed and direction in aerospace systems, change in air-drag and road friction for automotive systems.
- Changes in system parameters like load change in a DC motor.

2.2.1 Assumptions used regarding the environment

For using different identification models efficiently to estimate the unknown parameters of the system, certain assumptions have to be made about the region to which the system parameter belongs [17]. These assumptions are cited below:

- The unknown system parameters are assumed to belong to a closed and bounded set \mathcal{S} .
- The system parameter vector \mathbf{P} and estimator model parameter vector $\hat{\mathbf{P}}$ belong to \mathcal{S} .
- For N models set \mathcal{S} can be divided such that $\cup_{j=1}^N \mathcal{S}_j = \mathcal{S}$.

2.2.2 Switching and tuning among different environments

Let us consider that \mathcal{S} is a closed and bounded set in a finite dimensional parameter space and system parameter vector \mathbf{P} and model parameter vector \hat{P}_i belong to \mathcal{S} . Corresponding to each

parameter vector \hat{P}_i there exists a neighborhood $\mathcal{S}_i \subset \mathcal{S}$. Here, for N models $\cup_{j=1}^N \mathcal{S}_j = \mathcal{S}$. If at a particular instant, controller C_i is in use and the performance index J_j of \mathcal{S}_j happens to be the minimum in the set $\{J_j\}_{j=1}^N$, model \mathcal{S}_j will be selected and the controller will switch from C_i to C_j as shown in Figure 2.1 [18].

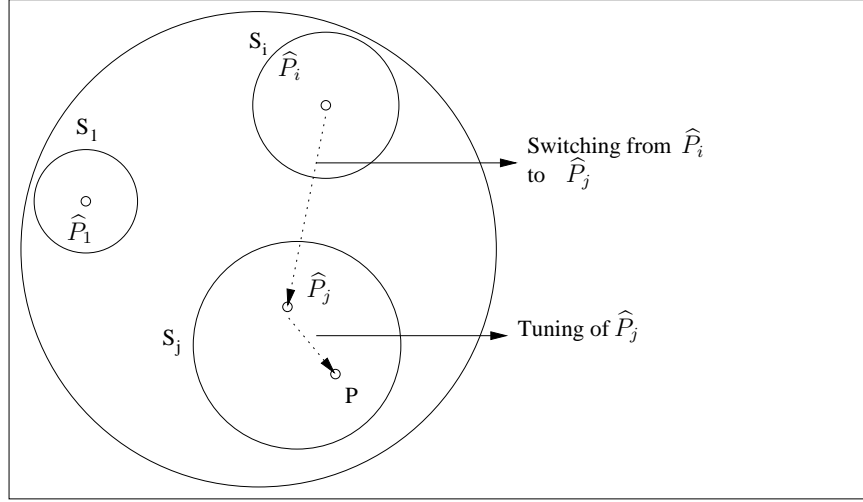


Figure 2.1: Multiple models in a system environment

For example, let us consider a system having two parameters a and b , whose values get changed due to change in environment. A bounded set for these parameters is considered as

$$\mathcal{S} = \{l_1 \leq a \leq l_4, l'_1 \leq b \leq l'_4\} \quad (2.1)$$

where l_1, l_4, l'_1, l'_4 are real constants. For $N=3$, the above parameter space can be divided into following 3 regions:

$$\mathcal{S}_1 = \{l_1 \leq a \leq l_2, l'_1 \leq b \leq l'_2\} \quad (2.2)$$

$$\mathcal{S}_2 = \{l_2 < a \leq l_3, l'_2 < b \leq l'_3\} \quad (2.3)$$

$$\mathcal{S}_3 = \{l_3 < a \leq l_4, l'_3 < b \leq l'_4\} \quad (2.4)$$

Further, using three identification models whose parameters belong to these three different sets, the model which is closest to the system will be chosen at a particular time. Parameter values of that chosen model are then considered as the true parameters of the system and accordingly the controller at that particular instant can be designed.

2.3 The Adaptive Control Problem

Regulation and tracking are the two most commonly studied control problems. In the regulation problem, the objective is to stabilize the system using input-output data around a fixed operating point. In the tracking problem, the aim is to make the system output follow a desired reference input. These problems can be further stated as follows:

Let us consider the following system:

$$\begin{aligned}\dot{\mathbf{x}}(t) &= \mathbf{A}\mathbf{x}(t) + \mathbf{B}u(t) \\ y_p(t) &= \mathbf{C}^T\mathbf{x}(t)\end{aligned}\tag{2.5}$$

where $\mathbf{x}(t) : \mathbb{R}^+ \rightarrow \mathbb{R}^n$ is the state vector, $u(t) : \mathbb{R}^+ \rightarrow \mathbb{R}$ is the control input and $y_p : \mathbb{R}^+ \rightarrow \mathbb{R}$ represents the output. Let $\{\mathbf{C}^T, \mathbf{A}, \mathbf{B}\}$ be observable and controllable and have unknown elements.

Regulation Problem: The objective is to find a control input u using only input-output data and a differentiator free controller, which stabilizes the system (2.5).

Tracking Problem: Let $y_m(t)$ be the uniformly bounded desired output. The aim is to determine a bounded input u using a differentiator free controller such that $\lim_{t \rightarrow \infty} |y_p(t) - y_m(t)| = 0$.

2.4 Multiple Model Adaptive Control (MMAC) with Switching

The concept of multiple models is used to represent different environments in which the system has to operate. If a system is required to operate in different environments (caused by external disturbance, parameter variations, change in subsystem dynamics), a fixed system model may not be able to estimate the controller parameters correctly. Use of multiple models and controllers have resulted in improved performance in presence of large parametric uncertainties [16–18].

2.4.1 Basic structure of MMAC

The basic structure of MMAC is given in Figure 2.2 [18]. The system has input u and output y_p . The control system has N identification models denoted as $\{I_j\}_{j=1}^N$ with identical structures but with different initial estimates of the system parameters. Corresponding to each I_j , the controllers $\{C_j\}_{j=1}^N$ with parameter vectors $\boldsymbol{\theta}_j$ and output u_j is designed. Each identification model I_j is paired with a controller C_j to form an indirect controller arrangement. Further, \hat{P}_j is the parameter vector belonging to model I_j . Here $e_j = \hat{y}_j - y_p$ is the identification error between j -th model and the actual

as $\boldsymbol{\theta} = [a(1), a(2), \dots, a(n)]^T$, where $\boldsymbol{\theta}$ is the vector of unknown parameters. Here parameters $a(1), a(2), \dots, a(n)$ are unknowns, $\mathbf{B} = [0, 0, \dots, 1]^T$ and $\mathbf{C}^T = [0 \ 0 \ \dots \ 1]$. Let us consider the reference model described by differential equation

$$\begin{aligned}\dot{\mathbf{x}}_m(t) &= \mathbf{A}_m \mathbf{x}_m(t) + \mathbf{B}_m r \\ y_m(t) &= \mathbf{C}_m^T \mathbf{x}_m(t)\end{aligned}\tag{2.7}$$

where $r : \mathbb{R}^+ \rightarrow \mathbb{R}$ is a known bounded piecewise continuous reference signal and $\mathbf{x}_m(t) : \mathbb{R}^+ \rightarrow \mathbb{R}^n$ is the reference model state. Here \mathbf{A}_m is stable, is in companion form and has last row as $\boldsymbol{\theta}_m^T$. Further, $\mathbf{C}_m^T = \mathbf{C}^T$.

Now, let us consider that the unknown parameter vector $\boldsymbol{\theta}^T \in \mathcal{S}$. The aim here is to determine input u to the system such that output of the system tracks the output of the reference model such that

$$\lim_{t \rightarrow \infty} [\mathbf{y}_p(t) - \mathbf{y}_m(t)] = 0.\tag{2.8}$$

Using (2.6), (2.7) in (2.8) yields

$$\lim_{t \rightarrow \infty} [\mathbf{x}(t) - \mathbf{x}_m(t)] = 0.\tag{2.9}$$

2.4.3 Single identification model

To control the system (2.6) by using an indirect method, an identification model is set up [38] as given below:

$$\dot{\hat{\mathbf{x}}}(t) = \mathbf{A}_m \hat{\mathbf{x}}(t) + [\hat{\mathbf{A}}(t) - \mathbf{A}_m] \mathbf{x}(t) + \mathbf{B}u(t)\tag{2.10}$$

Here also, $\hat{\mathbf{A}}(t)$ is assumed to be in companion form with its last row $\hat{\boldsymbol{\theta}}^T(t) = [\hat{a}_1(t), \hat{a}_2(t), \dots, \hat{a}_n(t)]$.

Further, $[\hat{a}_1(t), \hat{a}_2(t), \dots, \hat{a}_n(t)]$ are the estimates of the system parameters and can be adjusted adaptively. Parameter identification error is defined as $\tilde{\boldsymbol{\theta}}(t) = \hat{\boldsymbol{\theta}}(t) - \boldsymbol{\theta}$ and state identification error is defined as $\mathbf{e}_I(t) = \hat{\mathbf{x}}(t) - \mathbf{x}(t)$. Now, (2.6) - (2.10) give rise to

$$\begin{aligned}\dot{\mathbf{e}}_I(t) &= \mathbf{A}_m \hat{\mathbf{x}}(t) + [\hat{\mathbf{A}}(t) - \mathbf{A}_m] \mathbf{x}(t) + \mathbf{B}u(t) - \mathbf{A} \mathbf{x}(t) - \mathbf{B}u(t) \\ \text{or, } \dot{\mathbf{e}}_I(t) &= \mathbf{A}_m \mathbf{e}_I(t) + [\hat{\mathbf{A}}(t) - \mathbf{A}] \mathbf{x}(t)\end{aligned}\tag{2.11}$$

where $\hat{\mathbf{A}} - \mathbf{A}$ can be written as $\hat{\mathbf{A}} - \mathbf{A} = \mathbf{B}\tilde{\boldsymbol{\theta}}^T(t)$, using which, (2.11) can be written as

$$\dot{\mathbf{e}}_I(t) = \mathbf{A}_m \mathbf{e}_I(t) + \mathbf{B}\tilde{\boldsymbol{\theta}}^T(t)\mathbf{x}(t) \quad (2.12)$$

Adaptive laws for identification parameters: Lyapunov stability criterion can be used here to find an adaptive law for updating the parameters of the identification model. A suitable Lyapunov function candidate can be chosen as:

$$V(\mathbf{e}_I, \tilde{\boldsymbol{\theta}}) = \mathbf{e}_I^T \mathbf{P} \mathbf{e}_I + \tilde{\boldsymbol{\theta}}^T \tilde{\boldsymbol{\theta}} \quad (2.13)$$

where \mathbf{P} is the unique positive definite solution of Lyapunov equation $\mathbf{A}_m^T \mathbf{P} + \mathbf{P} \mathbf{A}_m = -\mathbf{Q}$, for a positive definite matrix \mathbf{Q} . Taking first time derivative of (2.13), gives

$$\dot{V}(\mathbf{e}_I, \tilde{\boldsymbol{\theta}}) = \dot{\mathbf{e}}_I^T \mathbf{P} \mathbf{e}_I + \mathbf{e}_I^T \mathbf{P} \dot{\mathbf{e}}_I + \dot{\tilde{\boldsymbol{\theta}}}^T \tilde{\boldsymbol{\theta}} + \tilde{\boldsymbol{\theta}}^T \dot{\tilde{\boldsymbol{\theta}}} \quad (2.14)$$

Using (2.12) in (2.14) gives

$$\dot{V}(\mathbf{e}_I, \tilde{\boldsymbol{\theta}}) = [\mathbf{e}_I^T \mathbf{A}_m^T + \mathbf{x}^T \tilde{\boldsymbol{\theta}} \mathbf{B}^T] \mathbf{P} \mathbf{e}_I + \mathbf{e}_I^T \mathbf{P} [\mathbf{A}_m \mathbf{e}_I + \mathbf{B} \tilde{\boldsymbol{\theta}}^T \mathbf{x}] + \dot{\tilde{\boldsymbol{\theta}}}^T \tilde{\boldsymbol{\theta}} + \tilde{\boldsymbol{\theta}}^T \dot{\tilde{\boldsymbol{\theta}}} \quad (2.15)$$

$$\text{or, } \dot{V}(\mathbf{e}_I, \tilde{\boldsymbol{\theta}}) = \mathbf{e}_I^T \mathbf{A}_m^T \mathbf{P} \mathbf{e}_I + \mathbf{x}^T \tilde{\boldsymbol{\theta}} \mathbf{B}^T \mathbf{P} \mathbf{e}_I + \mathbf{e}_I^T \mathbf{P} \mathbf{A}_m \mathbf{e}_I + \mathbf{e}_I^T \mathbf{P} \mathbf{B} \tilde{\boldsymbol{\theta}}^T \mathbf{x} + \dot{\tilde{\boldsymbol{\theta}}}^T \tilde{\boldsymbol{\theta}} + \tilde{\boldsymbol{\theta}}^T \dot{\tilde{\boldsymbol{\theta}}} \quad (2.16)$$

By choosing the adaptive law as $\dot{\tilde{\boldsymbol{\theta}}} = \dot{\hat{\boldsymbol{\theta}}}(t) = -\mathbf{e}_I^T \mathbf{P} \mathbf{B} \mathbf{x}(t)$ and using in (2.16) yields

$$\begin{aligned} \dot{V}(\mathbf{e}_I, \tilde{\boldsymbol{\theta}}) &= \mathbf{e}_I^T(t) \mathbf{A}_m^T \mathbf{P} \mathbf{e}_I(t) + \mathbf{e}_I^T \mathbf{P} \mathbf{A}_m \mathbf{e}_I(t) \\ \text{or, } \dot{V}(\mathbf{e}_I, \tilde{\boldsymbol{\theta}}) &= -\mathbf{e}_I^T \mathbf{Q} \mathbf{e}_I \leq 0 \end{aligned} \quad (2.17)$$

which shows that $\dot{V}(\mathbf{e}_I, \tilde{\boldsymbol{\theta}})$ is negative semidefinite. This confirms that $V(\mathbf{e}_I, \tilde{\boldsymbol{\theta}})$ is a suitable Lyapunov function for the system. Hence $\mathbf{e}_I(t)$ and $\tilde{\boldsymbol{\theta}}(t)$ or $\hat{\boldsymbol{\theta}}(t)$ are bounded.

Feedback control: Now feedback control is used to assure the stability of the system and boundedness of $\mathbf{x}(t)$. A feedback control input is chosen as

$$u(t) = -\Theta^T(t)\mathbf{x}(t) + r(t) \quad (2.18)$$

where $\Theta(t) = \boldsymbol{\theta}(t) - \boldsymbol{\theta}_m$ and the control error is defined as

$$\mathbf{e}(t) = \mathbf{x}(t) - \mathbf{x}_m(t). \quad (2.19)$$

An ideal control parameter is defined as $\Theta^* = \boldsymbol{\theta} - \boldsymbol{\theta}_m$. Similarly, control parameter error is defined as $\tilde{\Theta}(t) = \Theta^* - \Theta(t)$. Now, taking first time derivative of (2.19) and using (2.6) and (2.7) yields

$$\begin{aligned}\dot{\mathbf{e}}(t) &= \dot{\mathbf{x}}(t) - \dot{\mathbf{x}}_m(t) \\ \text{or, } \dot{\mathbf{e}}(t) &= \mathbf{A}_m \mathbf{e}(t) + \mathbf{B} \tilde{\Theta}^T(t) \mathbf{x}(t)\end{aligned}\tag{2.20}$$

Further, choosing a Lyapunov function candidate as

$$V(\mathbf{e}, \tilde{\Theta}) = \mathbf{e}^T \mathbf{P} \mathbf{e} + \tilde{\Theta}^T \tilde{\Theta}\tag{2.21}$$

and taking first time derivative of (2.21) gives

$$\dot{V}(\mathbf{e}, \tilde{\Theta}) = \dot{\mathbf{e}}^T \mathbf{P} \mathbf{e} + \mathbf{e}^T \mathbf{P} \dot{\mathbf{e}} + \dot{\tilde{\Theta}}^T \tilde{\Theta} + \tilde{\Theta}^T \dot{\tilde{\Theta}}.\tag{2.22}$$

By using control error equation (2.20) in (2.22) gives

$$\begin{aligned}\dot{V}(\mathbf{e}, \tilde{\Theta}) &= [\mathbf{e}^T(t) \mathbf{A}_m^T + \mathbf{x}^T(t) \tilde{k}(t) \mathbf{B}^T] \mathbf{P} \mathbf{e} + \mathbf{e}^T \mathbf{P} [\mathbf{A}_m \mathbf{e}(t) + \mathbf{B} \tilde{\Theta}^T(t) \mathbf{x}(t)] \\ &+ \dot{\tilde{\Theta}}^T(t) \tilde{\Theta}(t) + \tilde{\Theta}^T(t) \dot{\tilde{\Theta}}(t)\end{aligned}\tag{2.23}$$

$$\begin{aligned}\text{or, } \dot{V}(\mathbf{e}, \tilde{\Theta}) &= \mathbf{e}^T(t) \mathbf{A}_m^T \mathbf{P} \mathbf{e} + \mathbf{x}^T(t) \tilde{\Theta}(t) \mathbf{B}^T \mathbf{P} \mathbf{e} + \mathbf{e}^T \mathbf{P} \mathbf{A}_m \mathbf{e}(t) + \mathbf{e}^T \mathbf{P} \mathbf{B} \tilde{\Theta}^T(t) \mathbf{x}(t) \\ &+ \dot{\tilde{\Theta}}^T(t) \tilde{\Theta}(t) + \tilde{\Theta}^T(t) \dot{\tilde{\Theta}}(t).\end{aligned}\tag{2.24}$$

By choosing adaptive law as $\dot{\tilde{\Theta}}(t) = -\dot{\Theta}(t) = -\mathbf{e}^T(t) \mathbf{P} \mathbf{B} \mathbf{x}(t)$ and using in (2.24) yields

$$\begin{aligned}\dot{V}(\mathbf{e}, \tilde{\Theta}) &= \mathbf{e}^T(t) \mathbf{A}_m^T \mathbf{P} \mathbf{e}(t) + \mathbf{e}^T(t) \mathbf{P} \mathbf{A}_m \mathbf{e}(t) \\ \text{or, } \dot{V}(\mathbf{e}, \tilde{\Theta}) &= -\mathbf{e}^T \mathbf{Q} \mathbf{e} \leq 0\end{aligned}\tag{2.25}$$

which shows that $\dot{V}(\mathbf{e}, \tilde{\Theta})$ is negative semidefinite. This confirms the suitability of $V(\mathbf{e}, \tilde{\Theta})$ as Lyapunov function for the system. Hence $\mathbf{e}(t)$ and $\tilde{\Theta}(t)$ or $\Theta(t)$ are bounded. Integrating (2.25) from zero to infinity gives

$$-\int_0^{\infty} \dot{V}(\mathbf{e}, \tilde{\Theta}) dt = V(0) - V(\infty) < \infty\tag{2.26}$$

Using (2.25) and (2.26) yields

$$0 \leq \int_0^{\infty} \mathbf{e}^T \mathbf{Q} \mathbf{e} < \infty \quad (2.27)$$

which implies that $\mathbf{e} \in \mathcal{L}_2$, where \mathcal{L}_2 is the Euclidean norm. Since in (2.19) $\mathbf{x}_m(t)$ and $\mathbf{e}(t)$ are bounded, $\mathbf{x}(t)$ is also bounded. Similarly, because all the terms on the right hand side of (2.20) are bounded, it follows that $\dot{\mathbf{e}}(t)$ is also bounded. Since $\dot{\mathbf{e}}(t)$ is bounded and $\mathbf{e} \in \mathcal{L}_2$, implies that $\ddot{V}(\mathbf{e}, \tilde{\Theta})$ is also bounded. Hence $\dot{V}(\mathbf{e}, \tilde{\Theta})$ is uniformly continuous. Therefore, using Barbalat's lemma it follows that $\lim_{t \rightarrow \infty} \dot{V}(\mathbf{e}, \tilde{\Theta}) \rightarrow 0$ which also implies $\lim_{t \rightarrow \infty} \mathbf{e}(t) = 0$, meaning that the control objective $\lim_{t \rightarrow \infty} [\mathbf{x}(t) - \mathbf{x}_m(t)] = 0$ is achieved.

2.4.4 Multiple identification models

In adaptive control method, multiple identification models may be used to identify the system [5]. Here N identification models with the same structure as given for single identification model in Section 2.4.3 can be used to set up N estimates of the parameter vector. The j -th identification model ($j = 1, \dots, N$) can be found as [20]:

$$\begin{aligned} \dot{\mathbf{x}}_j(t) &= \mathbf{A}_m \mathbf{x}_j(t) + [\mathbf{A}_j(t) - \mathbf{A}_m] \mathbf{x}(t) + \mathbf{B}u(t) \\ \mathbf{x}_j(t_0) &= \mathbf{x}(t_0) \end{aligned} \quad (2.28)$$

All the N adaptive identification models can be described by identical differential equations with the same initial states as those of the system but with different initial values of the parameter vectors. When dealing with N identification models, at a time only one model can be chosen by using a suitable performance index. The model which provides the best approximation of the system parameters is selected. Then the problem reduces to the same as described in Section 2.4.3. At any particular time, the model chosen as the closest approximation according to the given performance index is used to find the parameters of the controller.

Switching scheme:

The switching scheme consists of monitoring a performance index $J_j(t)$ based on identification error $\mathbf{e}_j(t)$ for model I_j and switching to the controller corresponding to the model with the best performance

index. A good choice of performance index can be [20, 39]

$$J_j(t) = \alpha \mathbf{e}_j^2(t) + \beta \int_0^t e^{-\lambda(t-\tau)} \mathbf{e}_j^2(\tau) d\tau \quad (2.29)$$

where α, β, λ are positive constants.

2.4.5 Various combinations of fixed and adaptive models

Various combinations of fixed and adaptive models are suggested in the literature [20, 39]. Some of them are listed below:

- Single adaptive model
- Three fixed models
- Three adaptive models
- Three fixed and one adaptive model.

The first one is the basic adaptive control method, while the other three are multiple model adaptive control (MMAC) methods with switching among the models.

2.5 Summary

The purpose of this chapter is to familiarize with the basics of multiple model adaptive control (MMAC) technique. The main focus of this chapter is to discuss the motivation for using multiple models for different environments in which the system may have to operate. The reasons for change in the system environment are mentioned. Single and multiple identification models used in adaptive control method are described briefly.

3

Adaptive Controller Design for Linearly Parameterized SISO Nonlinear Systems Using Multiple Model Based Two Level Adaptation Technique

Contents

3.1	Introduction	19
3.2	Adaptive Control of Nonlinear Systems with Linear Parameterization .	20
3.3	Multiple Model based Two Level Adaptation (MMTLA) method	27
3.4	General Work Flow Chart	36
3.5	Simulation Results	36
3.6	Summary	45

3.1 Introduction

A highly desired feature of an adaptively controlled system is to sense the current operating condition and be able to make changes in the controller parameters accordingly. However, it was observed that in systems having highly uncertain parameters, or the systems having parameters which were unknown as well as changing with the change in their environment, using a classical adaptive controller with single adaptive model yielded slow and oscillatory response [16]. Hence multiple models with switching and tuning were introduced to enhance the performance of the classical adaptive control [15] [16]. Narendra et al. proposed adaptive control schemes for linear time invariant (LTI) systems using multiple models with switching and tuning [16–18] and it was found useful for uncertain systems in a changing environment. Similarly, an interesting use of multiple models in model predictive control (MPC) can be found in [29]. Here switching between multiple models is used to improve the tracking performance for hardware in loop (HIL) simulation platform dspace.

In this chapter, an adaptive control strategy with multiple model based two level adaptation (MMTLA) scheme is proposed for a class of nonlinear systems with linear parametrization. Feedback linearization technique [4,8,40] is used to design the control input. Multiple identification models are developed with similar structure but different initial parameter values which are chosen to optimally span the given compact parameter space. Adaptive laws for weights at the second level are derived using identifier error. Closed loop stability and tracking error convergence are guaranteed after introduction of the second level adaptation. A commonly accepted perception is that the number of models chosen has a direct bearing on the system performance. Here, selection of the least possible number of models in a given compact uncertain parameter space and their distribution in the parameter region is discussed. An important aspect of adaptive control studied by Boyd et al. in 1986 [41] and followed by Annaswamy et al. [42], was the convergence of unknown parameters of identification models. To ensure that the identifier parameters converge to their true values, the reference input signals are made persistently exciting (PE) [7]. Also, to restrict the parameters from leaving the compact parameter space, projection based adaptive laws [43,44] have been used. A comprehensive simulation work is presented for linearly parameterized systems and results are compared with existing adaptive control methods.

The chapter is organized as follows. In Section 3.2 the control problem is formulated followed by design of feedback control and estimator model for changing environments in the case of linearly

parameterized nonlinear systems. The proposed adaptive controller using multiple model based two level adaptation method is described in Section 3.3 including stability analysis for the overall system. Section 3.4 presents the general flowchart outlining the procedural steps followed in the proposed controller with multiple model based two level adaptation (MMTLA) scheme. Simulation results are presented in Section 3.5. The chapter is summarized in Section 3.6.

3.2 Adaptive Control of Nonlinear Systems with Linear Parameterization

Let us consider the following class of affine single-input single-output (SISO) nonlinear systems,

$$\begin{aligned}\dot{\mathbf{x}}(t) &= f(\mathbf{x}(t), \boldsymbol{\theta}(t)) + g(\mathbf{x}(t), \boldsymbol{\theta}(t))u(t) \\ y(t) &= h(\mathbf{x}(t))\end{aligned}\tag{3.1}$$

where $\mathbf{x}(t) : \mathbb{R}^+ \rightarrow \mathbb{R}^n$ is the state vector, which is assumed to be fully available for measurement. Next, $f, g : \mathbb{R}^n \rightarrow \mathbb{R}^n$ are sufficiently smooth vector fields and $h : \mathbb{R}^n \rightarrow \mathbb{R}$ is a scalar valued function. Further, $\boldsymbol{\theta}(t) = [\theta_1, \theta_2, \dots, \theta_p]^T \in \mathcal{S}_\theta$ is the unknown parameter vector, where p is the number of unknown parameters and $\mathcal{S}_\theta \subset \mathbb{R}^p$ is a compact set. Finally, $u(t) : \mathbb{R}^+ \rightarrow \mathbb{R}$ is the control input and $y(t) : \mathbb{R}^+ \rightarrow \mathbb{R}$ represents the output. Here origin of the state space is an equilibrium point for the system (3.1). The following assumptions are made about the system (3.1):

- (i) The system dynamics in (3.1) are assumed to be linearly parameterized, meaning that vector fields $f(\mathbf{x}, \boldsymbol{\theta})$, $g(\mathbf{x}, \boldsymbol{\theta})$ depend linearly on the unknown parameters $\boldsymbol{\theta}$ [45, 46]. Functions $f(\mathbf{x}, \boldsymbol{\theta})$ and $g(\mathbf{x}, \boldsymbol{\theta})$ can be characterized as

$$\begin{aligned}f(\mathbf{x}, \boldsymbol{\theta}) &= \boldsymbol{\omega}_f^T(\mathbf{x})\boldsymbol{\theta} \\ g(\mathbf{x}, \boldsymbol{\theta}) &= \boldsymbol{\omega}_g^T(\mathbf{x})\boldsymbol{\theta}\end{aligned}\tag{3.2}$$

where $\boldsymbol{\omega}_f, \boldsymbol{\omega}_g : \mathbb{R}^n \rightarrow \mathbb{R}^p$ are known smooth functions.

- (ii) The system has constant relative degree γ , meaning that

$$L_{g(\mathbf{x}, \boldsymbol{\theta})}L_{f(\mathbf{x}, \boldsymbol{\theta})}^{i-1}h(\mathbf{x}) = 0, \quad i = 1, 2, \dots, (\gamma - 1) \text{ and } L_{g(\mathbf{x}, \boldsymbol{\theta})}L_{f(\mathbf{x}, \boldsymbol{\theta})}^{\gamma-1}h(\mathbf{x}) \neq 0, \quad \forall \mathbf{x} \in \mathbb{R}^n, \boldsymbol{\theta} \in \mathcal{S}_\theta. \text{ Here, } L_f, L_g \text{ are the Lie derivative operators [45].}$$

- (iii) The equilibrium point of the zero dynamics of the system (3.1) is asymptotically stable [45].

3.2.1 Controller Input

For the system (3.1), a diffeomorphic coordinate transformation $\mathcal{T} = \Psi(\mathbf{x})$ is defined such that the transformed system becomes feedback linearizable [6,47]. Using this diffeomorphism, system (3.1) can be represented in terms of linearized states $\tau_1, \tau_2, \dots, \tau_\gamma$ as

$$\begin{aligned}
\dot{\tau}_1 &= \tau_2 \\
\dot{\tau}_2 &= \tau_3 \\
&\dots \\
\dot{\tau}_{\gamma-1} &= \tau_\gamma \\
\dot{\tau}_\gamma &= L_f^\gamma h(\mathbf{x})(\mathbf{x}, \boldsymbol{\theta}) + L_g L_f^{\gamma-1} h(\mathbf{x})(\mathbf{x}, \boldsymbol{\theta})u \\
\dot{\boldsymbol{\xi}} &= \varphi(\boldsymbol{\tau}, \boldsymbol{\xi}) \\
y &= \tau_1
\end{aligned} \tag{3.3}$$

where $\boldsymbol{\xi} : \mathbb{R}^+ \rightarrow \mathbb{R}^{n-\gamma}$ are the unobservable states of the system and $\dot{\boldsymbol{\xi}} = \varphi(\boldsymbol{\tau}, \boldsymbol{\xi})$ represents internal dynamics of the system which exists when relative degree is strictly lesser than the actual degree of the system. The zero dynamics $\dot{\boldsymbol{\xi}} = \varphi(0, \boldsymbol{\xi})$ of the system is assumed to be asymptotically stable.

Further, $L_f^\gamma h(\mathbf{x})(\mathbf{x}, \boldsymbol{\theta})$ and $L_g L_f^{\gamma-1} h(\mathbf{x})(\mathbf{x}, \boldsymbol{\theta})$ can be represented in terms of multilinear parameter elements [10] as

$$\begin{aligned}
L_f^\gamma h(\mathbf{x})(\mathbf{x}, \boldsymbol{\theta}) &= \mathcal{P}^T \mathcal{F}(\mathbf{x}) \\
L_g L_f^{\gamma-1} h(\mathbf{x})(\mathbf{x}, \boldsymbol{\theta}) &= \mathcal{P}^T \mathcal{G}(\mathbf{x})
\end{aligned} \tag{3.4}$$

where \mathcal{P} represents the multilinear parameter vector and \mathcal{F}, \mathcal{G} are known smooth functions. Consequently, using (3.4) in (3.3) yields

$$\dot{\tau}_\gamma = \mathcal{P}^T (\mathcal{F}(\mathbf{x}) + \mathcal{G}(\mathbf{x})u). \tag{3.5}$$

Choosing a virtual input v defined as $v = \mathcal{P}^T (\mathcal{F}(\mathbf{x}) + \mathcal{G}(\mathbf{x})u)$ yields

$$u = \frac{1}{\mathcal{P}^T \mathcal{G}(\mathbf{x})} (-\mathcal{P}^T \mathcal{F}(\mathbf{x}) + v). \tag{3.6}$$

The control objective here is to track a bounded desired trajectory $y_d(t)$, with bounded derivatives

$\dot{y}_d(t), \dots, y_d^{(\gamma)}(t)$. Based on the desired trajectory information, the control signal v can be designed as

$$v = y_d^{(\gamma)} + c_\gamma(y_d^{(\gamma-1)} - y^{(\gamma-1)}) + \dots + c_1(y_d - y) \quad (3.7)$$

where constants c_1, \dots, c_γ can be chosen such that $s^\gamma + c_\gamma s^{\gamma-1} + \dots + c_1$ yields a Hurwitz polynomial.

3.2.2 Estimation model design at the first level

As already assumed, the system dynamics (3.1) are linearly parameterized and can be written in the regressor form [45] as

$$\dot{\mathbf{x}} = \boldsymbol{\omega}^T(\mathbf{x}, u)\boldsymbol{\theta} \quad (3.8)$$

where $\boldsymbol{\omega}(\mathbf{x}, u) \in \mathbb{R}^{p \times n}$ is the known regressor matrix. A stable estimation model of the system is selected such that states and output converge to those of the system as time $t \rightarrow \infty$. The observer based estimation model [5, 45] for the system (3.8) is defined as

$$\dot{\hat{\mathbf{x}}} = \mathbf{A}(\hat{\mathbf{x}} - \mathbf{x}) + \boldsymbol{\omega}^T(\mathbf{x}, u)\hat{\boldsymbol{\theta}} \quad (3.9)$$

where $\hat{\mathbf{x}}$ and $\hat{\boldsymbol{\theta}}$ are the estimates of \mathbf{x} and $\boldsymbol{\theta}$ respectively and $\mathbf{A} \in \mathbb{R}^{n \times n}$ is a Hurwitz matrix. Considering the identification error $\mathbf{e}_I = \hat{\mathbf{x}} - \mathbf{x}$ and parameter error $\tilde{\boldsymbol{\theta}} = \hat{\boldsymbol{\theta}} - \boldsymbol{\theta}$, the identifier error dynamics of system (3.1) is given as,

$$\begin{aligned} \dot{\mathbf{e}}_I &= \mathbf{A}\mathbf{e}_I + \boldsymbol{\omega}^T(\mathbf{x}, u)\tilde{\boldsymbol{\theta}} \\ \dot{\tilde{\boldsymbol{\theta}}} &= -\boldsymbol{\omega}(\mathbf{x}, u)\mathbf{P}\mathbf{e}_I \end{aligned} \quad (3.10)$$

where \mathbf{P} is a symmetric positive definite matrix, which is the solution of the Lyapunov equation $\mathbf{A}^T\mathbf{P} + \mathbf{P}\mathbf{A} = -\mathbf{Q}$, with \mathbf{Q} being a symmetric positive definite matrix.

Theorem 3.1 [10]: Let us consider the identifier error dynamics of the system (3.1) given in (3.10).

If the nonlinear system is bounded-input bounded-state (BIBS) stable, then $\lim_{t \rightarrow \infty} \mathbf{e}_I(t) = 0$.

The proof of the above theorem can be found in [10]. Also, it should be noted that, when the regressor matrix $\boldsymbol{\omega}(\mathbf{x}, u)$ is sufficiently rich [7] (A.1 may be referred), $\tilde{\boldsymbol{\theta}}$ converges to zero asymptotically [6, 45]. Subsequent derivation proves the boundedness of the control error which in turn justifies the use of identification model (3.10).

The virtual control in (3.7) comprises of output y and its higher derivatives $\dot{y}, \ddot{y}, \dots, y^{(\gamma-1)}$. Since higher derivatives $\dot{y}, \ddot{y}, \dots, y^{(\gamma-1)}$ are functions of unknown parameter $\boldsymbol{\theta}$, certainty equivalence princi-

ple [7] (referred in A.1) is applied here to get

$$\hat{v} = y_d^{(\gamma)} + c_\gamma(y_d^{(\gamma-1)} - \hat{y}^{(\gamma-1)}) + \dots + c_1(y_d - y). \quad (3.11)$$

Using (3.11) and replacing the unknown parameter vector \mathcal{P} in (3.6) by its estimate $\hat{\mathcal{P}}$, the control input in (3.6) is obtained as

$$u = \frac{1}{\hat{\mathcal{P}}^T \mathcal{G}(\mathbf{x})} (-\hat{\mathcal{P}}^T \mathcal{F}(\mathbf{x}) + \hat{v}) \quad (3.12)$$

A projection technique [48] is used to keep the parameter estimate $\hat{\boldsymbol{\theta}}$ in a compact region \mathcal{S}_θ .

3.2.3 Closed loop error dynamics at the first level

Now, defining the multilinear parameter error vector as $\tilde{\mathcal{P}} = \hat{\mathcal{P}} - \mathcal{P}$, (3.5) can be obtained as

$$\begin{aligned} \dot{\tau}_\gamma &= \hat{\mathcal{P}}^T \mathcal{F}(\mathbf{x}) + \hat{\mathcal{P}}^T \mathcal{G}(\mathbf{x})u + \tilde{\mathcal{P}}^T \mathcal{F}(\mathbf{x}) + \tilde{\mathcal{P}}^T \mathcal{G}(\mathbf{x})u \\ \text{or, } \dot{\tau}_\gamma &= \hat{\mathcal{P}}^T \mathcal{F}(\mathbf{x}) + \hat{\mathcal{P}}^T \mathcal{G}(\mathbf{x})u + \tilde{\mathcal{P}}^T \boldsymbol{\Omega}_1(\mathbf{x}, u) \end{aligned} \quad (3.13)$$

where $\boldsymbol{\Omega}_1(\mathbf{x}, u)$ is a known regressor matrix. Substituting u from (3.12) in (3.13) yields

$$\dot{\tau}_\gamma = \hat{v} + \tilde{\mathcal{P}}^T \boldsymbol{\Omega}_1(\mathbf{x}, u). \quad (3.14)$$

Further,

$$\hat{v} = v + \tilde{\mathcal{P}}^T \boldsymbol{\Omega}_2(\mathbf{x}, u) \quad (3.15)$$

where $\boldsymbol{\Omega}_2(\mathbf{x}, u)$ is a known regressor matrix. Using (3.15) in (3.14) yields

$$\dot{\tau}_\gamma = v + \tilde{\mathcal{P}}^T (\boldsymbol{\Omega}_1(\mathbf{x}, u) + \boldsymbol{\Omega}_2(\mathbf{x}, u)). \quad (3.16)$$

Considering the multilinear parameter vector \mathcal{P} having dimension $\aleph \times 1$, another regressor matrix $\boldsymbol{\Omega} \in \mathbb{R}^{\aleph \times \gamma}$ is introduced as

$$\boldsymbol{\Omega} = [\boldsymbol{\Omega}_1 + \boldsymbol{\Omega}_2]. \quad (3.17)$$

Using (3.17), (3.16) can be written as

$$\dot{\tau}_\gamma = v + \tilde{\mathcal{P}}^T \boldsymbol{\Omega}(\mathbf{x}, u). \quad (3.18)$$

Further, the control error term is defined as

$$\mathbf{e}_i = \tau_i - y_d^{(i-1)}, i = 1, \dots, \gamma. \quad (3.19)$$

Rewriting (3.19) in vector form as

$$\mathbf{e} = \boldsymbol{\tau} - \mathbf{r} \quad (3.20)$$

where $\mathbf{r} = [y_d, \dot{y}_d, \dots, y_d^{(\gamma-1)}]^T$, $\boldsymbol{\tau} = [\tau_1, \tau_2, \dots, \tau_\gamma]^T$, $\mathbf{e} = [e_1, e_2, \dots, e_\gamma]^T$ and $y_d^{(0)} = y_d$. Taking first time derivative of (3.20) yields

$$\begin{aligned} \dot{e}_1 &= e_2 \\ \dot{e}_2 &= e_3 \\ &\dots \\ \dot{e}_{\gamma-1} &= e_\gamma \\ \dot{e}_\gamma &= \dot{\tau}_\gamma - y_d^{(\gamma)} \end{aligned} \quad (3.21)$$

Using (3.18) and (3.7), (3.21) can be written as

$$\dot{\mathbf{e}} = \mathbf{A}_m \mathbf{e} + \tilde{\mathcal{P}}^T \boldsymbol{\Omega}(\mathbf{x}, u) \quad (3.22)$$

where $\mathbf{A}_m = \begin{bmatrix} 0 & 1 & 0 & \dots & 0 \\ 0 & 0 & 1 & \dots & 0 \\ \dots & \dots & \dots & \dots & \dots \\ \dots & \dots & \dots & \dots & \dots \\ 0 & \dots & \dots & \dots & 1 \\ c_1 & c_2 & \dots & \dots & c_\gamma \end{bmatrix} \in \mathbb{R}^{\gamma \times \gamma}$ is a Hurwitz matrix. The complete closed loop error

dynamics can be found from (3.20), (3.22) and (3.3) as

$$\begin{aligned} \boldsymbol{\tau} &= \mathbf{e} + \mathbf{r} \\ \dot{\mathbf{e}} &= \mathbf{A}_m \mathbf{e} + \tilde{\mathcal{P}}^T \boldsymbol{\Omega}(\mathbf{x}, u) \\ \dot{\boldsymbol{\xi}} &= \boldsymbol{\varphi}(\boldsymbol{\tau}, \boldsymbol{\xi}). \end{aligned} \quad (3.23)$$

3.2.4 Closed loop stability at the first level

To assess the closed loop stability of the nonlinear system (3.1) with relative degree γ and having the linearized form as (3.3), following assumptions are made:

- (i) The zero dynamics $\varphi(0, \boldsymbol{\xi})$ is asymptotically stable and internal dynamics $\varphi(\boldsymbol{\tau}, \boldsymbol{\xi})$ is globally Lipschitz in $\boldsymbol{\tau}$ and $\boldsymbol{\xi}$. An upper bound b_φ is considered such that

$$\|\varphi(\boldsymbol{\tau}, \boldsymbol{\xi}) - \varphi(0, \boldsymbol{\xi})\| \leq b_\varphi \|\boldsymbol{\tau}\| \quad (3.24)$$

- (ii) The desired trajectory y_d to be tracked is considered bounded with bounded derivatives $\dot{y}_d, \dots, y_d^{(\gamma-1)}$. Defining b_d as an upper bound on y_d and its higher derivatives yields

$$\|\boldsymbol{\tau}\| \leq \|\mathbf{e}\| + b_d \quad (3.25)$$

- (iii) Since \mathbf{x} is a local diffeomorphism of $\boldsymbol{\tau}$ and $\boldsymbol{\xi}$,

$$\|\mathbf{x}\| \leq b_0(\|\boldsymbol{\tau}\| + \|\boldsymbol{\xi}\|), \quad b_0 > 0 \quad (3.26)$$

- (iv) For every control input u , the regressor matrix $\boldsymbol{\Omega}(\mathbf{x}, u)$ is bounded for bounded \mathbf{x} , such that for a small positive number b_Ω ,

$$\|\boldsymbol{\Omega}(\mathbf{x}, u)\| \leq b_\Omega \|\mathbf{x}\| \quad (3.27)$$

Using (3.26) and (3.27) gives

$$\|2\mathbf{P}\boldsymbol{\Omega}(\mathbf{x}, u)\| \leq b_1(\|\boldsymbol{\tau}\| + \|\boldsymbol{\xi}\|), \quad b_1 > 0 \quad (3.28)$$

where $b_1 = 2\|\mathbf{P}\|b_0b_\Omega$ and \mathbf{P} is the solution of Lyapunov equation $\mathbf{A}_m^T\mathbf{P} + \mathbf{P}\mathbf{A}_m = -\mathbf{I}$. Since the zero dynamics is assumed to be asymptotically stable, there exists a Lyapunov function $V_\varphi(\boldsymbol{\xi})$ such that

$$\begin{aligned} c_1\|\boldsymbol{\xi}\|^2 &\leq V_\varphi(\boldsymbol{\xi}) \leq c_2\|\boldsymbol{\xi}\|^2 \\ \frac{\partial V_\varphi}{\partial \boldsymbol{\xi}}\varphi(0, \boldsymbol{\xi}) &\leq -c_3\|\boldsymbol{\xi}\|^2 \\ \left\| \frac{\partial V_\varphi(\boldsymbol{\xi})}{\partial \boldsymbol{\xi}} \right\| &\leq c_4\|\boldsymbol{\xi}\| \end{aligned} \quad (3.29)$$

where c_1, c_2, c_3, c_4 are positive constants. A suitable Lyapunov function for the closed loop error dynamics (3.23) is chosen as

$$V(\mathbf{e}, \boldsymbol{\xi}) = \mathbf{e}^T \mathbf{P} \mathbf{e} + \mu V_\varphi(\boldsymbol{\xi}) \quad (3.30)$$

where \mathbf{P} is the solution of Lyapunov equation $\mathbf{A}_m^T \mathbf{P} + \mathbf{P} \mathbf{A}_m = -\mathbf{I}$ and μ is a small positive number.

Taking first time derivative of (3.30) yields

$$\dot{V}(\mathbf{e}, \boldsymbol{\xi}) = -\mathbf{e}^T \mathbf{e} + 2\mathbf{e}^T \mathbf{P} \tilde{\mathcal{P}}^T \Omega(\mathbf{x}, u) + \mu \frac{\partial V_\varphi}{\partial \boldsymbol{\xi}} \varphi(0, \boldsymbol{\xi}) + \left(\mu \frac{\partial V_\varphi}{\partial \boldsymbol{\xi}} \varphi(\boldsymbol{\tau}, \boldsymbol{\xi}) - \mu \frac{\partial V_\varphi}{\partial \boldsymbol{\xi}} \varphi(0, \boldsymbol{\xi}) \right) \quad (3.31)$$

Rewriting (3.31) yields

$$\begin{aligned} \dot{V}(\mathbf{e}, \boldsymbol{\xi}) &\leq -\|\mathbf{e}\|^2 + \|\mathbf{e}^T\| \|\tilde{\mathcal{P}}\| \|2\mathbf{P}\Omega(\mathbf{x}, u)\| + \mu \left\| \frac{\partial V_\varphi}{\partial \boldsymbol{\xi}} \varphi(0, \boldsymbol{\xi}) \right\| \\ &\quad + \mu \left\| \frac{\partial V_\varphi}{\partial \boldsymbol{\xi}} \right\| (\|\varphi(\boldsymbol{\tau}, \boldsymbol{\xi}) - \varphi(0, \boldsymbol{\xi})\|) \end{aligned} \quad (3.32)$$

Using (3.24) in (3.32) yields

$$\dot{V}(\mathbf{e}, \boldsymbol{\xi}) \leq -\|\mathbf{e}\|^2 + \|\mathbf{e}^T\| \|\tilde{\mathcal{P}}\| \|2\mathbf{P}\Omega(\mathbf{x}, u)\| + \mu \left\| \frac{\partial V_\varphi}{\partial \boldsymbol{\xi}} \varphi(0, \boldsymbol{\xi}) \right\| + \mu \left\| \frac{\partial V_\varphi}{\partial \boldsymbol{\xi}} b_\varphi \right\| \|\boldsymbol{\tau}\| \quad (3.33)$$

Again, using (3.29) in (3.33) gives

$$\dot{V}(\mathbf{e}, \boldsymbol{\xi}) \leq -\|\mathbf{e}\|^2 + \|\mathbf{e}^T\| \|\tilde{\mathcal{P}}\| \|2\mathbf{P}\Omega(\mathbf{x}, u)\| - \mu c_3 \|\boldsymbol{\xi}\|^2 + \mu c_4 \|\boldsymbol{\xi}\| b_\varphi \|\boldsymbol{\tau}\| \quad (3.34)$$

Using (3.28) in (3.34) yields

$$\dot{V}(\mathbf{e}, \boldsymbol{\xi}) \leq -\|\mathbf{e}\|^2 + b_1 \|\mathbf{e}\| (\|\boldsymbol{\tau}\| + \|\boldsymbol{\xi}\|) \|\tilde{\mathcal{P}}\| - \mu c_3 \|\boldsymbol{\xi}\|^2 + \mu c_4 \|\boldsymbol{\xi}\| b_\varphi \|\boldsymbol{\tau}\| \quad (3.35)$$

Finally, using (3.25) in (3.35) gives

$$\dot{V}(\mathbf{e}, \boldsymbol{\xi}) \leq -\|\mathbf{e}\|^2 + b_1 \|\mathbf{e}\| (\|\mathbf{e}\| + \|\boldsymbol{\xi}\| + b_d) \|\tilde{\mathcal{P}}\| - \mu c_3 \|\boldsymbol{\xi}\|^2 + \mu c_4 b_\varphi \|\boldsymbol{\xi}\| (\|\mathbf{e}\| + b_d) \quad (3.36)$$

Furthermore, (3.36) can be rearranged as

$$\begin{aligned} \dot{V}(\mathbf{e}, \boldsymbol{\xi}) &\leq -\left(\frac{1}{2} \|\mathbf{e}\| - b_1 b_d \|\tilde{\mathcal{P}}\| \right)^2 - \left(\frac{1}{2} \sqrt{\mu c_3} \|\boldsymbol{\xi}\| - \sqrt{\frac{\mu}{c_3}} c_4 b_\varphi b_d \right)^2 - \frac{3}{4} \|\mathbf{e}\|^2 + (b_1 b_d \|\tilde{\mathcal{P}}\|)^2 \\ &\quad - \frac{3}{4} \mu c_3 \|\boldsymbol{\xi}\|^2 + \frac{\mu}{c_3} (c_4 b_\varphi b_d)^2 + b_1 \|\tilde{\mathcal{P}}\| \|\mathbf{e}\|^2 + (b_1 \|\tilde{\mathcal{P}}\| + \mu c_4 b_\varphi) \|\mathbf{e}\| \|\boldsymbol{\xi}\| \end{aligned} \quad (3.37)$$

$$\text{or, } \dot{V}(\mathbf{e}, \boldsymbol{\xi}) \leq - \begin{bmatrix} \|\mathbf{e}\| \\ \|\boldsymbol{\xi}\| \end{bmatrix}^T \mathbf{Q} \begin{bmatrix} \|\mathbf{e}\| \\ \|\boldsymbol{\xi}\| \end{bmatrix} + (b_1 b_d \|\tilde{\mathcal{P}}\|)^2 + \frac{\mu}{c_3} (c_4 b_\varphi b_d)^2 \quad (3.38)$$

where

$$\mathbf{Q} = \begin{bmatrix} \frac{3}{4} - b_1 \|\tilde{\mathcal{P}}\| & -\frac{1}{2}(b_1 \|\tilde{\mathcal{P}}\| + \mu c_4 b_\varphi) \\ -\frac{1}{2}(b_1 \|\tilde{\mathcal{P}}\| + \mu c_4 b_\varphi) & \frac{3}{4} \mu c_3 \end{bmatrix} \quad (3.39)$$

The right hand side in (3.38) will be negative, if \mathbf{Q} is a positive definite matrix and the magnitude of the first term is greater than the sum of the other two terms. Since $\|\tilde{\mathcal{P}}\| \rightarrow 0$ as $t \rightarrow \infty$, the second term in (3.38) will go to zero asymptotically. The matrix \mathbf{Q} is positive definite for $\|\tilde{\mathcal{P}}\| \leq \frac{3}{4b_1}$ and $\mu \leq \frac{9c_3}{4(c_4 b_\varphi)^2}$. Therefore, a small positive value for $\mu < \frac{c_3}{(c_4 b_\varphi b_d)^2} \begin{bmatrix} \|\mathbf{e}\| \\ \|\boldsymbol{\xi}\| \end{bmatrix}^T \mathbf{Q} \begin{bmatrix} \|\mathbf{e}\| \\ \|\boldsymbol{\xi}\| \end{bmatrix}$ in (3.38) will ensure that the magnitude of the first term in (3.38) is greater than the sum of the other two terms. Consequently, $\dot{V} < 0$ whenever $\|\mathbf{e}\|$ and $\|\boldsymbol{\xi}\|$ become large, implies that $\|\mathbf{e}\| \in \mathcal{L}_\infty$ and $\|\boldsymbol{\xi}\| \in \mathcal{L}_\infty$.

3.3 Multiple Model based Two Level Adaptation (MMTLA) method

So far, the adaptive control of a class of linearly parameterized nonlinear system using single estimation model has been discussed. In this Section, the use of multiple estimation models and the concept of two level adaptation will be discussed at length. In case of multiple models, the same estimator structure (3.9) is used for all the models but with N different parameter vector estimates $\hat{\boldsymbol{\theta}}_j$, $j = 1, \dots, N$, placed at different starting points inside the compact space \mathcal{S}_θ . Dynamics of N estimation models are given as

$$\dot{\hat{\mathbf{x}}}_j = \mathbf{A}(\hat{\mathbf{x}}_j - \mathbf{x}) + \boldsymbol{\omega}^T(\mathbf{x}, u) \hat{\boldsymbol{\theta}}_j, \quad j = 1, \dots, N \quad (3.40)$$

where $\hat{\mathbf{x}}_j$ denotes the state vector of the j -th estimation model. The state estimation error and the parameter estimation error for the j -th estimation model are defined as $\mathbf{e}_{I_j} = \hat{\mathbf{x}}_j - \mathbf{x}$ and $\tilde{\boldsymbol{\theta}}_j = \hat{\boldsymbol{\theta}}_j - \boldsymbol{\theta}$ respectively. Now, following (3.10), the identifier error dynamics for N estimation models can be found as,

$$\dot{\mathbf{e}}_{I_j} = \mathbf{A} \mathbf{e}_{I_j} + \boldsymbol{\omega}^T(\mathbf{x}, u) \tilde{\boldsymbol{\theta}}_j, \quad j = 1, \dots, N. \quad (3.41)$$

Similarly, the adaptive laws for the j -th model parameter vector $\hat{\boldsymbol{\theta}}_j$ can be obtained as

$$\dot{\hat{\boldsymbol{\theta}}}_j = -\boldsymbol{\omega}(\mathbf{x}, u)\mathbf{P}\mathbf{e}_{I_j}, \quad j = 1, \dots, N. \quad (3.42)$$

The system parameter vector $\boldsymbol{\theta}$ and estimation model parameter vector $\hat{\boldsymbol{\theta}}_j$ are assumed to belong to a compact space \mathcal{S}_θ .

3.3.1 First level adaptation

In this section, selection and arrangement of multiple estimation models on the compact parameter space \mathcal{S}_θ are discussed. Here, the initially selected N identification models of the system are referred to as the first level models. At the first level, the parameters $\hat{\boldsymbol{\theta}}_j$ are adjusted using the tuning laws as derived in the previous sections and rewritten in (3.42) for N number of models.

Selection of models at the first level: The locations of initial values of parameter estimates $\hat{\boldsymbol{\theta}}_j(t_0)$ on parameter space \mathcal{S}_θ are selected such that $\hat{\boldsymbol{\theta}}_j(t_0)$ covers the full parameter space.

The parameter space \mathcal{S}_θ is a compact set implying that every element of the parameter vector $\boldsymbol{\theta}$ has a known upper and a lower bound. The parameter vector $\boldsymbol{\theta}$ is a p -dimensional vector given as $\boldsymbol{\theta} = [\theta_1, \theta_2, \dots, \theta_p]^T$. The above assumption implies $\theta_1 \in [\theta_1^{min}, \theta_1^{max}], \dots, \theta_p \in [\theta_p^{min}, \theta_p^{max}]$.

If $[\nu_1, \nu_2, \dots, \nu_p] \in \mathbb{Z}$ are the number of elements between minimum and maximum values of each parameter $[\theta_1, \dots, \theta_l, \dots, \theta_p]$ (including θ_l^{min} and θ_l^{max} , $l = 1, \dots, p$), the total number of models is given by

$$N = \nu_1 \times \nu_2 \dots \times \nu_p. \quad (3.43)$$

The space of the models \mathcal{Z} based on the arrangement given above will be the cartesian product of these sets, given as

$$\mathcal{Z} = [\theta_1^{min}, \dots, \theta_1^{max}] \times [\theta_2^{min}, \dots, \theta_2^{max}] \times \dots \times [\theta_p^{min}, \dots, \theta_p^{max}]. \quad (3.44)$$

For example, selecting two elements between maximum and minimum provides the number of model as $N = 2^p$.

3.3.2 Visualization of the parameter space

In this section, an example of a system with 3 unknown parameters is considered to have a visualization of the parameter space and adaptation at level one and level two. The combination

of models at the first level and advancement of the second level model to reach the actual system parameter is visible in Fig. 3.1, which shows the two level adaptation for a system with three unknown parameters. For number of parameters $\mathbf{p} = 3$, it has a 3-D co-ordinate system, one for each of

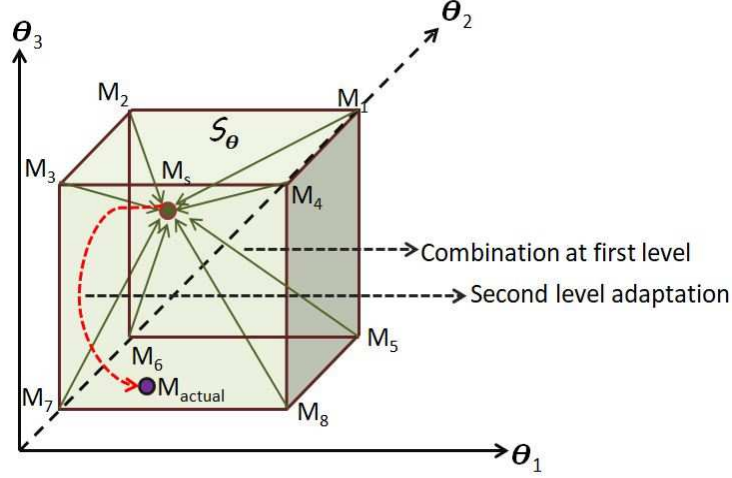


Figure 3.1: Two level adaptation (TLA)

the parameters θ_1 , θ_2 and θ_3 . Here M_1, \dots, M_8 are the first level adaptive models, M_{actual} and M_s are the actual system model and the second level model respectively. Further, selecting only the boundary values of the parameters for first level estimation models, meaning 2 models for each unknown parameter, the number of estimation models is obtained as $N = 2^{\mathbf{p}} = 8$. Therefore, a cube having vertices $[M_1, \dots, M_8]$ has formed a parameter space S_θ as can be observed in the Fig. 3.1. Here, the models M_1, \dots, M_8 are also adaptive in nature, but Fig. 3.1 shows only the adaptation at the second level at any particular instant.

3.3.3 Second level adaptation

In this section the concept of second level adaptation, introduced for linear systems in [20], is adopted for a class of nonlinear uncertain systems. The parameter estimates at first level $\hat{\theta}_j(t)$ are combined using suitable adaptive weights to get the parameter estimate at second level.

Theorem 3.2 [20]: If the system parameter vector θ lies in the convex hull $\mathcal{K}(t_0)$ of $\hat{\theta}_j(t_0)$, then θ lies in the convex hull $\mathcal{K}(t)$ of $\hat{\theta}_j(t)$ for all $t \geq t_0$.

Proof: The proof of this theorem is available in *Theorem 1* of [20].

Since the bounds on the parameters are assumed to be known, the initial values of $\hat{\theta}_j(t_0)$ at time t_0 can be suitably chosen such that the system parameter vector θ lies in their convex hull. Thus

it will always stay in the convex hull of $\hat{\boldsymbol{\theta}}_j(t)$ for all t . However, the convex parameters w_j are not known.

Adaptive law for updating the weights $w_j(t)$: The objective is to asymptotically find the adaptive weights $w_j(t)$ such that it satisfies Theorem 3.2 given as

$$\boldsymbol{\theta} = \sum_{j=1}^N w_j(t) \hat{\boldsymbol{\theta}}_j(t). \quad (3.45)$$

The tuning laws for the adaptive weights $w_j(t)$ can be found using the following Theorem.

Theorem 3.3 : The convex combination of first level adaptive models with suitably chosen adaptive weights $w_j(t)$ ensures that the estimation error dynamics at second level is Lyapunov stable.

Proof : The adaptive weights $w_j(t)$ satisfy the following conditions:

- The contribution from a model can never be negative, i.e. $w_j(t) \geq 0$.
- Sum of contributions from all the models must be unity i.e., $\sum_{j=1}^N w_j(t) = 1$.

Now, subtracting $\boldsymbol{\theta}$ from both sides of (3.45) and using properties of adaptive weights $w_j(t) \geq 0$ and $\sum_{j=1}^N w_j(t) = 1$, it can be shown that

$$\sum_{j=1}^N w_j(t) \tilde{\boldsymbol{\theta}}_j(t) = 0. \quad (3.46)$$

The adaptive weights at the second level depend on the estimation error. Therefore, considering the identification error (3.41) and using the property of linearity as well as the fact that the initial state errors can be chosen to be zero, it can be shown that

$$\sum_{j=1}^N w_j(t) \mathbf{e}_{I_j}(t) = 0. \quad (3.47)$$

Thus,

$$[e_{I_1}(t), e_{I_2}(t), \dots, e_{I_N}(t)] \mathbf{W} = \mathbf{E}(t)_{n \times N} \mathbf{W}_{N \times 1} = \mathbf{0}_{n \times 1} \quad (3.48)$$

where $\mathbf{W}(t) = [w_1(t), w_2(t), \dots, w_N(t)]^T$ and $\mathbf{E}(t) = [\mathbf{e}_{I_1}(t), \mathbf{e}_{I_2}(t), \dots, \mathbf{e}_{I_N}(t)]$. The error \mathbf{e}_{I_j} is the vector $\mathbf{e}_{I_j} = [e_{1j}, e_{2j}, \dots, e_{nj}]^T$, for n number of states of the actual system. Therefore, $\mathbf{E}(t) =$

$$\begin{bmatrix} e_{11} & \cdot & \cdot & e_{1N} \\ \cdot & \cdot & \cdot & \cdot \\ e_{n1} & \cdot & \cdot & e_{nN} \end{bmatrix}. \text{ Alternatively, } \mathbf{W} \text{ can be written as } \mathbf{W} = [\mathbf{W}(t)^T, w_N(t)]^T, \text{ where}$$

$\mathbf{W}(t) = [w_1(t), w_2(t), \dots, w_{N-1}(t)]^T$. By using the set of differential equations derived from (3.48), $\mathbf{W}(t)$ can be computed. As $\sum_{j=1}^N w_j(t) = 1$, $w_N(t) = 1 - \sum_{j=1}^{N-1} w_j(t)$. Rewriting (3.48) as

$$\begin{aligned} \mathbf{e}_{I_1} w_1 + \mathbf{e}_{I_2} w_2 \dots + \mathbf{e}_{I_N} w_N &= 0 \\ \text{or, } \mathbf{e}_{I_1} w_1 + \mathbf{e}_{I_2} w_2 \dots + \mathbf{e}_{I_{N-1}} w_{N-1} &= -\mathbf{e}_{I_N} w_N \end{aligned} \quad (3.49)$$

the following can be obtained:

$$\mathbf{H}(t)\mathbf{W} = \mathbf{k}(t) \quad (3.50)$$

where

$$\begin{aligned} \mathbf{H}(t) &= [\mathbf{e}_{I_1}(t), \mathbf{e}_{I_2}(t), \dots, \mathbf{e}_{I_{N-1}}(t)] \\ \mathbf{k}(t) &= -\mathbf{e}_{I_N} w_N \end{aligned} \quad (3.51)$$

To estimate the values of \mathbf{W} , an estimation model is built as

$$\mathbf{H}(t)\hat{\mathbf{W}}(t) = \hat{\mathbf{k}}(t) \quad (3.52)$$

Subtracting (3.50) from (3.52) yields

$$\mathbf{H}(t)\tilde{\mathbf{W}}(t) = \tilde{\mathbf{k}}(t) \quad (3.53)$$

where $\tilde{\mathbf{W}} = \hat{\mathbf{W}} - \mathbf{W}$ and $\tilde{\mathbf{k}} = \hat{\mathbf{k}} - \mathbf{k}$. Taking first time derivative of (3.53) gives

$$\mathbf{H}(t)\dot{\tilde{\mathbf{W}}}(t) = \dot{\tilde{\mathbf{k}}}(t). \quad (3.54)$$

To design a suitable adaptive law for the weights at second level, let us choose a Lyapunov function candidate as

$$V(t) = \frac{\tilde{\mathbf{W}}^T \tilde{\mathbf{W}}}{2} + \frac{\tilde{\mathbf{k}}^T \tilde{\mathbf{k}}}{2}. \quad (3.55)$$

Taking first time derivative of (3.55) and using (3.53) yields

$$\dot{V}(t) = \tilde{\mathbf{W}}^T \dot{\tilde{\mathbf{W}}} + \tilde{\mathbf{k}}^T \mathbf{H}(t) \dot{\tilde{\mathbf{W}}} \quad (3.56)$$

Now, using adaptive law for weights as

$$\begin{aligned}\dot{\tilde{\mathbf{W}}}(t) &= -\mathbf{H}^T(t)\tilde{\mathbf{k}}(t) \\ &= -\mathbf{H}^T(t)\mathbf{H}(t)\hat{\tilde{\mathbf{W}}}(t) + \mathbf{H}^T(t)\mathbf{k}(t).\end{aligned}\quad (3.57)$$

Using (3.57) in (3.56) yields

$$\dot{V}(t) = -\tilde{\mathbf{k}}^T(t)\tilde{\mathbf{k}}(t) - (\mathbf{H}^T(t)\tilde{\mathbf{k}}(t))^T(\mathbf{H}^T(t)\tilde{\mathbf{k}}(t)).\quad (3.58)$$

From (3.58), it is observed that $\dot{V}(t)$ is negative semidefinite and hence proves that $V(t)$ in (3.55) is a suitable Lyapunov function. This implies that the error dynamics at the second level is Lyapunov stable with the adaptive law (3.57). \square

Finally, using the combination of first level estimates of system parameter vector $\hat{\boldsymbol{\theta}}_j$ with adaptive weights $W(t)$ at every instant, the virtual estimate of system parameter values $\boldsymbol{\theta}_s(t)$ can be obtained as

$$\boldsymbol{\theta}_s(t) = \sum_{j=1}^N w_j(t)\hat{\boldsymbol{\theta}}_j(t)\quad (3.59)$$

and can be used to find the new control input as

$$u_s = \frac{1}{q(\mathbf{x}, \boldsymbol{\theta}_s)}(-p(\mathbf{x}, \boldsymbol{\theta}_s) + \hat{v})\quad (3.60)$$

where $p(\mathbf{x}, \boldsymbol{\theta}_s), q(\mathbf{x}, \boldsymbol{\theta}_s) : \mathbb{R}^n \rightarrow \mathbb{R}^n$ are sufficiently smooth vector fields. In (3.60) above, $q(\mathbf{x}, \boldsymbol{\theta}_s)$ is assumed to be bounded away from zero, because of the fact that $\boldsymbol{\theta}_s$ always resides inside the convex hull of $\hat{\boldsymbol{\theta}}_j$ [6, 48]. The parameters $\hat{\boldsymbol{\theta}}_j$ are kept in a certain range [48], such that, at every point inside their convex hull, $q(\mathbf{x}, \boldsymbol{\theta}_s)$ is bounded away from zero.

In this work, projection based adaptive laws [43,44] are used to ensure the boundedness of estimated parameters in the already defined compact region \mathcal{S}_θ . Applying projection, the system parameter estimate in (3.59) can be rewritten as

$$\boldsymbol{\theta}_s(t) = Proj_{\boldsymbol{\theta}_s(t) \in \mathcal{S}_\theta} \left\{ \sum_{j=1}^N w_j(t)\boldsymbol{\theta}_j(t) \right\}\quad (3.61)$$

In adaptive control problems, the convergence of estimated parameters depends on the richness of its reference input with respect to the frequency content [7, 44]. For that purpose, persistence of excitation (PE) of input signal is used in simulations to ensure the convergence of estimated parameters to their

actual values. The basic control block diagram with two level adaptation is shown in Figure 3.2.

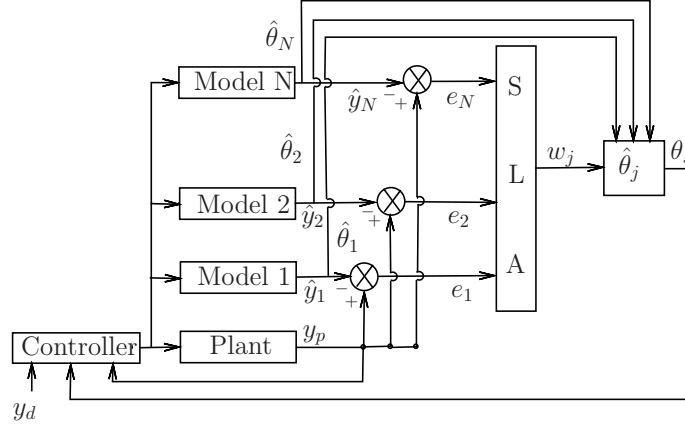


Figure 3.2: Control block diagram with second level adaptation (SLA)

3.3.4 Overall stability assessment

This subsection is dedicated to provide the overall system stability with two level adaptation as well as convergence of control and parameter errors. From the discussions in the previous section and using (3.23), the control error equation at the second level can be found as

$$\dot{\mathbf{e}}_s = \mathbf{A}_m \mathbf{e}_s + \boldsymbol{\Omega}^T(\mathbf{x}, u_s) \tilde{\mathcal{P}}_s \quad (3.62)$$

where $u_s = \frac{1}{\hat{\mathcal{P}}_s^T \mathcal{G}(x)} (-\hat{\mathcal{P}}_s^T \mathcal{F}(x) + \hat{v})$, \mathbf{e}_s is the control error at the second level and $\tilde{\mathcal{P}}_s = \mathcal{P}_s - \mathcal{P}$, with \mathcal{P}_s being the multilinear parameter estimate at the second level. Similar to (3.23), the complete closed loop error dynamics can be written as

$$\begin{aligned} \boldsymbol{\tau} &= \mathbf{e}_s + \mathbf{r} \\ \dot{\mathbf{e}}_s &= \mathbf{A}_m \mathbf{e}_s + \boldsymbol{\Omega}^T(\mathbf{x}, u_s) \tilde{\mathcal{P}}_s. \\ \dot{\boldsymbol{\xi}} &= \boldsymbol{\varphi}(\boldsymbol{\tau}, \boldsymbol{\xi}) \end{aligned} \quad (3.63)$$

A suitable Lyapunov function for closed loop error dynamics (3.63) is chosen as

$$V(\mathbf{e}_s, \tilde{\boldsymbol{\theta}}_s, \boldsymbol{\xi}) = \mathbf{e}_s^T \mathbf{P} \mathbf{e}_s + \tilde{\boldsymbol{\theta}}_s^T \tilde{\boldsymbol{\theta}}_s + \mu V_\varphi(\boldsymbol{\xi}) \quad (3.64)$$

where \mathbf{P} is the solution of Lyapunov equation $\mathbf{A}_m^T \mathbf{P} + \mathbf{P} \mathbf{A}_m = -\mathbf{I}$. First time differentiation of (3.64) yields

$$\begin{aligned} \dot{V}(\mathbf{e}_s, \tilde{\boldsymbol{\theta}}_s, \boldsymbol{\xi}) &= -\mathbf{e}_s^T \mathbf{e}_s + 2\mathbf{e}_s^T \mathbf{P} \boldsymbol{\Omega}^T(\mathbf{x}, u_s) \tilde{\mathcal{P}}_s + 2\tilde{\boldsymbol{\theta}}_s^T \dot{\tilde{\boldsymbol{\theta}}}_s + \mu \frac{\partial V_\varphi}{\partial \boldsymbol{\xi}} \varphi(0, \boldsymbol{\xi}) \\ &+ \left(\mu \frac{\partial V_\varphi}{\partial \boldsymbol{\xi}} \varphi(\tau, \boldsymbol{\xi}) - \mu \frac{\partial V_\varphi}{\partial \boldsymbol{\xi}} \varphi(0, \boldsymbol{\xi}) \right) \end{aligned} \quad (3.65)$$

Now, taking first time differentiation of (3.59) gives

$$\dot{\boldsymbol{\theta}}_s(t) = \sum_{j=1}^N w_j \dot{\boldsymbol{\theta}}_j(t) + \sum_{j=1}^N \dot{w}_j(t) \hat{\boldsymbol{\theta}}_j \quad (3.66)$$

Since $\tilde{\boldsymbol{\theta}}_s = \boldsymbol{\theta}_s - \boldsymbol{\theta}$, its first time differentiation provides,

$$\dot{\tilde{\boldsymbol{\theta}}}_s(t) = \dot{\boldsymbol{\theta}}_s(t) \quad (3.67)$$

Therefore, using (3.67) in (3.66) gives,

$$\dot{\boldsymbol{\theta}}_s(t) = \dot{\tilde{\boldsymbol{\theta}}}_s(t) = \sum_{j=1}^N w_j \dot{\boldsymbol{\theta}}_j(t) + \sum_{j=1}^N \dot{w}_j(t) \hat{\boldsymbol{\theta}}_j \quad (3.68)$$

Similarly, using (3.68) in (3.65) gives

$$\begin{aligned} \dot{V}(\mathbf{e}_s, \tilde{\boldsymbol{\theta}}_s, \boldsymbol{\xi}) &= -\mathbf{e}_s^T \mathbf{e}_s + 2\mathbf{e}_s^T \mathbf{P} \boldsymbol{\Omega}^T(\mathbf{x}, u_s) \tilde{\mathcal{P}}_s + 2\tilde{\boldsymbol{\theta}}_s^T \left(\sum_{j=1}^N w_j \dot{\boldsymbol{\theta}}_j + \sum_{j=1}^N \dot{w}_j \hat{\boldsymbol{\theta}}_j \right) \\ &+ \mu \frac{\partial V_\varphi}{\partial \boldsymbol{\xi}} \varphi(0, \boldsymbol{\xi}) + \left(\mu \frac{\partial V_\varphi}{\partial \boldsymbol{\xi}} \varphi(\tau, \boldsymbol{\xi}) - \mu \frac{\partial V_\varphi}{\partial \boldsymbol{\xi}} \varphi(0, \boldsymbol{\xi}) \right) \end{aligned} \quad (3.69)$$

Extending the adaptive law of the single model for N number of models, the following can be written,

$$\dot{\hat{\boldsymbol{\theta}}}_j = -\boldsymbol{\omega}(\mathbf{x}, u_s) \mathbf{P} \mathbf{e}_j, \quad j = 1, \dots, N \quad (3.70)$$

Taking first time derivative of $\sum_{j=1}^N w_j(t) = 1$ yields $\sum_{j=1}^N \dot{w}_j(t) = 0$, and hence $\dot{w}_N = -(\dot{w}_1 + \dots + \dot{w}_{N-1})$, giving

$$\begin{aligned} \sum_{j=1}^N \dot{w}_j \hat{\boldsymbol{\theta}}_j &= \dot{w}_1 \hat{\boldsymbol{\theta}}_1 + \dots + \dot{w}_{N-1} \hat{\boldsymbol{\theta}}_{N-1} - (\dot{w}_1 + \dots + \dot{w}_{N-1}) \hat{\boldsymbol{\theta}}_N \\ &= \dot{w}_1 (\hat{\boldsymbol{\theta}}_1 - \hat{\boldsymbol{\theta}}_N) + \dots + \dot{w}_{N-1} (\hat{\boldsymbol{\theta}}_{N-1} - \hat{\boldsymbol{\theta}}_N) \\ &= \hat{\mathbf{W}}^T \mathbf{Z}(t) \end{aligned} \quad (3.71)$$

where $\hat{\mathbf{W}}$ is the estimate of \mathbf{W} as in (3.52) and $\mathbf{Z}(t) = [(\hat{\boldsymbol{\theta}}_1 - \hat{\boldsymbol{\theta}}_N), \dots, (\hat{\boldsymbol{\theta}}_{N-1} - \hat{\boldsymbol{\theta}}_N)]^T$. Using (3.70)

and (3.71), (3.69) can be written as

$$\begin{aligned} \dot{V}(\mathbf{e}_s, \tilde{\boldsymbol{\theta}}_s, \boldsymbol{\xi}) &= -\mathbf{e}_s^T \mathbf{e}_s + 2\mathbf{e}_s^T \mathbf{P} \boldsymbol{\Omega}^T(\mathbf{x}, u_s) \tilde{\mathcal{P}}_s + 2\tilde{\boldsymbol{\theta}}_s^T \left(-\sum_{j=1}^N w_j \boldsymbol{\omega}(\mathbf{x}, u_s) \mathbf{P} \mathbf{e}_j + \dot{\mathbf{W}} \mathbf{Z}(t) \right) \\ &\quad + \mu \frac{\partial V_\varphi}{\partial \boldsymbol{\xi}} \varphi(0, \boldsymbol{\xi}) + \left(\mu \frac{\partial V_\varphi}{\partial \boldsymbol{\xi}} \varphi(\boldsymbol{\tau}, \boldsymbol{\xi}) - \mu \frac{\partial V_\varphi}{\partial \boldsymbol{\xi}} \varphi(0, \boldsymbol{\xi}) \right) \end{aligned} \quad (3.72)$$

Lastly, using $\sum_{j=1}^N w_j \mathbf{e}_j = 0$, (3.48) and (3.57), (3.72) can be written as

$$\begin{aligned} \dot{V}(\mathbf{e}_s, \tilde{\boldsymbol{\theta}}_s, \boldsymbol{\xi}) &= -\mathbf{e}_s^T \mathbf{e}_s + 2\mathbf{e}_s^T \mathbf{P} \boldsymbol{\Omega}^T(\mathbf{x}, u_s) \tilde{\mathcal{P}}_s - 2\mathbf{H}(t) \tilde{\mathbf{k}}(t) \mathbf{Z}(t) \tilde{\boldsymbol{\theta}}_s \\ &\quad + \mu \frac{\partial V_\varphi}{\partial \boldsymbol{\xi}} \varphi(0, \boldsymbol{\xi}) + \left(\mu \frac{\partial V_\varphi}{\partial \boldsymbol{\xi}} \varphi(\boldsymbol{\tau}, \boldsymbol{\xi}) - \mu \frac{\partial V_\varphi}{\partial \boldsymbol{\xi}} \varphi(0, \boldsymbol{\xi}) \right). \end{aligned} \quad (3.73)$$

Using the assumption (3.24) in (3.73) gives

$$\begin{aligned} \dot{V}(\mathbf{e}_s, \tilde{\boldsymbol{\theta}}_s, \boldsymbol{\xi}) &= -\mathbf{e}_s^T \mathbf{e}_s + 2\mathbf{e}_s^T \mathbf{P} \boldsymbol{\Omega}^T(\mathbf{x}, u_s) \tilde{\mathcal{P}}_s - 2\mathbf{H}(t) \tilde{\mathbf{k}}(t) \mathbf{Z}(t) \tilde{\boldsymbol{\theta}}_s \\ &\quad + \mu \frac{\partial V_\varphi}{\partial \boldsymbol{\xi}} \varphi(0, \boldsymbol{\xi}) + \mu \frac{\partial V_\varphi}{\partial \boldsymbol{\xi}} \varphi(\boldsymbol{\tau}, \boldsymbol{\xi}) b_\varphi \|\boldsymbol{\tau}\| \end{aligned} \quad (3.74)$$

Using the assumption (3.25) in (3.74) gives

$$\begin{aligned} \dot{V}(\mathbf{e}_s, \tilde{\boldsymbol{\theta}}_s, \boldsymbol{\xi}) &= -\mathbf{e}_s^T \mathbf{e}_s + 2\mathbf{e}_s^T \mathbf{P} \boldsymbol{\Omega}^T(\mathbf{x}, u_s) \tilde{\mathcal{P}}_s - 2\mathbf{H}(t) \tilde{\mathbf{k}}(t) \mathbf{Z}(t) \tilde{\boldsymbol{\theta}}_s \\ &\quad + \mu \frac{\partial V_\varphi}{\partial \boldsymbol{\xi}} \varphi(0, \boldsymbol{\xi}) + \mu \frac{\partial V_\varphi}{\partial \boldsymbol{\xi}} \varphi(\boldsymbol{\tau}, \boldsymbol{\xi}) b_\varphi (\|\mathbf{e}_s\| + b_d) \end{aligned} \quad (3.75)$$

Using (3.28) in (3.75) gives

$$\begin{aligned} \dot{V}(\mathbf{e}_s, \tilde{\boldsymbol{\theta}}_s, \boldsymbol{\xi}) &= -\|\mathbf{e}_s\|^2 + \|\mathbf{e}_s\| b_1 (\|\boldsymbol{\tau}\| + \|\boldsymbol{\xi}\|) \|\tilde{\mathcal{P}}_s\| - 2\|\mathbf{H}(t)\| \|\tilde{\mathbf{k}}(t)\| \|\mathbf{Z}(t)\| \|\tilde{\boldsymbol{\theta}}_s\| \\ &\quad + \mu \frac{\partial V_\varphi}{\partial \boldsymbol{\xi}} \varphi(0, \boldsymbol{\xi}) + \mu \frac{\partial V_\varphi}{\partial \boldsymbol{\xi}} \varphi(\boldsymbol{\tau}, \boldsymbol{\xi}) b_\varphi (\|\mathbf{e}_s\| + b_d) \end{aligned} \quad (3.76)$$

Finally, using (3.29) in (3.76) gives

$$\begin{aligned} \dot{V}(\mathbf{e}_s, \tilde{\boldsymbol{\theta}}_s, \boldsymbol{\xi}) &\leq -\|\mathbf{e}_s\|^2 + b_1 \|\mathbf{e}_s\| (\|\mathbf{e}_s\| + \|\boldsymbol{\xi}\| + b_d) \|\tilde{\mathcal{P}}_s\| \\ &\quad - 2\|\mathbf{H}\| \|\tilde{\mathbf{k}}\| \|\mathbf{Z}\| \|\tilde{\boldsymbol{\theta}}_s\| - \mu c_3 \|\boldsymbol{\xi}\|^2 + \mu c_4 b_\varphi \|\boldsymbol{\xi}\| (\|\mathbf{e}_s\| + b_d) \end{aligned} \quad (3.77)$$

Using the stability analysis of the first level that is, $\|\tilde{\mathcal{P}}_s\| \rightarrow 0$ and $\|\tilde{\boldsymbol{\theta}}_s\| \rightarrow 0$ as $t \rightarrow \infty$, (3.77) can be rewritten as

$$\dot{V}(\mathbf{e}_s, \tilde{\boldsymbol{\theta}}_s, \boldsymbol{\xi}) \leq -\|\mathbf{e}_s\|^2 - \mu c_3 \|\boldsymbol{\xi}\|^2 + \mu c_4 b_\varphi \|\boldsymbol{\xi}\| \|\mathbf{e}_s\| + \mu c_4 b_d b_\varphi \|\boldsymbol{\xi}\| \quad (3.78)$$

Rearranging the terms in (3.78) yields

$$\begin{aligned} \dot{V}(\mathbf{e}_s, \tilde{\boldsymbol{\theta}}_s, \boldsymbol{\xi}) &\leq - \left(\|\mathbf{e}_s\| - \frac{\mu c_4 b_\varphi \|\boldsymbol{\xi}\|}{2} \right)^2 + \frac{(\mu c_4 b_\varphi \|\boldsymbol{\xi}\|)^2}{4} - \mu c_3 \|\boldsymbol{\xi}\|^2 + \mu c_4 b_d b_\varphi \|\boldsymbol{\xi}\| \\ \text{or, } \dot{V}(\mathbf{e}_s, \tilde{\boldsymbol{\theta}}_s, \boldsymbol{\xi}) &\leq \frac{(\mu c_4 b_\varphi \|\boldsymbol{\xi}\|)^2}{4} - \mu c_3 \|\boldsymbol{\xi}\|^2 + \mu c_4 b_d b_\varphi \|\boldsymbol{\xi}\| \end{aligned} \quad (3.79)$$

$$\text{or, } \dot{V}(\mathbf{e}_s, \tilde{\boldsymbol{\theta}}_s, \boldsymbol{\xi}) \leq - \left(\sqrt{\mu c_3 - \frac{(\mu c_4 b_\varphi)^2}{4}} \|\boldsymbol{\xi}\| - \frac{\mu c_4 b_d b_\varphi}{2\sqrt{\mu c_3 - \frac{(\mu c_4 b_\varphi)^2}{4}}} \right)^2 + \frac{(\mu c_4 b_d b_\varphi)^2}{4 \left(\mu c_3 - \frac{(\mu c_4 b_\varphi)^2}{4} \right)} \quad (3.80)$$

$$\text{or, } \dot{V}(\mathbf{e}_s, \tilde{\boldsymbol{\theta}}_s, \boldsymbol{\xi}) \leq \frac{(\mu c_4 b_d b_\varphi)^2}{4 \left(\mu c_3 - \frac{(\mu c_4 b_\varphi)^2}{4} \right)} \quad (3.81)$$

Right hand side in (3.81) is negative for

$$\mu c_3 - \frac{(\mu c_4 b_\varphi)^2}{4} < 0 \quad (3.82)$$

or,

$$\mu > \frac{4c_3}{(c_4 b_\varphi)^2} \quad (3.83)$$

Choosing a positive value for $\mu > \frac{4c_3}{(c_4 b_\varphi)^2}$ will ensure that Lyapunov function $\dot{V}(\mathbf{e}_s, \tilde{\boldsymbol{\theta}}_s, \boldsymbol{\xi})$ is always negative definite and hence $V(\mathbf{e}_s, \tilde{\boldsymbol{\theta}}_s, \boldsymbol{\xi})$ is a decreasing function whose minimum is at zero. Thus the overall system is asymptotically stable and both $\|\tilde{\boldsymbol{\theta}}_s\| \rightarrow 0$ and $\mathbf{e}_s(t) \rightarrow 0$ as $t \rightarrow \infty$.

3.4 General Work Flow Chart

The procedural steps undergone in this multiple model based two level adaptation (MMTLA) method and also followed in the subsequent chapters can be represented using a general work flow chart given in Figure 3.3.

3.5 Simulation Results

The proposed multiple model based two level adaptation (MMTLA) technique is applied to two linearly parameterized nonlinear systems. The proposed MMTLA method is compared with already existing adaptive control techniques having multiple models with switching.

Case 1: Numerical example

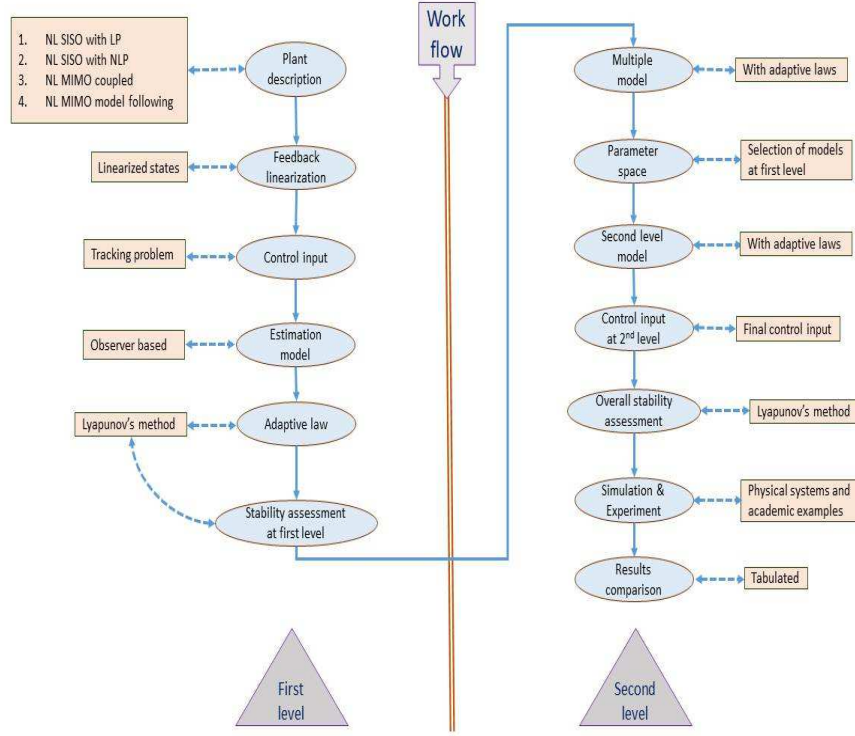


Figure 3.3: General work flow chart

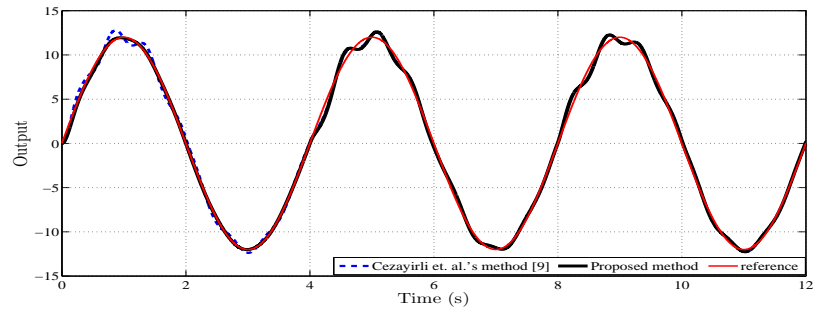
Let us consider the following nonlinear system [9],

$$\begin{aligned}
 \dot{x}_1 &= \cos x_2 + x_3 + \theta \tan^{-1} x_1 \\
 \dot{x}_2 &= x_1 - x_2 \\
 \dot{x}_3 &= u \\
 y &= x_1
 \end{aligned} \tag{3.84}$$

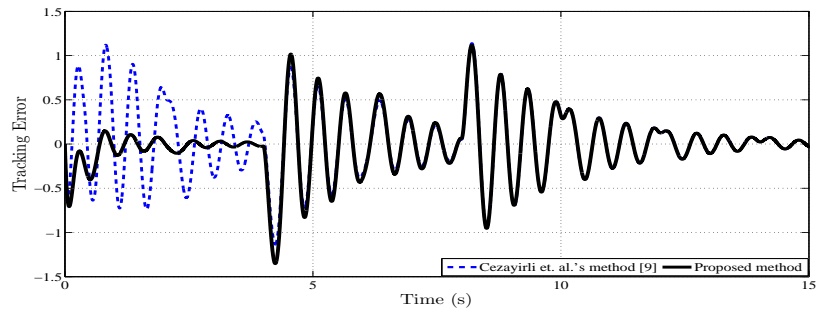
where θ is the unknown parameter. For designing the estimator model, the system dynamics can be written in regressor form using (3.8) as

$$\begin{aligned}
 \dot{\mathbf{x}} &= \boldsymbol{\omega}^T(\mathbf{x}, u) \mathcal{P} \\
 &= \begin{pmatrix} \cos x_2 & x_3 & \tan^{-1} x_1 \\ x_1 & -x_2 & 0 \\ u & 0 & 0 \end{pmatrix} \begin{pmatrix} 1 \\ 1 \\ \theta \end{pmatrix}
 \end{aligned} \tag{3.85}$$

Using Theorem 3.1, the BIBS stability of the system (3.84) can be proved. The uncertain parameter θ belongs to the compact set $\mathcal{S}_\theta = [-7, 8]$. For simulation purpose, the initial value of the parameter is considered as $\theta = 5$. At $t = 4s$, the value of the parameter is changed to $\theta = -5$. At $t = 8s$, it is again changed to $\theta = 5$. In the method followed by Cezayirli et al. [10] (Appendix A.2 may be referred), 6 fixed identification models are used with parameters initialized at $\theta_j = [-7, -4, -1, 2, 5, 8]$ [9]. In the proposed MMTLA control, two identical identification models are initiated at $\theta_j = ([-7, 8])$. All the states for the system and the identification models start from 0. Here, the reference trajectory is considered as $y_d = 12\sin(0.5\pi)t$. Simulation results are shown in Figure 3.4 - Figure 3.6.



(a) Output tracking

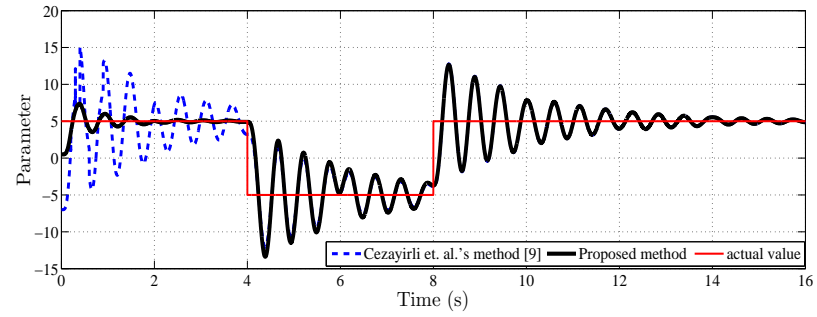


(b) Tracking Error

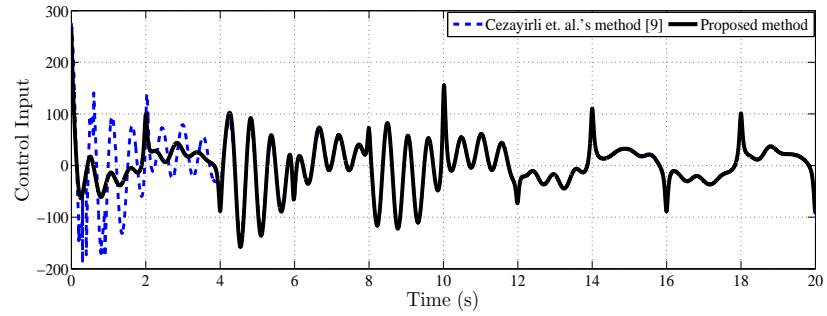
Figure 3.4: Case 1: Trajectory tracking

For fair comparison with [9], parameter variation for the system is considered in the range of $[-7, 8]$ and this is the reason for selecting the estimator models in this range. Figure 3.4 compares tracking results obtained by using the proposed MMTLA control method with those of [9]. In Figure 3.5 parameter convergence and control input profiles for both the methods can be found. Moreover, Figure 3.6 presents the parameter convergence at the first and second levels and also the adaptive weight convergence for both the models in the proposed MMTLA control.

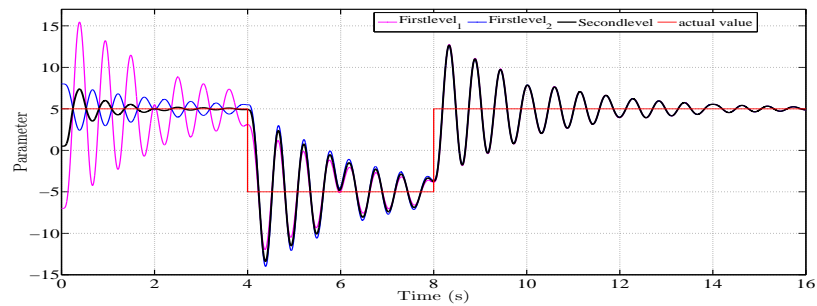
The comparison between the transient and steady state performances of the proposed scheme with



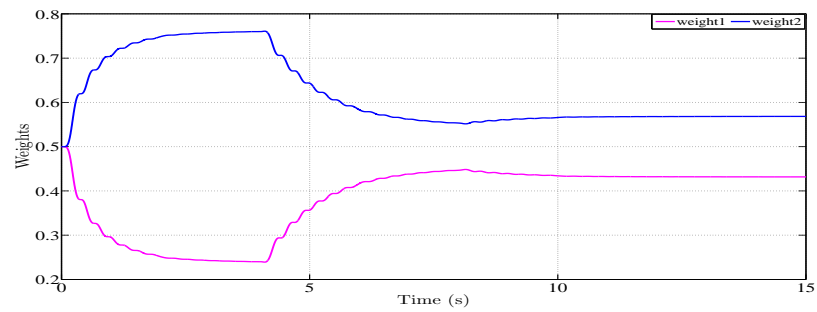
(a) Parameter



(b) Control input

Figure 3.5: Case 1: Parameter convergence and control input

(a) Parameter



(b) Weight

Figure 3.6: Case 1: Parameter and adaptive weight convergence

the method followed by [9] is provided in Table 3.1. The input and output performance measures used

Table 3.1: Comparison between schemes: Case 1

Adaptation Mechanism	Performance Specification							
	M_p	M_u	t_s	e_{ss}	t_c (θ)	TV	CE	RMSE
Cezayirli et al. [9]	6.41 %	3.08 %	18.02 s	0.0165	22.19 s	367.04	8.24×10^3	0.2402
MMTLA Contol	5.16 %	2.08 %	17.5 s	0.0165	22.19 s	359.5	7.4×10^3	0.2091

M_p : Peak overshoot, M_u : Peak undershoot

t_s : Settling time, e_{ss} : Steady state error

t_c (θ): Convergence time for parameter

TV : Total variation, CE : Control energy

RMSE : Root mean square error

in Table (3.1) for comparison purpose are defined in Appendix A.5. It is evident that from Table 3.1 that the proposed MMTLA scheme outperforms the method followed in [9] in transient performance. The steady state performance and parameter convergence time in both the methods are equal. The proposed MMTLA control method spends lesser energy and attains better output performance in terms of RMSE than [9]. Smoothness of the control inputs in the two methods are almost comparable. All these features are achieved even when the proposed MMTLA method uses only 2 models against 6 models used by [9]

Case 2: Single link robot arm driven by brushed DC motor

The proposed MMTLA control technique is next applied to a 1-link robot arm driven by a brushed DC-motor shown in Figure 3.7 [49]. This is an example of a nonlinear single-input single-output (SISO) system with linear parameterization. The system comprises of mechanical and electrical subsystems with dynamics given as

$$\begin{aligned}
 J_l \ddot{q}(t) + B_f \dot{q}(t) + L_l \sin q(t) &= I_a(t) \\
 L \dot{I}_a(t) + R I_a(t) + k_b \dot{q}(t) &= v(t)
 \end{aligned}
 \tag{3.86}$$

where J_l is the lumped inertia, B_f stands for friction coefficient, L_l denotes lumped load and $q(t)$ is the angular position. Similarly, $I_a(t)$ is the rotor armature current, L denotes the rotor inductance, R stands for rotor resistance, k_b is the back emf constant and $v(t)$ is the input voltage.

The constants J_l , L_l are given as $J_l = (J/k_t) + (m_l l^2/3k_t) + (m_0 l^2/k_t) + (2m_0 r_0^2/5k_t)$ and $L_l = (m_l l G/2k_t) + (m_0 l G/k_t)$. The description and values of constants for the given electromechanical system are given in Table 3.2. Considering $x_1 = q$, $x_2 = \dot{q}$, $x_3 = I_a$ as state variables and $u = v(t)$ as

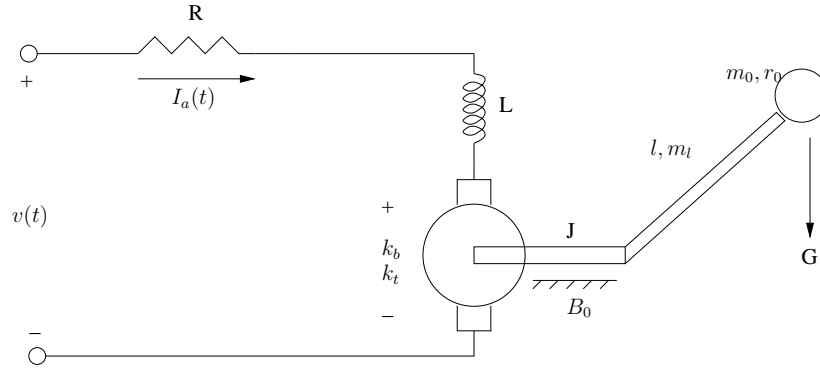


Figure 3.7: Model of 1-link robot arm driven by a brushed DC-motor

input, the complete system dynamics can be represented in the state-space form as

$$\begin{aligned}
 \dot{x}_1 &= x_2 \\
 \dot{x}_2 &= \theta_2 \sin x_1 - B_f \theta_1 x_2 + \theta_1 x_3 \\
 \dot{x}_3 &= \varrho_1 x_2 + \varrho_2 x_3 + \varrho_0 u \\
 y &= x_1
 \end{aligned} \tag{3.87}$$

where $\varrho_0 = 1/L$, $\varrho_1 = -k_b/L$, $\varrho_2 = -R/L$, $B_f = B_0/k_t$, $\theta_1 = 1/J_l$, $\theta_2 = -L_l/J_l$. The system (3.87) can easily be represented in form of (3.8) as

$$\dot{\mathbf{x}} = \begin{pmatrix} x_2 & 0 & 0 \\ 0 & -B_f \theta_1 x_2 + x_3 & \sin x_1 \\ \varrho_1 x_2 + \varrho_2 x_3 + \varrho_0 u & 0 & 0 \end{pmatrix} \begin{bmatrix} 1 \\ \theta_1 \\ \theta_2 \end{bmatrix} \tag{3.88}$$

Accordingly, using Theorem 3.1, the BIBS stability of system (3.87) can be easily deduced. Here u (input voltage v) is the manipulated variable and x_1 (the angular position q) is the controlled variable. Further, parameters θ_1 and θ_2 are uncertain, because of the unknown and sudden changes in the load. It is observed that the relative degree of the system, $\gamma = 3$. The transformation used to linearize the system is given by the diffeomorphism

$$\begin{pmatrix} \tau_1 \\ \tau_2 \\ \tau_3 \end{pmatrix} = \begin{pmatrix} x_1 \\ x_2 \\ \theta_2 \sin x_1 - B_f \theta_1 x_2 + \theta_1 x_3 \end{pmatrix} \tag{3.89}$$

Table 3.2: Electromechanical system constants for single link robot arm.

Symbol	Description	Value	Unit
J	motor inertia	1.625×10^{-3}	$kg - m^2/rad$
r_0	radius of the load	0.02	m
l	link length	0.3	m
R	rotor resistance	5.0	Ω
L	rotor inductance	25×10^{-3}	H
m_0	load mass	0.45	kg
m_l	link mass	0.5	kg
G	gravity constant	9.81	$kg - m/s^2$
B_0	viscous friction coefficient	16.25×10^{-3}	$N - m - s/rad$
k_t	torque constant of motor	0.90	$N - m/A$
k_b	back-emf constant	0.90	$N - m/A$

where unknown parameter vector $\theta = [\theta_1, \theta_2]^T$ are the elements of compact set $\mathcal{S}_\theta = [7, 16] \times [-37, -32]$. For fair comparison, the initial values of load mass and load radius are set to $m_0 = 1.55kg$ and $r_0 = 0.34m$ as in [10], which makes the initial values of parameters as $\theta_1 = 10$ and $\theta_2 = -33$. At $t = 10s$, sudden change in load parameters to $m_0 = 1.26kg$ and $r_0 = 0.256m$ made the values of parameters as $\theta_1 = 14.5$ and $\theta_2 = -36.7$.

Cezayirli et al. [10] (Appendix A.2 may be referred) used 24 fixed identification models with parameters initialized at $\theta_j =$

$$\begin{aligned}
 &([11.5, -34.5], [11.5, -36], [11.5, -34], [11.5, -32], [7, -34.5], [7, -36], [7, -34], [7, -32], \\
 &[9, -34.5], [9, -36], [9, -34], [9, -32], [11, -34.5], [11, -36], [11, -34], [11, -32], \\
 &[13, -34.5], [13, -36], [13, -34], [13, -32], [16, -34.5], [16, -36], [16, -34], [16, -32]).
 \end{aligned}$$

On the contrary, in the proposed MMTLA method, only 4 identical identification models are initiated at $\theta_j = ([7, -37], [7, -32], [16, -37], [16, -32])$. All the states for the system as well as the identification models start from 0. Here the reference trajectory is considered as $y_d = 2(1 - e^{-0.6t}) \sin(1.8\pi)t$. Simulation results obtained by using the proposed MMTLA control method are shown in Figure 3.8 - Figure 3.12. Figure 3.8 compares tracking results obtained by using the proposed MMTLA control method with those of [10]. In Figure 3.9 parameter convergence in both the methods can be observed. Figure 3.10 presents the control inputs for both the methods. Moreover, Figure 3.11 shows the parameter estimation profile in the proposed MMTLA approach for first and second levels for both the parameters. Finally, Figure 3.12 shows the adaptive weight convergence in all the four models in the proposed MMTLA approach. Table 3.3 compares the transient and steady state performances of the proposed MMTLA scheme with Cezayirli et al.'s method [10]. It is evident from Table 3.3 that

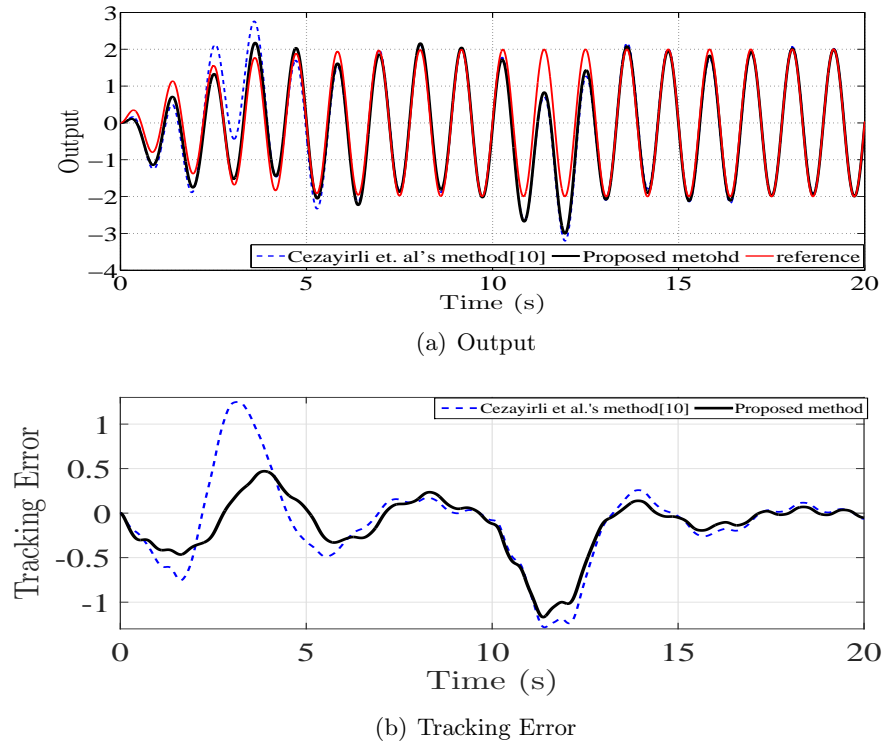


Figure 3.8: Case 2: Trajectory tracking by angular position of robot arm

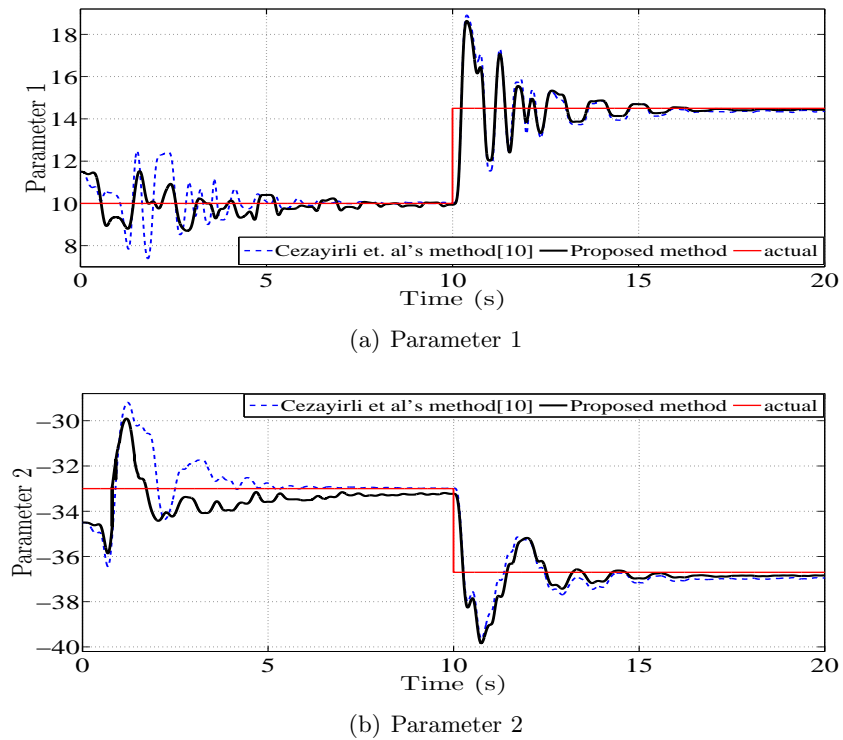


Figure 3.9: Case 2: Parameter Convergence

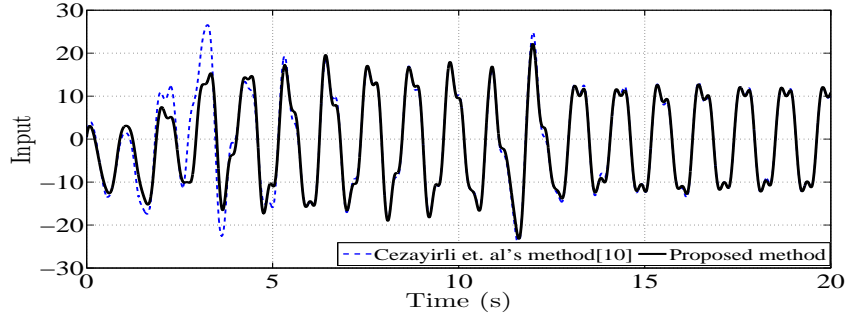
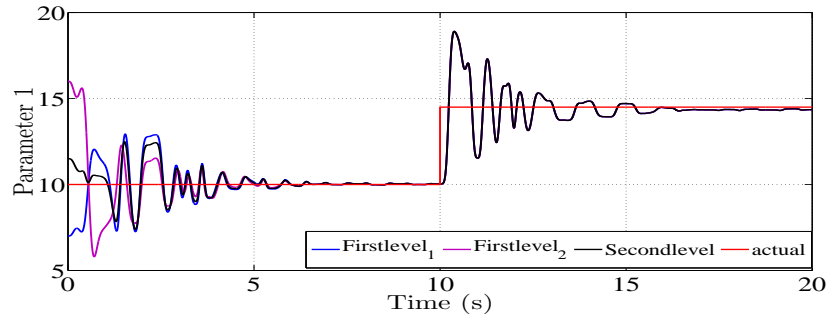
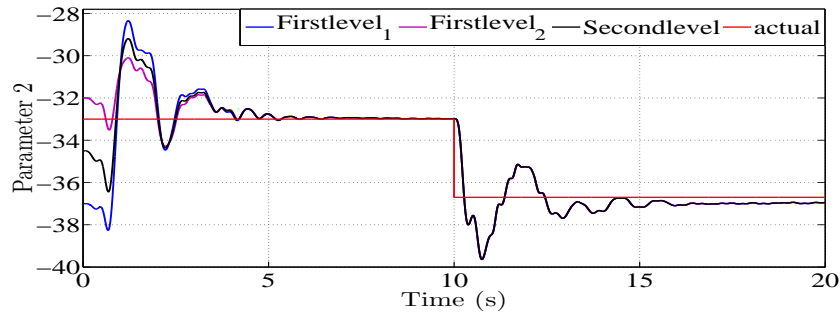


Figure 3.10: Case 2: Control input



(a) Parameter1



(b) Parameter2

Figure 3.11: Case 2: First and second level Parameter convergence

Table 3.3: Comparison between schemes: Case 2

Adaptation Mechanism	Performance Specification								
	M_p	M_u	t_s	e_{ss}	$t_c(\theta_1)$	$t_c(\theta_2)$	TV	CE	RMSE
Cezayirli et al. [10]	57.87 %	21.3 %	27.2 s	0.134	32.1 s	29.25 s	10.52	1.85×10^3	0.4037
MMTLA Control	22.17 %	6.3 %	23.9 s	0.093	26.7 s	25.1 s	10.50	1.77×10^3	0.2916

M_p : Peak overshoot, M_u : Peak undershoot

t_s : Settling time, e_{ss} : Steady state error

$t_c(\theta_1), t_c(\theta_2)$: Convergence time for first and second parameter respectively

TV : Total variation, CE : Control energy

RMSE : Root mean square error

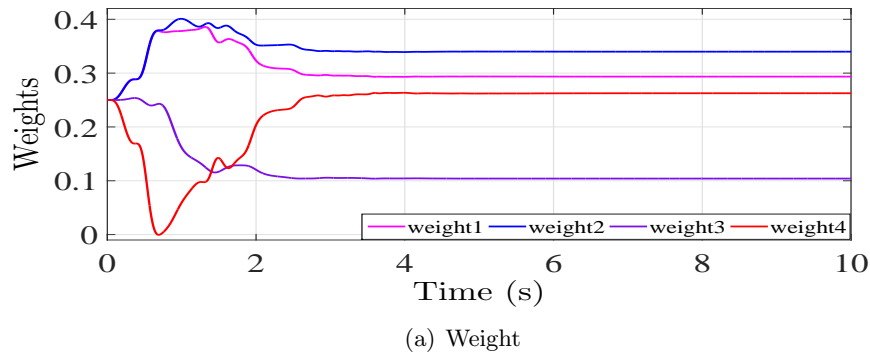


Figure 3.12: Case 2: Adaptive weight convergence

all the transient performance indices like peak overshoot, peak undershoot, settling time are lesser in the proposed MMTLA control. Also, the steady state error in the proposed MMTLA method is substantially reduced than the Cezayirli et al.'s method [10]. In the proposed MMTLA control, the convergence time for both the parameters is lesser than [10]. Smoothness of the control input is comparable in both the methods. However, control energy spent by the proposed MMTLA control is reduced and the output performance in terms of RMSE is substantially improved in the proposed method. Most importantly, the number of models used in the proposed scheme is significantly lesser compared to the number of models used by [10]. Furthermore, the parameter convergence time in the proposed MMTLA method is decreased which is crucial for online tuning.

3.6 Summary

A multiple model based two level adaptation (MMTLA) control method is proposed in this chapter. The proposed control scheme is designed for a nonlinear system with linear parameterization. The control input is found by using feedback linearization technique. The adaptive laws for unknown parameters at the first level are obtained using Lyapunov stability criterion. Multiple identification models have been developed with the same structure and different initial parameters which are chosen to optimally span the given compact parameter space. All the identification models are adaptive in nature. Adaptive laws for weights at the second level are derived using the identifier error. It is observed from simulation studies that the positions of identification models need to be selected judiciously to minimize the control effort. Simulation results confirm that the proposed MMTLA control method outperforms existing switching based multiple model adaptive control method. The underly-

ing importance of the proposed MMTLA control method is that the number of identification models required in the proposed MMTLA method is significantly lesser than that of existing multiple model based techniques. Moreover, parameter convergence in the proposed MMTLA method is reasonably fast. This is a significant benefit of the proposed MMTLA control method which makes it appropriate for practical applications. Also, the control effort required is reduced in MMTLA control method.

4

Adaptive Controller Design for Nonlinearly Parameterized SISO Nonlinear Systems Using Multiple Model Based Two Level Adaptation Technique

Contents

4.1	Introduction	48
4.2	Nonlinearly Parameterized Nonlinear System Description	49
4.3	Adaptive Feedback Controller and Estimation Model Design	50
4.4	Multiple Model Based Two Level Adaptation Technique	54
4.5	Simulation Results	57
4.6	Summary	66

4.1 Introduction

Adaptive control of nonlinear systems [3, 4, 6–8, 12, 50, 51] has continued to be a topic of extensive research in the past. However, most of the results in the literature are available for linearly parameterized nonlinear systems, although, nonlinear parameterization is often observed in many physical systems like the cart-pendulum system [12], fermentation process [32, 33], adaptive brake control [34], robotic manipulators [35], electro-hydraulic system [36] and bioreactors [37]. In [1], Boskovic et al. presented a stable adaptive control method based on modified adaptive algorithms developed for first order nonlinearly parameterized plants. Furthermore, Ge et al. [12] used weighted control Lyapunov function (WCLF) for adaptive tracking control of nonlinearly parameterized nonlinear systems. Anuradha et al. [42, 52] discussed the problem of parameter convergence using error model approach to establish new adaptation algorithms for nonlinearly parameterized systems.

A few recent works on multiple model adaptive control (MMAC) includes control of nonlinear systems using multiple model adaptive control based parallel dynamic neural networks (PDNNs) [53]. A multiple model based adaptive control methodology for uncertain linear systems was proposed in [54] which was able to ensure stability and guarantee performance. Recently, Xie et al. [55] applied MMAC to switched systems. A smooth controller design using only fixed models for nonlinear systems was reported in [56]. However, it was later observed that lack of proper switching schemes for controllers in MMAC made this approach not very useful practically. Therefore, researchers started looking for methods to reduce number of models or to find alternative for switching.

In this chapter, a multiple model with two level adaptation (MMTLA) control is introduced for nonlinear systems having nonlinear parameterization. The control input is designed using feedback linearization for the nonlinearly parameterized system [40, 45, 47]. State estimation error between the system and its estimation model is used to find the tuning law for the unknown parameters using Lyapunov stability criterion [5]. Multiple adaptive estimation models having same structure but distinct initializations for estimated parameters are designed. The tuning laws for estimation of parameters for every model are combined to find a single tuning law for each parameter and this is known as second level adaptation. The asymptotic stability and parameter convergence for the system after two levels is established using Lyapunov stability criterion.

Simulation studies are carried out to establish the theoretical propositions. A numerical example and a cart-pendulum system are simulated and the relevant results are compared with an already

existing method [12]. From simulation results it is found that there is a significant improvement in transient performance using the proposed MMTLA control method and in addition, the control energy expense is considerably reduced.

4.2 Nonlinearly Parameterized Nonlinear System Description

A class of nonlinearly parameterized system is considered as:

$$\begin{aligned} \dot{x}_i &= x_{i+1}, \quad i = 1, \dots, n-1 \\ \dot{x}_n &= \frac{1}{d(\mathbf{x}, \boldsymbol{\theta})} [f(\mathbf{x}, \boldsymbol{\theta}) + g(\mathbf{x})u] \\ y &= x_1 \end{aligned} \tag{4.1}$$

where the state vector $\mathbf{x} : \mathbb{R}^+ \rightarrow \mathbb{R}^n$ is considered measurable. Moreover, $u : \mathbb{R}^+ \rightarrow \mathbb{R}$ is the control input and $y : \mathbb{R}^+ \rightarrow \mathbb{R}$ represents the output. Further, $f(\mathbf{x}, \boldsymbol{\theta}), d(\mathbf{x}, \boldsymbol{\theta}) : \mathbb{R}^n \rightarrow \mathbb{R}^n$ are sufficiently smooth vector fields and $g(\mathbf{x}) : \mathbb{R}^n \rightarrow \mathbb{R}$ is a known continuous function. Functions $f(\mathbf{x}, \boldsymbol{\theta})$ and $d(\mathbf{x}, \boldsymbol{\theta})$ can be characterized as

$$\begin{aligned} f(\mathbf{x}, \boldsymbol{\theta}) &= \sum_{l=1}^p \theta_l f_l(\mathbf{x}) = \boldsymbol{\omega}_f^T(\mathbf{x})\boldsymbol{\theta} \\ d(\mathbf{x}, \boldsymbol{\theta}) &= \sum_{l=1}^p \theta_l d_l(\mathbf{x}) = \boldsymbol{\omega}_d^T(\mathbf{x})\boldsymbol{\theta} \end{aligned} \tag{4.2}$$

where $\boldsymbol{\theta} = [\theta_1, \theta_2, \dots, \theta_p]^T$ and p is the number of unknown parameters, $\boldsymbol{\omega}_f(x) \in \mathbb{R}^p$ and $\boldsymbol{\omega}_d(x) \in \mathbb{R}^p$ are known smooth functions. Here $f(\mathbf{x}, \boldsymbol{\theta}), d(\mathbf{x}, \boldsymbol{\theta})$ are linearly parameterized functions, but $d(\mathbf{x}, \boldsymbol{\theta})$ in the denominator of (4.1) causes the unknown parameter $\boldsymbol{\theta}$ enter into the system in a nonlinear fashion, making it a nonlinearly parameterized system. The following assumptions are made about the system (4.1):

- (i) It is assumed that $g(\mathbf{x})/d(\mathbf{x}, \boldsymbol{\theta}) \neq 0, \forall \mathbf{x} \in \mathbb{R}^n$. Without losing generality, it is assumed that $g(\mathbf{x}) > 0$ and $d(\mathbf{x}, \boldsymbol{\theta}) > 0 \forall \mathbf{x} \in \mathbb{R}^n$.
- (ii) The unknown parameter $\boldsymbol{\theta} \in \mathcal{S}_\theta$, where $\mathcal{S}_\theta \subset \mathbb{R}^p$ is a compact set.
- (iii) The system has full relative degree n .
- (iv) The equilibrium point of the zero dynamics of the system (4.1) is asymptotically stable.

4.3 Adaptive Feedback Controller and Estimation Model Design

Feedback linearization [40] is a widely explored nonlinear control technique where a nonlinear state feedback in the control converts the nonlinear system into a stable linear system. This common methodology includes two consecutive operations, (i) nonlinear change of coordinates, (ii) nonlinear state feedback controller design. Here, step (i) is not required as the system (4.1) is assumed to have full degree.

Therefore, a virtual input $v = \frac{1}{d(\mathbf{x}, \boldsymbol{\theta})} [f(\mathbf{x}, \boldsymbol{\theta}) + g(\mathbf{x})u]$ can be considered to get the control input as

$$u = \frac{1}{g(\mathbf{x})} (-f(\mathbf{x}, \boldsymbol{\theta}) + d(\mathbf{x}, \boldsymbol{\theta})v). \quad (4.3)$$

Using (4.2) in (4.3) gives

$$u = \frac{1}{g(\mathbf{x})} (-\boldsymbol{\omega}_f^T(\mathbf{x})\boldsymbol{\theta} + \boldsymbol{\omega}_d^T(\mathbf{x})\boldsymbol{\theta}v). \quad (4.4)$$

The virtual input v for a tracking problem can be designed using the required trajectory information as [10, 45]

$$v = y_d^{(n)} + c_n(y_d^{(n-1)} - y^{(n-1)}) + \dots + c_1(y_d - y) \quad (4.5)$$

where c_1, \dots, c_n are the constant coefficients of a Hurwitz Polynomial $s^n + c_n s^{n-1} + \dots + c_1$ and y_d is the desired trajectory.

The designed controller in (4.4) is impractical because it contains unknown parameter vector $\boldsymbol{\theta}$. Therefore, a stable estimation model [5, 45] for the system (4.1) is developed as

$$\begin{aligned} \dot{\hat{x}}_i &= \lambda_i(\hat{x}_i - x_i) + x_{i+1}, \quad i = 1, 2, \dots, n-1 \\ \dot{\hat{x}}_n &= \lambda_n(\hat{x}_n - x_n) + \frac{1}{\hat{d}(\mathbf{x}, \hat{\boldsymbol{\theta}})} \left[\hat{f}(\mathbf{x}, \hat{\boldsymbol{\theta}}) + g(\mathbf{x})u \right] \end{aligned} \quad (4.6)$$

such that its states and output converge to the system as time $t \rightarrow \infty$. Here, $\{\hat{x}_i, i = 1, 2, \dots, n\}$ is the estimate of $\{x_i, i = 1, 2, \dots, n\}$, $\hat{\boldsymbol{\theta}}$ is the estimate of $\boldsymbol{\theta}$ and λ_i, λ_n are negative constants. Also, $\hat{f}(\mathbf{x}, \hat{\boldsymbol{\theta}}) = \boldsymbol{\omega}_f^T(\mathbf{x})\hat{\boldsymbol{\theta}}$ and $\hat{d}(\mathbf{x}, \hat{\boldsymbol{\theta}}) = \boldsymbol{\omega}_d^T(\mathbf{x})\hat{\boldsymbol{\theta}}$. Now, subtracting (4.1) from (4.6) and using (4.2), the

identifier error dynamics of system (4.1) are found as

$$\begin{aligned}\dot{e}_{I_i} &= \lambda_i e_{I_i} \\ \dot{e}_{I_n} &= \lambda_n e_{I_n} + \frac{1}{\omega_d^T(\mathbf{x})\hat{\boldsymbol{\theta}}} \left[\omega_f^T(\mathbf{x})\hat{\boldsymbol{\theta}} + g(\mathbf{x})u \right] - \frac{1}{\omega_d^T(\mathbf{x})\boldsymbol{\theta}} \left[\omega_f^T(\mathbf{x})\boldsymbol{\theta} + g(\mathbf{x})u \right]\end{aligned}\quad (4.7)$$

or,

$$\begin{aligned}\dot{e}_{I_i} &= \lambda_i e_{I_i} \\ \dot{e}_{I_n} &= \lambda_n e_{I_n} + \frac{\omega_d^T(\mathbf{x})\boldsymbol{\theta}[\omega_f^T(\mathbf{x})\hat{\boldsymbol{\theta}} + g(\mathbf{x})u] - \omega_d^T(\mathbf{x})\hat{\boldsymbol{\theta}}[\omega_f^T(\mathbf{x})\boldsymbol{\theta} + g(\mathbf{x})u]}{(\omega_d^T(\mathbf{x})\hat{\boldsymbol{\theta}})(\omega_d^T(\mathbf{x})\boldsymbol{\theta})}\end{aligned}\quad (4.8)$$

where $e_{I_i} = \hat{x}_i - x_i$, $i = 1, 2, \dots, n$. The above error equation can be rewritten as

$$\begin{aligned}\dot{e}_{I_i} &= \lambda_i e_{I_i} \\ \dot{e}_{I_n} &= \lambda_n e_{I_n} + \frac{(\omega_d^T(\mathbf{x})\hat{\boldsymbol{\theta}})(\omega_f^T(\mathbf{x})\tilde{\boldsymbol{\theta}}) - (\omega_d^T(\mathbf{x})\tilde{\boldsymbol{\theta}})(\omega_f^T(\mathbf{x})\hat{\boldsymbol{\theta}}) - (\omega_d^T(\mathbf{x})\tilde{\boldsymbol{\theta}})g(\mathbf{x})u}{(\omega_d^T(\mathbf{x})\hat{\boldsymbol{\theta}})(\omega_d^T(\mathbf{x})\boldsymbol{\theta})}\end{aligned}\quad (4.9)$$

where $\tilde{\boldsymbol{\theta}} = \hat{\boldsymbol{\theta}} - \boldsymbol{\theta}$ is the parameter error.

4.3.1 System stability and adaptive law design

To investigate the stability properties of the nonlinear system (4.1), a suitable Lyapunov function is considered as

$$V(\mathbf{e}_I, \tilde{\boldsymbol{\theta}}) = \sigma_1 \frac{\mathbf{e}_I^T \mathbf{e}_I}{2} + \sigma_2 \frac{\tilde{\boldsymbol{\theta}}^T \tilde{\boldsymbol{\theta}}}{2}\quad (4.10)$$

where $\mathbf{e}_I = [e_{I_1}, e_{I_2}, \dots, e_{I_n}]^T$ and σ_1 and σ_2 are positive constants. The adaptive law is used as

$$\begin{aligned}\dot{\tilde{\boldsymbol{\theta}}} &= -\frac{\sigma_1}{\sigma_2} \frac{(\omega_d^T \hat{\boldsymbol{\theta}})\omega_f^T - \omega_d^T(\omega_f^T \hat{\boldsymbol{\theta}}) - \omega_d^T g u}{(\omega_d^T \hat{\boldsymbol{\theta}})(\omega_d^T \boldsymbol{\theta})} e_{I_n} \\ \text{or, } \dot{\tilde{\boldsymbol{\theta}}} &= -\frac{\sigma_1}{\sigma_2} \frac{(\omega_d^T \hat{\boldsymbol{\theta}})\omega_f^T - \omega_d^T(\omega_f^T \hat{\boldsymbol{\theta}}) - \omega_d^T g u}{(\omega_d^T \hat{\boldsymbol{\theta}})(\omega_d^T \boldsymbol{\theta})} e_{I_n}.\end{aligned}\quad (4.11)$$

Using estimate $\hat{\boldsymbol{\theta}}$ in place of unknown parameter vector $\boldsymbol{\theta}$ in (4.11) yields the final adaptive law,

$$\dot{\tilde{\boldsymbol{\theta}}} = -\frac{\sigma_1}{\sigma_2} \frac{\omega_f(\omega_d^T \hat{\boldsymbol{\theta}}) - \omega_d(\omega_f^T \hat{\boldsymbol{\theta}}) - \omega_d^T g u}{(\omega_d^T \hat{\boldsymbol{\theta}})^2} e_{I_n}.\quad (4.12)$$

Taking first time derivative of Lyapunov equation (4.10) and using adaptive law (4.12) gives

$$\dot{V}(\mathbf{e}_I, \tilde{\boldsymbol{\theta}}) = \sigma_1 \sum_{i=1}^{n-1} \lambda_i e_{I_i}^2 + \sigma_1 \lambda_n e_{I_n}^2 \leq 0.\quad (4.13)$$

From (4.13), boundedness of the parameter error $\tilde{\boldsymbol{\theta}}$ and the estimation error \mathbf{e}_I are established. Since all the terms in the right hand side of (4.9) are bounded, boundedness of $\dot{\mathbf{e}}_I$ is assured. Now, taking first time derivative on both sides of (4.13) gives

$$\ddot{V}(\mathbf{e}_I, \tilde{\boldsymbol{\theta}}) = 2\sigma_1 \sum_{i=1}^{n-1} \lambda_i e_{I_i} \dot{e}_{I_i} + 2\sigma_1 \lambda_n e_{I_n} \dot{e}_{I_n}. \quad (4.14)$$

As is evident in (4.14), boundedness of \mathbf{e}_I and $\dot{\mathbf{e}}_I$ implies that $\ddot{V}(\mathbf{e}_I, \tilde{\boldsymbol{\theta}})$ has a finite value and hence, $\lim_{t \rightarrow \infty} \dot{V}(\mathbf{e}_I, \tilde{\boldsymbol{\theta}}) \rightarrow 0$ satisfies Barbalat's lemma meaning that $\lim_{t \rightarrow \infty} \mathbf{e}_I(t) = 0$. Moreover, having sufficiently rich [7] (A.1 may be referred) regressor vectors $\boldsymbol{\omega}_f, \boldsymbol{\omega}_d$ in (4.11), implies that $\lim_{t \rightarrow \infty} \tilde{\boldsymbol{\theta}}(t) = 0$ (using *Theorem 2.1* in [45]).

Furthermore, the virtual control signal v in (4.5) consists of y and its derivatives $\dot{y}, \ddot{y}, \dots, y^{(n-1)}$, which are functions of unknown parameter $\boldsymbol{\theta}$. Now, certainty equivalence principle [7] (A.1 may be referred) is applied to yield $\hat{v} = y_d^{(\gamma)} + c_\gamma(y_d^{(\gamma-1)} - \hat{y}^{(\gamma-1)}) + \dots + c_1(y_d - y)$. Consequently, the control input in (4.4) can be deduced by replacing $\boldsymbol{\theta}$ and v with their estimate $\hat{\boldsymbol{\theta}}$ and \hat{v} respectively yielding

$$u = \frac{1}{g(\mathbf{x})} (-\boldsymbol{\omega}_f^T(\mathbf{x})\hat{\boldsymbol{\theta}} + \boldsymbol{\omega}_d^T(\mathbf{x})\hat{\boldsymbol{\theta}}\hat{v}). \quad (4.15)$$

In the preceding paragraphs, the convergence of estimation and parameter errors was established. Now, the closed loop stability of the system at the first level including boundedness of the control error will be discussed.

The control error is represented as

$$e_i = x_i - y_d^{(i-1)}, \quad i = 1, \dots, n. \quad (4.16)$$

Taking first time derivative of (4.16) gives

$$\begin{aligned} \dot{e}_1 &= e_2 \\ \dot{e}_2 &= e_3 \\ &\dots \\ \dot{e}_{n-1} &= e_n \\ \dot{e}_n &= \dot{x}_n - y_d^{(n)} \end{aligned} \quad (4.17)$$

Using (4.17) and properties of \hat{v} , the vector form of control error equation is represented as

$$\dot{\mathbf{e}} = \mathbf{A}\mathbf{e} + \mathbf{B}(\dot{x}_n - \hat{v}) \quad (4.18)$$

where $\mathbf{A} = \begin{bmatrix} 0 & 1 & 0 & \dots & 0 \\ 0 & 0 & 1 & \dots & 0 \\ \vdots & \vdots & \vdots & \ddots & \vdots \\ 0 & \dots & \dots & \dots & 1 \\ c_1 & c_2 & \dots & \dots & c_n \end{bmatrix}$ is a Hurwitz matrix and $\mathbf{B} = [0, 0, \dots, 1]^T$. Using (4.1) and (4.15), (4.18) can be written as

$$\dot{\mathbf{e}} = \mathbf{A}\mathbf{e} + \frac{1}{\boldsymbol{\theta}^T \boldsymbol{\omega}_d} [\boldsymbol{\theta}^T \boldsymbol{\omega}_f + gu] - \frac{1}{\hat{\boldsymbol{\theta}}^T \boldsymbol{\omega}_d} [\hat{\boldsymbol{\theta}}^T \boldsymbol{\omega}_f + gu]. \quad (4.19)$$

Following assumptions are made to analyze the closed loop stability of the system (4.1):

- (i) The reference trajectory y_d is bounded with bounded derivatives $\dot{y}_d, \dots, y_d^{n-1}$. For y_d and its higher derivatives upper bounded by b_d , one can write

$$\|\mathbf{x}\| \leq \|\mathbf{e}\| + b_d \quad (4.20)$$

- (ii) Since $\boldsymbol{\omega}_f$ and $\boldsymbol{\omega}_d$ are known regressor vectors and are bounded, parameter estimate $\hat{\boldsymbol{\theta}}$ is a known bounded vector and this gives

$$\left\| \frac{(\boldsymbol{\omega}_f)(\hat{\boldsymbol{\theta}}^T \boldsymbol{\omega}_d) - (\boldsymbol{\omega}_d)(\hat{\boldsymbol{\theta}}^T \boldsymbol{\omega}_f) - (\boldsymbol{\omega}_d)g(\mathbf{x})u}{(\hat{\boldsymbol{\theta}}^T \boldsymbol{\omega}_d)^2} \right\| \|\tilde{\boldsymbol{\theta}}^T\| \leq b_\omega \|\mathbf{x}\| \|\tilde{\boldsymbol{\theta}}^T\| \quad (4.21)$$

where $\tilde{\boldsymbol{\theta}} = \hat{\boldsymbol{\theta}} - \boldsymbol{\theta}$ and b_ω is a small positive constant chosen by the designer.

Consequently, a Lyapunov function for closed loop error dynamics (4.19) can be selected as

$$V(\mathbf{e}) = \mathbf{e}^T \mathbf{P} \mathbf{e}. \quad (4.22)$$

Taking first differentiation of (4.22) with respect to time and using (4.19) gives

$$\dot{V}(\mathbf{e}) = \mathbf{e}^T (\mathbf{A}^T \mathbf{P} + \mathbf{P} \mathbf{A}) \mathbf{e} + 2\mathbf{e}^T \mathbf{P} \frac{(\tilde{\boldsymbol{\theta}}^T \boldsymbol{\omega}_f)(\hat{\boldsymbol{\theta}}^T \boldsymbol{\omega}_d) - (\tilde{\boldsymbol{\theta}}^T \boldsymbol{\omega}_d)(\hat{\boldsymbol{\theta}}^T \boldsymbol{\omega}_f) - (\tilde{\boldsymbol{\theta}}^T \boldsymbol{\omega}_d)g(\mathbf{x})u}{(\hat{\boldsymbol{\theta}}^T \boldsymbol{\omega}_d)(\boldsymbol{\theta}^T \boldsymbol{\omega}_d)} \quad (4.23)$$

where \mathbf{P} is a symmetric positive definite matrix, found by solving Lyapunov equation $\mathbf{A}^T \mathbf{P} + \mathbf{P} \mathbf{A} = -\mathbf{I}$.

Again, using estimate $\hat{\boldsymbol{\theta}}$ in place of the unknown parameter vector $\boldsymbol{\theta}$, (4.23) can be written as

$$\dot{V}(\mathbf{e}) = -\mathbf{e}^T \mathbf{e} + 2\mathbf{e}^T \mathbf{P} \frac{(\tilde{\boldsymbol{\theta}}^T \boldsymbol{\omega}_f)(\hat{\boldsymbol{\theta}}^T \boldsymbol{\omega}_d) - (\tilde{\boldsymbol{\theta}}^T \boldsymbol{\omega}_d)(\hat{\boldsymbol{\theta}}^T \boldsymbol{\omega}_f) - (\tilde{\boldsymbol{\theta}}^T \boldsymbol{\omega}_d)g(\mathbf{x})u}{(\hat{\boldsymbol{\theta}}^T \boldsymbol{\omega}_d)^2}. \quad (4.24)$$

Now, using (4.20) and (4.21), (4.24) yields

$$\dot{V}(\mathbf{e}) \leq -\|\mathbf{e}\|^2 + 2\mathbf{P}b_\omega \|\mathbf{x}\| \|\tilde{\boldsymbol{\theta}}^T\| \|\mathbf{e}\| \quad (4.25)$$

$$\text{or, } \dot{V}(\mathbf{e}) \leq -\left(\|\mathbf{e}\| - \frac{1}{2}b_\omega \|\mathbf{x}\| \|\tilde{\boldsymbol{\theta}}^T\|\right)^2 + \frac{1}{4}\left(b_\omega \|\mathbf{x}\| \|\tilde{\boldsymbol{\theta}}^T\|\right)^2 \quad (4.26)$$

If the magnitude of the second term in (4.26) is lesser than the magnitude of the first term, $\dot{V}(\mathbf{e})$ will become negative definite. Therefore, design parameter b_ω can be chosen such that

$$\frac{b_\omega^2}{4}\left(\|\mathbf{x}\| \|\tilde{\boldsymbol{\theta}}^T\|\right)^2 \leq \left(\|\mathbf{e}\| - \frac{1}{2}b_\omega \|\mathbf{x}\| \|\tilde{\boldsymbol{\theta}}^T\|\right)^2. \quad (4.27)$$

Consequently, $b_\omega \leq \frac{\|\mathbf{e}\|}{\|\mathbf{x}\| \|\tilde{\boldsymbol{\theta}}^T\|}$ will ensure that $\dot{V}(\mathbf{e}) \leq 0$, which implies that $\|\mathbf{e}\| \in \mathcal{L}_\infty$.

4.4 Multiple Model Based Two Level Adaptation Technique

This section is devoted to discuss the concept of two level adaptation using multiple estimation models $M_j(j = 1, \dots, N)$. Therefore, extending the basic structure of the single estimator model as given in (4.6) for N multiple models provides

$$\begin{aligned} \dot{\hat{x}}_{i_j} &= \lambda_{i_j}(\hat{x}_{i_j} - x_i) + x_{i+1}, \quad i = 1, 2, \dots, n-1 \\ \dot{\hat{x}}_{n_j} &= \lambda_{n_j}(\hat{x}_{n_j} - x_n) + \frac{1}{\hat{d}(\mathbf{x}, \hat{\boldsymbol{\theta}}_j)} \left[\hat{f}(\mathbf{x}, \hat{\boldsymbol{\theta}}_j) + g(\mathbf{x})u \right], \quad j = 1, \dots, N \end{aligned} \quad (4.28)$$

where parameter vector estimates $\hat{\boldsymbol{\theta}}_j$, $j = 1, \dots, N$ are placed at different starting points inside the compact space \mathcal{S}_θ . Here, $\hat{x}_{i_j}, \hat{x}_{n_j}$, $j = 1, \dots, N$ is the state vector of the j -th model and $\lambda_{i_j}, \lambda_{n_j}$ are negative constants. Defining the identifier error dynamics for each model as,

$$\begin{aligned} \dot{e}_{I_{i_j}} &= \lambda_{i_j} e_{I_{i_j}} \\ \dot{e}_{I_{n_j}} &= \lambda_{n_j} e_{I_{n_j}} + \frac{(\boldsymbol{\omega}_d^T(\mathbf{x})\hat{\boldsymbol{\theta}}_j)(\boldsymbol{\omega}_f^T(\mathbf{x})\tilde{\boldsymbol{\theta}}_j) - (\boldsymbol{\omega}_d^T(\mathbf{x})\tilde{\boldsymbol{\theta}}_j)(\boldsymbol{\omega}_f^T(\mathbf{x})\hat{\boldsymbol{\theta}}_j) - (\boldsymbol{\omega}_d^T(\mathbf{x})\tilde{\boldsymbol{\theta}}_j)g(\mathbf{x})u}{(\boldsymbol{\omega}_d^T(\mathbf{x})\hat{\boldsymbol{\theta}}_j)(\boldsymbol{\omega}_d^T(\mathbf{x})\boldsymbol{\theta})} \end{aligned} \quad (4.29)$$

where $e_{I_{i_j}} = \hat{x}_{i_j} - x_i$, $e_{I_{n_j}} = \hat{x}_{n_j} - x_n$ and $\tilde{\boldsymbol{\theta}}_j = \hat{\boldsymbol{\theta}}_j - \boldsymbol{\theta}$ are the state estimation error and the parameter error for the j -th model respectively. Using (4.12), the adaptive law for the j -th parameter vector is

deduced as

$$\dot{\hat{\boldsymbol{\theta}}}_j = -\frac{\sigma_{1_j} \boldsymbol{\omega}_f(\boldsymbol{\omega}_d^T \hat{\boldsymbol{\theta}}_j) - \boldsymbol{\omega}_d(\boldsymbol{\omega}_f^T \hat{\boldsymbol{\theta}}_j) - \boldsymbol{\omega}_d^T g u}{\sigma_{2_j} (\boldsymbol{\omega}_d^T \hat{\boldsymbol{\theta}}_j)^2} e_{I_{n_j}} \quad (4.30)$$

where $\sigma_{1_j}, \sigma_{2_j}$ are positive constants.

The first level models $\hat{\boldsymbol{\theta}}_j(t)$ are combined in a convex manner, using weights $w_j(t)$ which are also adaptive in nature, resulting in the desired second level model $\boldsymbol{\theta}_s(t)$ given as

$$\boldsymbol{\theta}_s(t) = \sum_{j=1}^N w_j(t) \hat{\boldsymbol{\theta}}_j(t) \quad (4.31)$$

where the weights $w_j(t)$ satisfy the rules given in Section 3.3.3. Therefore, identification of $\boldsymbol{\theta}$ is now transformed to estimation of $w_j(t)$ at the second level. Thus, as discussed in Section 3.3.3, the error and weight relationship can be written as

$$[\mathbf{e}_1(t), \mathbf{e}_2(t), \dots, \mathbf{e}_N(t)] \mathbf{W} = \mathbf{E}(t)_{n \times N} \mathbf{W}_{N \times 1} = \mathbf{0}_{n \times 1} \quad (4.32)$$

where $\mathbf{W}(t) = [w_1(t), w_2(t), \dots, w_N(t)]^T$ and $\mathbf{E}(t) = [\mathbf{e}_1(t), \mathbf{e}_2(t), \dots, \mathbf{e}_N(t)]$.

Similarly, using (3.57) the adaptive weights have the tuning laws given as

$$\begin{aligned} \dot{\tilde{\mathbf{W}}}(t) &= -\mathbf{H}(t) \tilde{k}(t) \\ &= -\mathbf{H}^T(t) \mathbf{H}(t) \tilde{\mathbf{W}}(t) + \mathbf{H}^T(t) k(t). \end{aligned} \quad (4.33)$$

Finally, using the estimate of system parameter $\boldsymbol{\theta}_s$, the control input at the second level can be derived as

$$u_s = \frac{1}{g(\mathbf{x})} (-\boldsymbol{\omega}_f^T(\mathbf{x}) \boldsymbol{\theta}_s + \boldsymbol{\omega}_d^T(\mathbf{x}) \boldsymbol{\theta}_s \hat{v}). \quad (4.34)$$

4.4.1 Complete system stability after two level adaptation

To achieve the overall system stability and tracking convergence, control error equation (4.19) is modified here by replacing $\hat{\boldsymbol{\theta}}$ with second level estimate $\boldsymbol{\theta}_s$ as

$$\dot{\mathbf{e}}_s = \mathbf{A} \mathbf{e}_s + \frac{1}{\boldsymbol{\theta}_s^T \boldsymbol{\omega}_d} [\boldsymbol{\theta}_s^T \boldsymbol{\omega}_f + g u_s] - \frac{1}{\boldsymbol{\theta}^T \boldsymbol{\omega}_d} [\boldsymbol{\theta}^T \boldsymbol{\omega}_f + g u_s] \quad (4.35)$$

where $u_s = \frac{1}{g(\mathbf{x})}(-\boldsymbol{\omega}_f^T(\mathbf{x})\boldsymbol{\theta}_s + \boldsymbol{\omega}_d^T(\mathbf{x})\boldsymbol{\theta}_s\hat{v})$. Rewriting (4.21) for second level parameter estimate $\boldsymbol{\theta}_s$, which is also a known bounded vector, gives

$$\left\| \frac{(\boldsymbol{\omega}_f)(\boldsymbol{\theta}_s^T \boldsymbol{\omega}_d) - (\boldsymbol{\omega}_d)(\boldsymbol{\theta}_s^T \boldsymbol{\omega}_f) - (\boldsymbol{\omega}_d)g(\mathbf{x})u_s}{(\boldsymbol{\theta}_s^T \boldsymbol{\omega}_d)^2} \right\| \|\tilde{\boldsymbol{\theta}}_s^T\| \leq b_\omega \|\mathbf{x}\| \|\tilde{\boldsymbol{\theta}}_s^T\| \quad (4.36)$$

where $\tilde{\boldsymbol{\theta}}_s = \boldsymbol{\theta}_s - \boldsymbol{\theta}$. An appropriate Lyapunov function for closed loop error dynamics (4.35) is chosen as

$$V_s(\mathbf{e}_s, \tilde{\boldsymbol{\theta}}_s) = \mathbf{e}_s^T \mathbf{P} \mathbf{e}_s + \tilde{\boldsymbol{\theta}}_s^T \tilde{\boldsymbol{\theta}}_s \quad (4.37)$$

where \mathbf{P} is a symmetric positive definite matrix, obtained by solving Lyapunov equation $\mathbf{A}^T \mathbf{P} + \mathbf{P} \mathbf{A} = -\mathbf{I}$. Differentiating (4.37) with respect to time and using (4.35) yields

$$\dot{V}_s(\mathbf{e}_s, \tilde{\boldsymbol{\theta}}_s) = \mathbf{e}_s^T (\mathbf{A}^T \mathbf{P} + \mathbf{P} \mathbf{A}) \mathbf{e}_s + 2\tilde{\boldsymbol{\theta}}_s^T \dot{\tilde{\boldsymbol{\theta}}}_s + 2\mathbf{e}_s^T \mathbf{P} \frac{(\tilde{\boldsymbol{\theta}}_s^T \boldsymbol{\omega}_f)(\boldsymbol{\theta}_s^T \boldsymbol{\omega}_d) - (\tilde{\boldsymbol{\theta}}_s^T \boldsymbol{\omega}_d)(\boldsymbol{\theta}_s^T \boldsymbol{\omega}_f) - (\tilde{\boldsymbol{\theta}}_s^T \boldsymbol{\omega}_d)g(\mathbf{x})u_s}{(\boldsymbol{\theta}_s^T \boldsymbol{\omega}_d)(\boldsymbol{\theta}_s^T \boldsymbol{\omega}_d)} \quad (4.38)$$

Replacing unknown parameter $\boldsymbol{\theta}$ with its estimate $\boldsymbol{\theta}_s$, (4.38) is rewritten as

$$\dot{V}_s(\mathbf{e}_s, \tilde{\boldsymbol{\theta}}_s) = -\mathbf{e}_s^T \mathbf{e}_s + 2\tilde{\boldsymbol{\theta}}_s^T \dot{\tilde{\boldsymbol{\theta}}}_s + 2\mathbf{e}_s^T \mathbf{P} \frac{(\tilde{\boldsymbol{\theta}}_s^T \boldsymbol{\omega}_f)(\boldsymbol{\theta}_s^T \boldsymbol{\omega}_d) - (\tilde{\boldsymbol{\theta}}_s^T \boldsymbol{\omega}_d)(\boldsymbol{\theta}_s^T \boldsymbol{\omega}_f) - (\tilde{\boldsymbol{\theta}}_s^T \boldsymbol{\omega}_d)g(\mathbf{x})u_s}{(\boldsymbol{\theta}_s^T \boldsymbol{\omega}_d)^2} \quad (4.39)$$

Now, differentiating $\tilde{\boldsymbol{\theta}}_s$ in (4.31) with respect to time yields

$$\dot{\tilde{\boldsymbol{\theta}}}_s = \dot{\boldsymbol{\theta}}_s = \sum_{j=1}^N w_j \dot{\boldsymbol{\theta}}_j + \sum_{j=1}^N \dot{w}_j \hat{\boldsymbol{\theta}}_j \quad (4.40)$$

Using (4.40) in (4.39) gives

$$\begin{aligned} \dot{V}_s(\mathbf{e}_s, \tilde{\boldsymbol{\theta}}_s) = & -\mathbf{e}_s^T \mathbf{e}_s + 2\mathbf{e}_s^T \mathbf{P} \frac{(\tilde{\boldsymbol{\theta}}_s^T \boldsymbol{\omega}_f)(\boldsymbol{\theta}_s^T \boldsymbol{\omega}_d) - (\tilde{\boldsymbol{\theta}}_s^T \boldsymbol{\omega}_d)(\boldsymbol{\theta}_s^T \boldsymbol{\omega}_f) - (\tilde{\boldsymbol{\theta}}_s^T \boldsymbol{\omega}_d)g(\mathbf{x})u_s}{(\boldsymbol{\theta}_s^T \boldsymbol{\omega}_d)^2} \\ & + 2\tilde{\boldsymbol{\theta}}_s^T \left(\sum_{j=1}^N w_j \dot{\boldsymbol{\theta}}_j + \sum_{j=1}^N \dot{w}_j \hat{\boldsymbol{\theta}}_j \right) \end{aligned} \quad (4.41)$$

Using

$$\begin{aligned} \sum_{j=1}^N w_j(t) &= 1 \\ \text{or, } \sum_{j=1}^N \dot{w}_j(t) &= 0 \end{aligned} \quad (4.42)$$

for $j = 1, \dots, N$, (4.42) can be written as

$$\dot{w}_N = -(\dot{w}_1 + \dots + \dot{w}_{N-1}). \quad (4.43)$$

The above discussion gives

$$\begin{aligned} \sum_{j=1}^N \dot{w}_j \hat{\theta}_j &= \dot{w}_1 \hat{\theta}_1 + \dots + \dot{w}_N \hat{\theta}_N \\ &= \dot{w}_1 (\hat{\theta}_1 - \hat{\theta}_N) + \dots + \dot{w}_{N-1} (\hat{\theta}_{N-1} - \hat{\theta}_N) \\ &= \dot{\mathbf{W}} \mathbf{Z}(t) \end{aligned} \quad (4.44)$$

where \mathbf{W} is estimated by $\hat{\mathbf{W}}$ and $\mathbf{Z}(t) = [(\hat{\theta}_1 - \hat{\theta}_N), \dots, (\hat{\theta}_{N-1} - \hat{\theta}_N)]$. Using (4.30) and (4.44), (4.41) is represented by

$$\begin{aligned} \dot{V}_s(\mathbf{e}_s, \tilde{\theta}_s) &= -\mathbf{e}_s^T \mathbf{e}_s + 2\mathbf{e}_s^T \mathbf{P} \frac{(\tilde{\theta}_s^T \boldsymbol{\omega}_f)(\boldsymbol{\theta}_s^T \boldsymbol{\omega}_d) - (\tilde{\theta}_s^T \boldsymbol{\omega}_d)(\boldsymbol{\theta}_s^T \boldsymbol{\omega}_f) - (\tilde{\theta}_s^T \boldsymbol{\omega}_d)g(\mathbf{x})u_s}{(\boldsymbol{\theta}_s^T \boldsymbol{\omega}_d)^2} \\ &\quad + 2\tilde{\theta}_s^T \left(-\sum_{j=1}^N w_j \frac{\sigma_1 (\boldsymbol{\omega}_d^T \hat{\theta}_j) \boldsymbol{\omega}_f^T - \boldsymbol{\omega}_d^T (\boldsymbol{\omega}_f^T \hat{\theta}_j) - \boldsymbol{\omega}_d^T g u_s}{(\boldsymbol{\omega}_d^T \hat{\theta}_j)^2} \right) e_{n_j} + \dot{\mathbf{W}} \mathbf{Z}(t). \end{aligned} \quad (4.45)$$

Using (4.32) and (4.33), (4.45) can be written as

$$\dot{V}_s(\mathbf{e}_s, \tilde{\theta}_s) = -\mathbf{e}_s^T \mathbf{e}_s + 2\mathbf{e}_s^T \mathbf{P} \frac{(\tilde{\theta}_s^T \boldsymbol{\omega}_f)(\boldsymbol{\theta}_s^T \boldsymbol{\omega}_d) - (\tilde{\theta}_s^T \boldsymbol{\omega}_d)(\boldsymbol{\theta}_s^T \boldsymbol{\omega}_f) - (\tilde{\theta}_s^T \boldsymbol{\omega}_d)g(\mathbf{x})u_s}{(\boldsymbol{\theta}_s^T \boldsymbol{\omega}_d)^2} - 2\mathbf{H}(t)\tilde{k}(t)\mathbf{Z}(t)\tilde{\theta}_s \quad (4.46)$$

Now, using (4.21) and (4.36) in (4.46) gives

$$\dot{V}_s(\mathbf{e}_s, \tilde{\theta}_s) \leq -\|\mathbf{e}_s\|^2 + 2\|\mathbf{P}\|b_\omega \|\mathbf{x}\| \|\tilde{\theta}_s\| \|\mathbf{e}_s\| + 2\|\mathbf{H}\| \|\tilde{k}\| \|\mathbf{Z}\| \|\tilde{\theta}_s\|. \quad (4.47)$$

A suitable design parameter b_ω can be chosen such that $b_\omega < \frac{\|\mathbf{e}_s\|^2 - 2\|\mathbf{H}\|\|\tilde{k}\|\|\mathbf{Z}\|\|\tilde{\theta}_s\|}{2\|\mathbf{P}\|\|\mathbf{x}\|\|\tilde{\theta}_s\|\|\mathbf{e}_s\|}$ for ensuring negative definiteness of the Lyapunov function $\dot{V}_s(\mathbf{e}_s, \tilde{\theta}_s)$. Consequently, the asymptotic stability of the overall system is attained. Since \dot{V}_s is negative definite, V_s is a decreasing function whose minimum value is zero. Also, V_s is positive definite, which implies that it will be zero only when $\mathbf{e}_s(t)$ and $\tilde{\theta}_s(t)$ are both zero, inferring that $\lim_{t \rightarrow \infty} \mathbf{e}_s(t) = 0$ and $\lim_{t \rightarrow \infty} \tilde{\theta}_s(t) = 0$.

4.5 Simulation Results

The proposed MMTLA controller is applied to a numerical example and a cart-pendulum system which are nonlinearly parameterized nonlinear systems. Moreover, the results obtained with MMTLA

control method are compared with a single model adaptive control method developed by Ge et al. [12] discussed in A.3.

Case 1: Numerical example

Let us consider a nonlinearly parameterized nonlinear system as given below [12]:

$$\begin{aligned}\dot{x}_1 &= x_2 \\ \dot{x}_2 &= \frac{x_1^2 + u}{e^{-x_1^2}(\theta_1 + \theta_2 x_2^2)}\end{aligned}\quad (4.48)$$

where θ_1 and θ_2 are the unknown parameters. Using (4.6), the estimation model for system (4.48) is built as

$$\begin{aligned}\dot{\hat{x}}_1 &= \lambda_1(\hat{x}_1 - x_1) + x_2 \\ \dot{\hat{x}}_2 &= \lambda_2(\hat{x}_2 - x_2) + \frac{x_1^2 + u}{e^{-x_1^2}(\hat{\theta}_1 + \hat{\theta}_2 x_2^2)}\end{aligned}\quad (4.49)$$

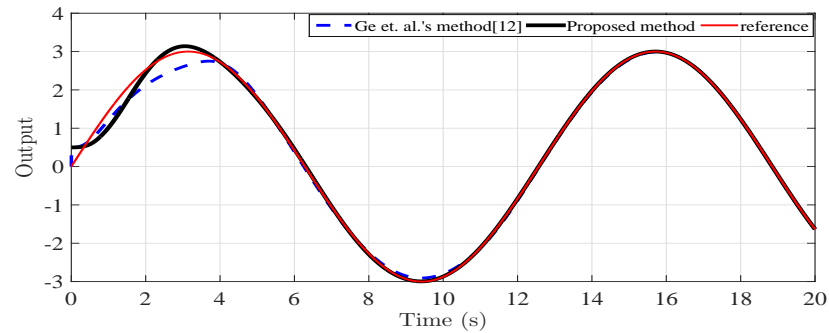
The control input for system (4.48) is found using (4.15) resulting in

$$u = -x_1^2 + \hat{v}(\hat{\theta}_1 + \hat{\theta}_2 x_2^2)e^{-x_1^2}\quad (4.50)$$

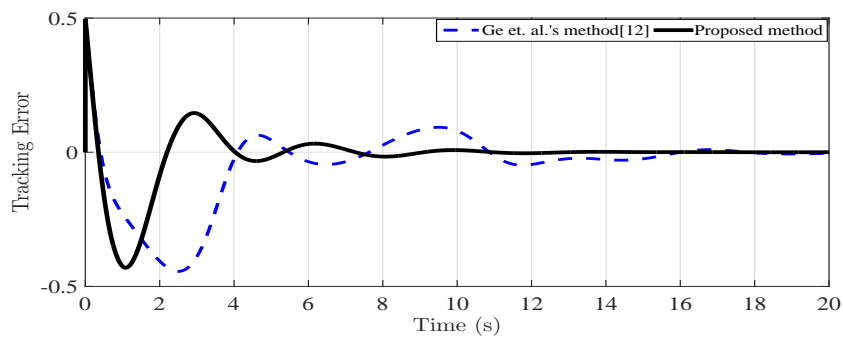
Adaptive laws for system (4.48) are found using (4.30) yielding

$$\begin{aligned}\dot{\hat{\theta}}_1 &= \iota_1 \frac{(x_1^2 + u)e_2}{e^{-x_1^2}(\hat{\theta}_1 + \hat{\theta}_2 x_2^2)^2} \\ \dot{\hat{\theta}}_2 &= \iota_2 \frac{(x_1^2 + u)x_2^2 e_2}{e^{-x_1^2}(\hat{\theta}_1 + \hat{\theta}_2 x_2^2)^2}\end{aligned}\quad (4.51)$$

where $e_2 = \hat{x}_2 - x_2$. Controller gains for virtual input v in (4.5) are chosen as $c_1 = 3, c_2 = 1$ and gains ι_1, ι_2 in (4.51) are chosen as $\iota_1 = 10, \iota_2 = 25$ as per [12] for fair comparison. The unknown parameter vector for this system $\theta_p = [\theta_1, \theta_2]^T = [2, 0.5]^T$ lies in the compact and bounded set $\mathcal{S}_\theta = [0.5, 3.5] \times [-0.5, 1.5]$. In Ge et al. [12] given in A.3, a single identification model is used where starting values of parameters are $\hat{\theta} = [0, 0]^T$. In the proposed MMTLA control method, 4 models are initialized at $\theta_j = ([0.5, -0.5], [0.5, 1.5], [3.5, -0.5], [3.5, 1.5])$. The system and the estimation model states start from $[0.5, 0]$. The reference trajectory to be tracked is chosen as $y_d = 3\sin(0.5t)$. The simulation results are plotted in Figure 4.1 - Figure 4.4. Table 4.1 compares the transient and steady state performances of the MMTLA control method with those of Ge et al.'s method [12]. The definitions of performance specifications can be found in A.5.



(a) Output



(b) Tracking Error

Figure 4.1: Case 1: Trajectory tracking**Table 4.1:** Simulation results: Case 1

Adaptation Mechanism	Performance Specification								
	M_p	M_u	t_s	e_{ss}	$t_c(\theta_1)$	$t_c(\theta_2)$	TV	CE	RMSE
Ge et al. [12]	13.076 %	14.63 %	19.87 s	0	23.6 s	18.7 s	5.53	1.57×10^3	0.072
MMTLA Control	9.94 %	8.60 %	10.8 s	0	9.8 s	8.89 s	4.75	1.54×10^3	0.051

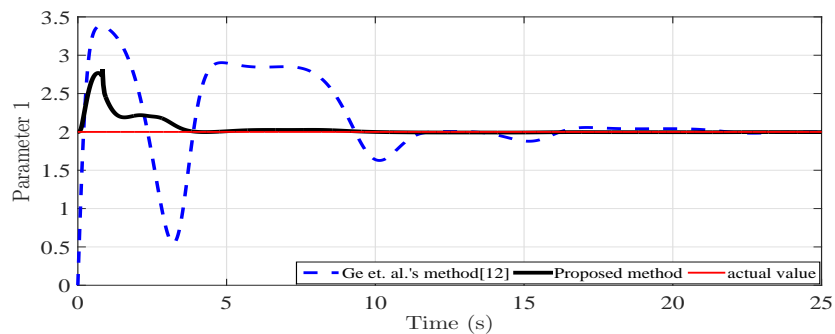
M_p : Peak overshoot, M_u : Peak undershoot

t_s : Settling time, e_{ss} : Steady state error

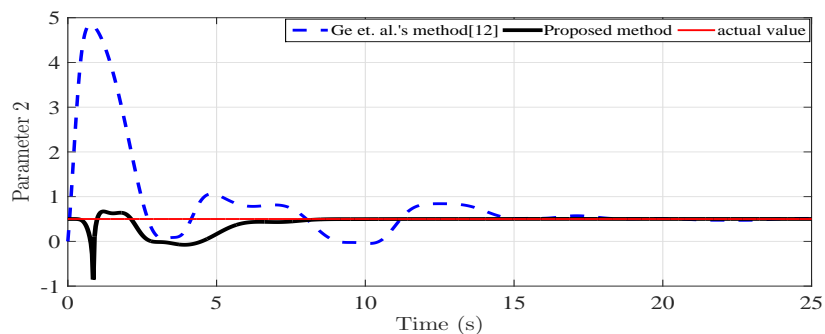
$t_c(\theta_1), t_c(\theta_2)$: Convergence time for first and second parameter respectively

TV : Total variation, CE : Control energy

RMSE : Root mean square error



(a) Parameter 1



(b) Parameter 2

Figure 4.2: Case 1: Parameter Convergence

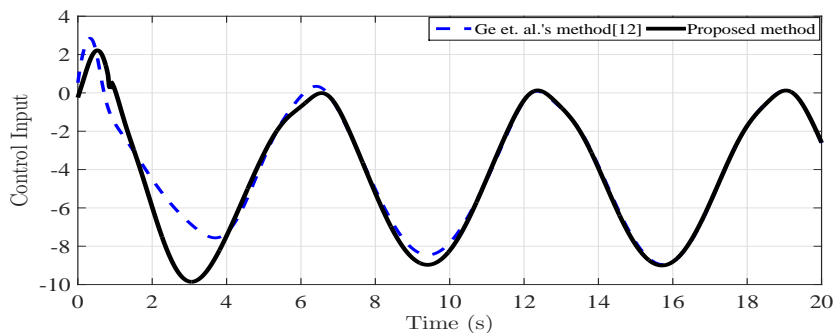


Figure 4.3: Case 1: Control Input

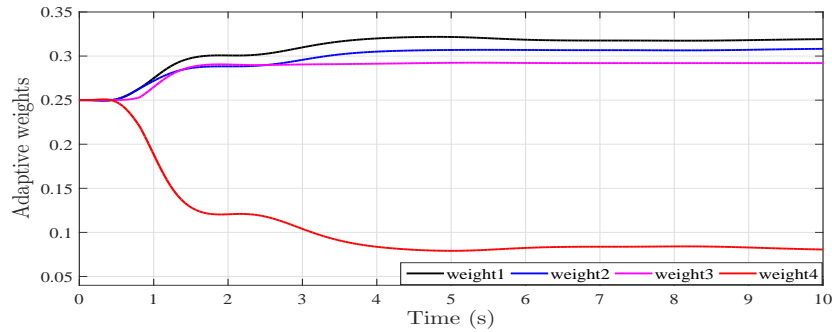


Figure 4.4: Case 1: Adaptive weights

From Table 4.1 it is evident that transient performance of the MMTLA control technique is far superior than that of Ge et al.'s [12] method. The control energy for both the methods are almost equal. However, smoother control input and faster convergence of parameters are advantages of the proposed MMTLA control method. It may be noted that parameter convergence time is drastically reduced in the MMTLA control method making it a potential candidate for online tuning problems.

Case 2: Cart-pendulum system

The proposed MMTLA control method is applied next to a cart-pendulum system shown in Figure 4.5. The design objective here is to control the vertical angle of the inverted pendulum by manipulating the balanced force applied to the cart. Attitude control of booster rocket at take-off is a real-world application of inverted pendulum control example. The cart-pendulum system is a second order nonlinearly parameterized nonlinear single-input single-output (SISO) system as described below [12]:

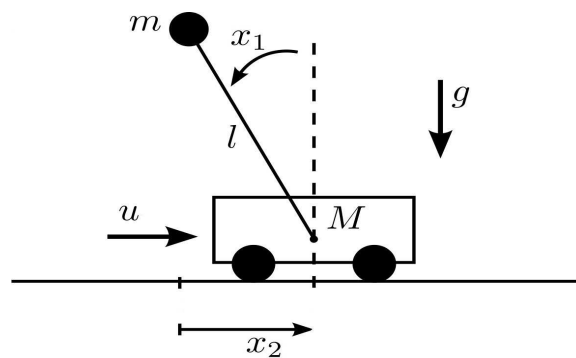


Figure 4.5: Cart-pendulum system

$$\begin{aligned}
 \dot{x}_1 &= x_2 \\
 \dot{x}_2 &= \frac{g \sin x_1 - \frac{mlx_2^2 \sin x_1 \cos x_1}{M+m}}{l \left(\frac{4}{3} - \frac{m \cos^2 x_1}{M+m} \right)} + \frac{\frac{\cos x_1}{M+m}}{l \left(\frac{4}{3} - \frac{m \cos^2 x_1}{M+m} \right)} u \\
 y &= x_1
 \end{aligned} \tag{4.52}$$

where x_1 and x_2 are the two states of the system, which physically represent the angular displacement and angular velocity of the pendulum respectively. Further, u is the applied control force. For simplicity, the system dynamics with respect to cart (cart distance, cart velocity) are ignored in the simulation study. The physical constants involved in the system (4.52) are specified in Table 4.2. System (4.52) can be described in the form of (4.1 - 4.2) as

Table 4.2: Physical system constants of cart-pendulum system

Symbol	Description	Value	Unit
M	Mass of cart	1	kg
m	Mass of the pendulum	0.2	kg
l	Half length of the pendulum	0.5	m
g	gravity constant	9.81	$kg - m/s^2$

$$\begin{aligned}
 \dot{x}_1 &= x_2 \\
 \dot{x}_2 &= \frac{g \sin x_1 + \frac{\theta_2 x_2^2 \sin x_1 \cos x_1}{\theta_1}}{\left(\frac{4l}{3} + \frac{\theta_2 \cos^2 x_1}{\theta_1} \right)} + \frac{\frac{\cos x_1}{\theta_1}}{\left(\frac{4l}{3} + \frac{\theta_2 \cos^2 x_1}{\theta_1} \right)} u \\
 y &= x_1
 \end{aligned} \tag{4.53}$$

with

$$\boldsymbol{\theta}_p = \begin{bmatrix} \theta_1 \\ \theta_2 \\ \theta_3 \end{bmatrix} = \begin{bmatrix} M + m \\ -ml \\ \frac{4}{3}l(M + m) \end{bmatrix} \tag{4.54}$$

$$\boldsymbol{\omega}_f(\mathbf{x}) = \begin{bmatrix} g \sin x_1 \\ x_2^2 \sin x_1 \cos x_1 \\ 0 \end{bmatrix}, \quad \boldsymbol{\omega}_d(\mathbf{x}) = \begin{bmatrix} 0 \\ \cos^2 x_1 \\ 1 \end{bmatrix} \quad \text{and}$$

$$g(\mathbf{x}) = \cos x_1 \tag{4.55}$$

which gives rise to control input,

$$u = \frac{1}{g(\mathbf{x})} \left[-\hat{\boldsymbol{\theta}}^T \boldsymbol{\omega}_f + \hat{\boldsymbol{\theta}}^T \boldsymbol{\omega}_d \hat{v} \right] \quad (4.56)$$

with adaptive laws given by (4.12) as

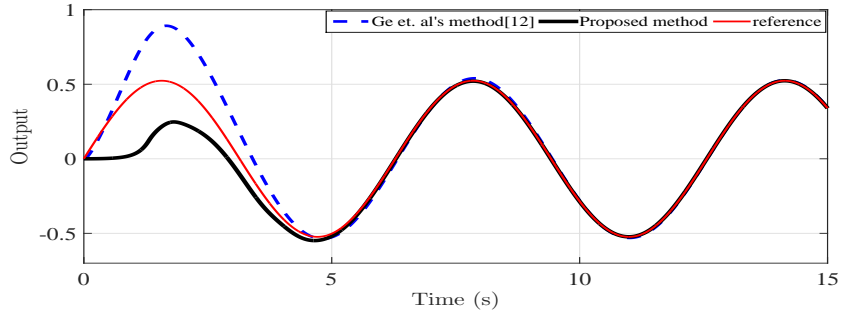
$$\begin{aligned} \dot{\hat{\theta}}_1 &= -\mathbf{g}_1(\hat{\theta}_2 g \sin x_1 \cos^2 x_1 + \hat{\theta}_3 g \sin x_1) e_2 / (\hat{\theta}_2 \cos^2 x_1 + \hat{\theta}_3)^2 \\ \dot{\hat{\theta}}_2 &= -\mathbf{g}_2(\hat{\theta}_3 x_2^2 \sin x_1 \cos x_1 - \hat{\theta}_1 g \sin x_1 \cos^2 x_1 - u \cos^3 x_1) e_2 / (\hat{\theta}_2 \cos^2 x_1 + \hat{\theta}_3)^2 \\ \dot{\hat{\theta}}_3 &= -\mathbf{g}_3(-\hat{\theta}_1 g \sin x_1 - \hat{\theta}_2 x_2^2 \sin x_1 \cos x_1 - u \cos x_1) e_2 / (\hat{\theta}_2 \cos^2 x_1 + \hat{\theta}_3)^2. \end{aligned} \quad (4.57)$$

Constants used in the virtual control v are chosen as $c_1 = 8, c_2 = 10$ and for controller parameters in (4.57), $\mathbf{g}_1 = 1, \mathbf{g}_2 = 1, \mathbf{g}_3 = 1$ are selected as per [12] for fair comparison. Assumption (i) in Section 4.2 for $g(\mathbf{x}) = \cos x_1$ is satisfied only for $|x_1| < \pi/2$. Hence, the simulation parameters need to be selected such that $|x_1| < \pi/2$ holds true for all time. Elements of the unknown parameter vector $\boldsymbol{\theta}_p = [\theta_1, \theta_2, \theta_3]^T = [1.2, -0.1, 0.8]^T$ belong to the compact and bounded set $\mathcal{S}_\theta = [-3, -0.4, -3] \times [3, 0.4, 3]$. In Ge et al. [12] given in A.3, a single adaptive identification model is used with parameters initialized at $\hat{\boldsymbol{\theta}} = [0, 0, 0]^T$. Likewise, for the proposed MMTLA control method $N = 8$ models are initialized at

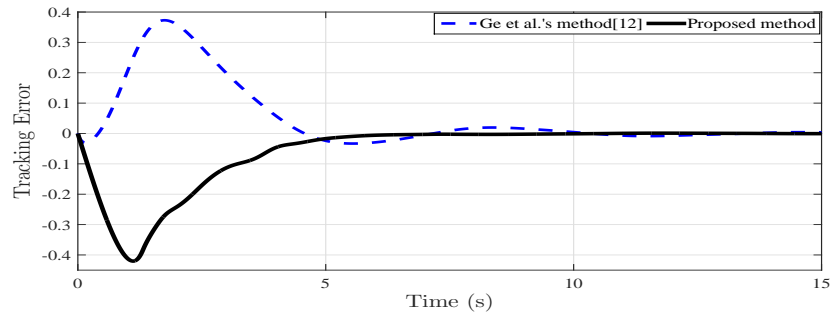
$$\boldsymbol{\theta}_j = ([-3, -0.4, -3], [-3, -0.4, 3], [-3, 0.4, -3], [-3, 0.4, 3], [3, -0.4, -3], [3, -0.4, 3], [3, 0.4, -3], [3, 0.4, 3]).$$

All the states of system and the identification models are initialized at 0. For tracking, $y_d = (\pi/6) \sin(t)$ is chosen as the desired trajectory. Figure 4.6 - Figure 4.9 compare the simulation results obtained using the proposed MMTLA control method with those obtained using Ge et al.'s method [12].

Further, Table 4.3 compares the transient and steady state performances of the system using the proposed MMTLA controller with those of Ge et al.'s method [12]. Table 4.3 clearly shows superiority of the proposed MMTLA control scheme over Ge et al.'s method [12] for all the transient and steady state performance specifications. The control input in the proposed MMTLA control method is far smoother than that of Ge et al.'s method [12]. Moreover, convergence time of the unknown parameters in the MMTLA method is significantly lesser. Additionally, the MMTLA controller achieves comparable output performance in terms of RMSE with those of [12] by spending lesser control energy.



(a) Output



(b) Tracking Error

Figure 4.6: Case 2: Trajectory tracking

Table 4.3: Simulation results: Case 2

Adaptation Mechanism	Performance Specification									
	M_p	M_u	t_s	e_{ss}	$t_c(\theta_1)$	$t_c(\theta_2)$	$t_c(\theta_3)$	TV	CE	RMSE
Ge et al. [12]	70.35 %	5.4 %	18.62 s	0	20.1 s	40.3 s	30.56 s	3.54	1.217×10^3	0.0663
MMTLA Control	52.7 %	4.57 %	9.47 s	0	7.72 s	40.1 s	25.1 s	1.74	1.091×10^3	0.0662

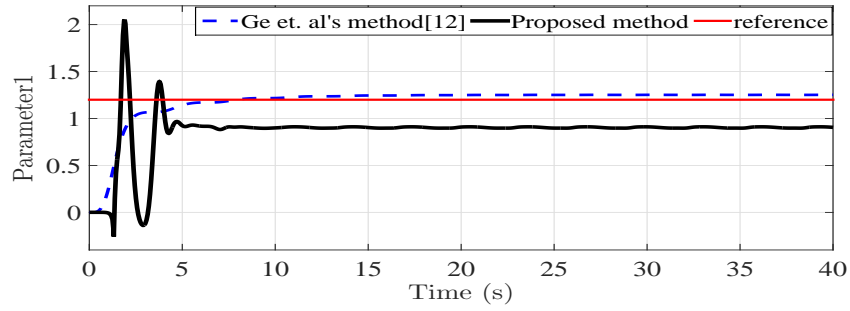
M_p : Peak overshoot, M_u : Peak undershoot

t_s : Settling time, e_{ss} : Steady state error

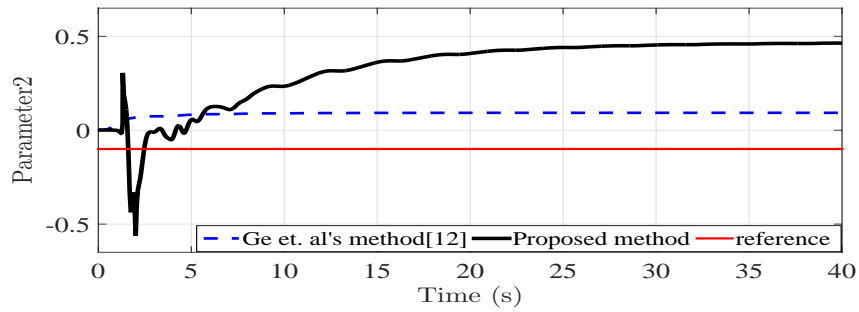
$t_c(\theta_1)$, $t_c(\theta_2)$, $t_c(\theta_3)$: Convergence time for first, second and third parameter respectively

TV : Total variation, CE : Control energy

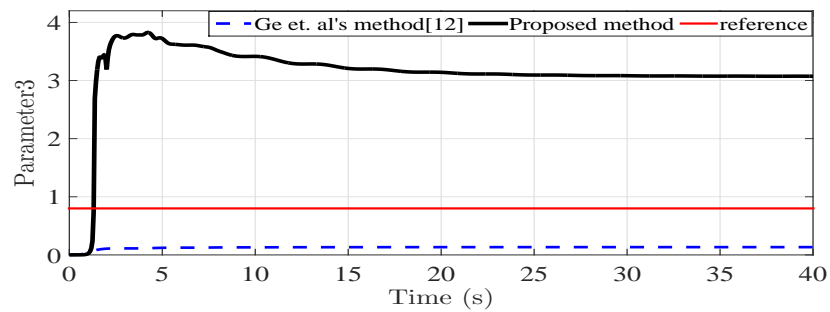
RMSE : Root mean square error



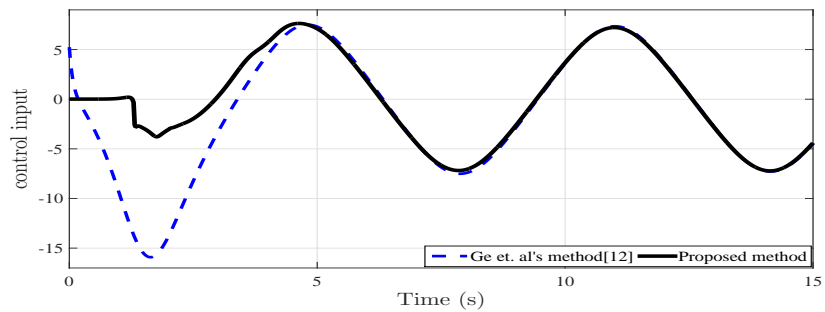
(a) Parameter 1



(b) Parameter 2



(c) Parameter 3

Figure 4.7: Case 2: Parameter Convergence**Figure 4.8: Case 2: Control Input**

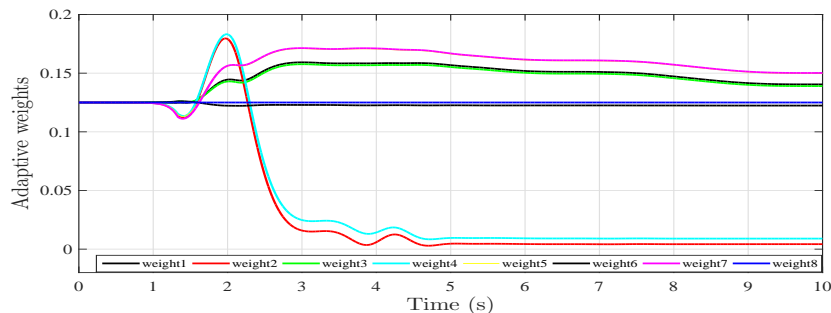


Figure 4.9: Case 2: Adaptive weights

4.6 Summary

A nonlinearly parameterized nonlinear system is adaptively controlled using the multiple model based two level adaptation (MMTLA) control method. The control input is found using the feedback linearization technique. The tuning laws for identifier parameter are obtained using Lyapunov stability criterion. Identification models at the first level are combined using adaptive weights efficiently to get the single second level model. Overall closed loop stability of the system and tracking error convergence with MMTLA control are established using Lyapunov criterion. Simulation results suggest that the offline selection of starting values of identifier parameters should be precise to minimize the control effort. Simulation results confirm improvement in transient, input and output performances with the MMTLA controller compared to an existing adaptive control technique. The MMTLA control technique is best suited for systems where parametric errors are large and convergence of first level models are slow.

5

Adaptive Controller Design for Nonlinear Coupled MIMO Systems Using Multiple Model Based Two Level Adaptation Technique

Contents

5.1	Introduction	68
5.2	System Description	69
5.3	Design of Estimation Model	70
5.4	Controller Design Using Feedback Linearization	70
5.5	Introduction of Multiple Models	75
5.6	Two Level Adaptation for Nonlinear MIMO Systems	75
5.7	Simulation and Experimental Results	81
5.8	Summary	98

5.1 Introduction

Controller design for nonlinear coupled MIMO systems is a challenging problem. Efforts are continuing to design controllers for nonlinear coupled MIMO systems by effectively handling the coupling [57–59]. In [57], a robust adaptive sliding mode controller was designed using fuzzy modeling for a class of uncertain MIMO nonlinear systems. Lee et al. [59] presented an adaptive control method for a class of nonlinear MIMO coupled systems where backstepping and adaptive fuzzy logic control were combined effectively to design a robust controller.

In this chapter, an adaptive controller using multiple model based two level adaptation (MMTLA) approach is designed for a class of nonlinear MIMO systems with cross-coupling. Unlike the MMAC with switching and tuning, in MMTLA the information from each and every model is used efficiently and all of them contribute simultaneously to control the system. Well known feedback linearization technique is used to design the control input which also decouples the nonlinear system [4, 6, 8, 40, 48]. The unknown parameters present in the model are estimated using an observer based estimation model [5, 45]. Adaptive tuning laws for the unknown parameters are derived using Lyapunov stability criterion. Further, for validating the proposed MMTLA method, a twin rotor MIMO system (TRMS) is considered. A TRMS is a nonlinear MIMO aerodynamical system with high cross-coupling between its two propellers [60]. A high nonlinearity, unstable system dynamics, inter-axis cross-coupling and parameter uncertainty are some basic challenges in designing a controller for the TRMS, which mimics a helicopter. In a real helicopter, the aerodynamic force is controlled by varying the angle of attack of the propeller blades. On the contrary, the TRMS is designed such that the angle of attack is fixed and the aerodynamic force is controlled by changing the speed of the motors [61]. A twin rotor MIMO system (TRMS) is an excellent and widely used laboratory model to test the performance of controllers designed for nonlinear MIMO cross-coupled systems. A good number of techniques has already been reported in the literature for designing controllers for the TRMS. Most of the methods available in literature use decoupling techniques to separate the system in the horizontal and vertical subsystems and treat the couplings as the uncertainty between subsystems [62–64]. Few other techniques using decoupling method include sliding mode controller [65, 66], backstepping controller [67], T-S fuzzy model based controller [68]. Similarly, there are methods available where coupling effects are treated as an integral part of the system and the controllers are designed without creating decoupled subsystems [26, 69]. Further, many other research groups like Liu et al. [70–72] contributed useful techniques and

results on helicopter control. Few recent works on helicopter control includes the robust controller design using backstepping decentralized method [73]. Similarly, a fault tolerant control (FTC) method using adaptive neural network is recently published [74].

Extensive simulation and experimental studies are conducted on the TRMS for pitch and yaw control using the proposed MMTLA method.

5.2 System Description

A class of nonlinear multi-input multi-output (MIMO) system [6] is considered as

$$\begin{aligned}\dot{\mathbf{x}} &= f(\mathbf{x}, \boldsymbol{\theta}_f) + \sum_{i=1}^m g_i(\mathbf{x}, \boldsymbol{\theta}_g) u_i \\ y_i &= h_i(\mathbf{x}), \quad i = 1, \dots, m\end{aligned}\tag{5.1}$$

where $\mathbf{x} : \mathbb{R}^+ \rightarrow \mathbb{R}^n$ is the state vector which is assumed to be fully available for measurement. Next, $u_i, y_i : \mathbb{R}^+ \rightarrow \mathbb{R}$ are the control inputs and system outputs respectively. Further, $f, g_i : \mathbb{R}^n \rightarrow \mathbb{R}^n$, and $h_i : \mathbb{R}^n \rightarrow \mathbb{R}$ are sufficiently smooth vector fields. Lastly, $\boldsymbol{\theta}_f \in \mathcal{S}_f, \boldsymbol{\theta}_g \in \mathcal{S}_g$ are the unknown parameter vectors with compact sets $\mathcal{S}_f \subset \mathbb{R}^{p_f}, \mathcal{S}_g \subset \mathbb{R}^{p_g}$. Here, it is assumed that all the inputs u_i 's are interacting with all the outputs y_i 's or the system (5.1) is a coupled system. Additionally, the following properties are assumed about the system (5.1):

- (i) Functions $f(\mathbf{x}, \boldsymbol{\theta}_f)$ and $g_i(\mathbf{x}, \boldsymbol{\theta}_g)$ are characterized as

$$\begin{aligned}f(\mathbf{x}, \boldsymbol{\theta}_f) &= \boldsymbol{\omega}_f^T(\mathbf{x}) \boldsymbol{\theta}_f \\ g_i(\mathbf{x}, \boldsymbol{\theta}_g) &= \boldsymbol{\omega}_{g_i}^T(\mathbf{x}) \boldsymbol{\theta}_g\end{aligned}\tag{5.2}$$

where $\boldsymbol{\omega}_f(\mathbf{x})$ and $\boldsymbol{\omega}_{g_i}(\mathbf{x})$ are known matrices.

- (ii) The system has constant relative degree γ_i [6], i.e.

- (a) $L_{g_i(\mathbf{x}, \boldsymbol{\theta}_g)} L_{f(\mathbf{x}, \boldsymbol{\theta}_f)}^{i-1} h_i(\mathbf{x}) = 0, \quad i = 1, 2, \dots, (\gamma_i - 1)$
(b) $L_{g_i(\mathbf{x}, \boldsymbol{\theta}_g)} L_{f(\mathbf{x}, \boldsymbol{\theta}_f)}^{\gamma_i-1} h_i(\mathbf{x}) \neq 0, \quad \forall \mathbf{x} \in \mathbb{R}^n, \boldsymbol{\theta}_f \in \mathcal{S}_f, \boldsymbol{\theta}_g \in \mathcal{S}_g.$

where L is the Lie derivative defined as $L_f h(\mathbf{x}) = \frac{dh(\mathbf{x})}{dx} f(\mathbf{x})$.

- (iii) The equilibrium point of the zero dynamics of the system (5.1) is asymptotically stable [6].

5.3 Design of Estimation Model

In this section, an observer based estimation model [5,45] is designed for the system (5.1). Using (5.2), (5.1) can be written as

$$\dot{\mathbf{x}} = \boldsymbol{\omega}_f^T(\mathbf{x})\boldsymbol{\theta}_f + \sum_{i=1}^m \boldsymbol{\omega}_{g_i}^T(\mathbf{x})\boldsymbol{\theta}_g u_i \quad (5.3)$$

The observer based estimation model [5,45] for the system (5.3) is defined as

$$\dot{\hat{\mathbf{x}}} = \mathbf{A}(\hat{\mathbf{x}} - \mathbf{x}) + \boldsymbol{\omega}_f^T(\mathbf{x})\hat{\boldsymbol{\theta}}_f + \sum_{i=1}^m \boldsymbol{\omega}_{g_i}^T(\mathbf{x})\hat{\boldsymbol{\theta}}_g u_i \quad (5.4)$$

Consequently, the estimation error dynamics for (5.2) are given as

$$\dot{\mathbf{e}}_I = \mathbf{A}\mathbf{e}_I + \boldsymbol{\omega}_f^T(\mathbf{x})\tilde{\boldsymbol{\theta}}_f + \sum_{i=1}^m \boldsymbol{\omega}_{g_i}^T(\mathbf{x})\tilde{\boldsymbol{\theta}}_g u_i \quad (5.5)$$

with $\mathbf{e}_I = \hat{\mathbf{x}} - \mathbf{x}$, $\tilde{\boldsymbol{\theta}}_f = \hat{\boldsymbol{\theta}}_f - \boldsymbol{\theta}_f$, $\tilde{\boldsymbol{\theta}}_g = \hat{\boldsymbol{\theta}}_g - \boldsymbol{\theta}_g$. Also, the matrix $\mathbf{A} \in \mathbb{R}^{n \times n}$ is a stable matrix chosen by the designer. A suitable Lyapunov function $V(\mathbf{e}_I, \tilde{\boldsymbol{\theta}}_f, \tilde{\boldsymbol{\theta}}_g) = \mathbf{e}_I^T \mathbf{P} \mathbf{e}_I + \tilde{\boldsymbol{\theta}}_f^T \tilde{\boldsymbol{\theta}}_f + \tilde{\boldsymbol{\theta}}_g^T \tilde{\boldsymbol{\theta}}_g$ is chosen, where \mathbf{P} is the positive definite matrix solution of the Lyapunov function $\mathbf{A}^T \mathbf{P} + \mathbf{P} \mathbf{A} = -\mathbf{Q}$ and $\mathbf{Q} = \mathbf{Q}^T > 0$.

Thereupon, using adaptive laws for the parameter estimates as

$$\begin{aligned} \dot{\tilde{\boldsymbol{\theta}}}_f &= \dot{\hat{\boldsymbol{\theta}}}_f = -\boldsymbol{\omega}_f^T(\mathbf{x})\mathbf{P}\mathbf{e}_I \\ \dot{\tilde{\boldsymbol{\theta}}}_{g_i} &= \dot{\hat{\boldsymbol{\theta}}}_{g_i} = -\boldsymbol{\omega}_{g_i}^T(\mathbf{x})u_i\mathbf{P}\mathbf{e}_I \end{aligned} \quad (5.6)$$

it can be guaranteed that $\mathbf{e}_I \rightarrow 0$ as $t \rightarrow \infty$, following *Theorem 2.1* in [45]. Also, if the regressor vectors $\boldsymbol{\omega}_f(\mathbf{x}), \boldsymbol{\omega}_{g_i}(\mathbf{x})$ are rich enough [7] (A.1), $\tilde{\boldsymbol{\theta}} = [\tilde{\boldsymbol{\theta}}_f, \tilde{\boldsymbol{\theta}}_g]^T$ converges to zero asymptotically [6,45].

5.4 Controller Design Using Feedback Linearization

A tracking control problem is considered now. For a MIMO system with a well defined relative degree ' γ_i ', a virtual control input ' v_i ' can be defined such that the system nonlinearity is cancelled. This gives a simple integrator system between output and new input ' v_i ', making the design of the controller simple using a linear technique. If the desired output and its derivatives $[y_{d_i}, \dot{y}_{d_i}, \dots, y_{d_i}^{(\gamma_i)}]$ are smooth and bounded, ' v_i ' can be designed to follow the desired trajectory y_{d_i} , such that the whole system remains bounded and tracking error $e_i = y_{d_i} - y_i$ converges to zero asymptotically. The feedback linearization technique used to design a state feedback controller for a nonlinear coupled MIMO system which is also decoupled in the process is discussed in this section. The decoupling

problem or noninteracting control problem is solvable using static state feedback if and only if the system has a relative degree γ_i [8] at the equilibrium point.

The outputs y_i in (5.1) are differentiated γ_i times with respect to time, such that at least one of the inputs appears in $y_i^{(\gamma_i)}$ [6], i.e.

$$y_i^{(\gamma_i)} = L_{f(\mathbf{x}, \boldsymbol{\theta}_f)}^{\gamma_i} h_i(\mathbf{x}) + \sum_{i=1}^m L_{g_i}(L_{f(\mathbf{x}, \boldsymbol{\theta}_f)}^{\gamma_i-1} h_i(\mathbf{x})) u_i \quad (5.7)$$

with at least one of the $L_{g_i}(L_{f(\mathbf{x}, \boldsymbol{\theta}_f)}^{\gamma_i-1} h_i(\mathbf{x})) \neq 0, \forall \mathbf{x} \in \mathbb{R}^n, \boldsymbol{\theta}_f \in \mathcal{S}_f, \boldsymbol{\theta}_g \in \mathcal{S}_g$. Thereafter, a $m \times 1$ matrix $\mathfrak{B}(\mathbf{x}, \boldsymbol{\theta}_f)$ and a $m \times m$ matrix $\mathfrak{A}(\mathbf{x}, \boldsymbol{\theta}_f, \boldsymbol{\theta}_g)$ are defined respectively as

$$\mathfrak{B}(\mathbf{x}, \boldsymbol{\theta}_f) = \begin{bmatrix} L_{f(\mathbf{x}, \boldsymbol{\theta}_f)}^{\gamma_1} h_1(\mathbf{x}) \\ \cdot \\ \cdot \\ \cdot \\ L_{f(\mathbf{x}, \boldsymbol{\theta}_f)}^{\gamma_m} h_m(\mathbf{x}) \end{bmatrix}, \quad \mathfrak{A}(\mathbf{x}, \boldsymbol{\theta}_f, \boldsymbol{\theta}_g) = \begin{bmatrix} L_{g_1(\mathbf{x}, \boldsymbol{\theta}_g)}(L_{f(\mathbf{x}, \boldsymbol{\theta}_f)}^{\gamma_1-1} h_1(\mathbf{x})) & \cdot & \cdot & \cdot & L_{g_m(\mathbf{x}, \boldsymbol{\theta}_g)}(L_{f(\mathbf{x}, \boldsymbol{\theta}_f)}^{\gamma_1-1} h_1(\mathbf{x})) \\ \cdot & & & & \cdot \\ \cdot & & & & \cdot \\ \cdot & & & & \cdot \\ L_{g_1(\mathbf{x}, \boldsymbol{\theta}_g)}(L_{f(\mathbf{x}, \boldsymbol{\theta}_f)}^{\gamma_m-1} h_m(\mathbf{x})) & \cdot & \cdot & \cdot & L_{g_m(\mathbf{x}, \boldsymbol{\theta}_g)}(L_{f(\mathbf{x}, \boldsymbol{\theta}_f)}^{\gamma_m-1} h_m(\mathbf{x})) \end{bmatrix} \quad (5.8)$$

such that (5.7) can be written as

$$y_i^{(\gamma_i)} = \mathfrak{B}(\mathbf{x}, \boldsymbol{\theta}_f) + \mathfrak{A}(\mathbf{x}, \boldsymbol{\theta}_f, \boldsymbol{\theta}_g) u_i. \quad (5.9)$$

Here matrix \mathfrak{A} is referred to as decoupling matrix. As stated earlier, the decoupling problem is solvable if and only if the system has a vector relative degree or the decoupling matrix \mathfrak{A} is nonsingular. Subsequently, if $\mathfrak{A}(\mathbf{x}, \boldsymbol{\theta}_f, \boldsymbol{\theta}_g) \in \mathbb{R}^{m \times m}$ is bounded away from singularity, the state feedback control law

$$u_i = \mathfrak{A}(\mathbf{x}, \boldsymbol{\theta}_f, \boldsymbol{\theta}_g)^{-1} [-\mathfrak{B}(\mathbf{x}, \boldsymbol{\theta}_f) + v_i], \quad i = 1, \dots, m \quad (5.10)$$

yields the closed-loop decoupled, linear system

$$y_i^{(\gamma_i)} = v_i, \quad i = 1, \dots, m \quad (5.11)$$

Here control v_i is chosen to make the outputs $y_i(t)$ track their respective desired outputs $y_{d_i}(t)$, i.e.,

$$v_i = y_{d_i}^{(\gamma_i)} + c_{1_i}(y_{d_i}^{(\gamma_i-1)} - y_i^{(\gamma_i-1)}) + \dots + c_{\gamma_i}(y_{d_i} - y_i) \quad (5.12)$$

with all $c_{1_i}, \dots, c_{\gamma_i}$ chosen so that $s^{\gamma_i} + c_{1_i}s^{\gamma_i-1} + \dots + c_{\gamma_i}$ are Hurwitz polynomials. The feedback law in (5.10) is popularly known as *static state-feedback linearizing control law* [6].

Further, as $\theta = [\theta_f, \theta_g]^T$ is the unknown parameter vector, at any time t , the estimates of f and g are

$$\begin{aligned} f(\mathbf{x}, \hat{\theta}_f) &= \omega_f^T(\mathbf{x})\hat{\theta}_f \\ g_i(\mathbf{x}, \hat{\theta}_g) &= \omega_{g_i}^T(\mathbf{x})\hat{\theta}_g \end{aligned} \quad (5.13)$$

with $\hat{\theta}, \hat{\theta}_f, \hat{\theta}_g$ being the estimates of $\theta, \theta_f, \theta_g$ respectively at time t . Therefore, the control law (5.10) is rewritten as

$$u_i = \mathfrak{A}(\mathbf{x}, \hat{\theta}_f, \hat{\theta}_g)^{-1}[-\mathfrak{B}(\mathbf{x}, \hat{\theta}_f) + \hat{v}_i] \quad (5.14)$$

with the unknown parameter vector $\theta = [\theta_f, \theta_g]$ in (5.10) being replaced by its estimate $\hat{\theta} = [\hat{\theta}_f, \hat{\theta}_g]^T$. In (5.14), the parameter estimate $\hat{\theta}$ can be chosen such that $\mathfrak{A}(\mathbf{x}, \hat{\theta})$ is non-singular [6]. To do so, projection technique [44] is used to keep parameter estimates $\hat{\theta}$ in a compact region \mathcal{S}_θ [48]. Also, \hat{v}_i is the estimate of v_i given as,

$$\hat{v}_i = y_{d_i}^{(\gamma_i)} + c_{1_i}(y_{d_i}^{(\gamma_i-1)} - \hat{y}_i^{(\gamma_i-1)}) + \dots + c_{\gamma_i}(y_{d_i} - \hat{y}_i). \quad (5.15)$$

The estimate \hat{v}_i is required since derivatives of output $\dot{y}_i, \ddot{y}_i, \dots, y_i^{(\gamma_i-1)}$ in (5.7) are functions of unknown parameters θ .

Moreover, if $\mathfrak{A}(\mathbf{x}, \theta)$ defined in (5.8) is nonsingular for all $\mathbf{x} \in \mathbb{R}^n$, a diffeomorphism $(\tau, \xi) = \psi(\mathbf{x})$ can be defined [6] as

$$\tau = \begin{bmatrix} h_1 & L_f h_1 & \cdot & \cdot & L_f^{\gamma_1-1} h_1 \\ \cdot & \cdot & & & \cdot \\ \cdot & \cdot & & & \cdot \\ h_m & L_f h_m & \cdot & \cdot & L_f^{\gamma_m-1} h_m \end{bmatrix} \quad (5.16)$$

Therefore, (5.1) can be reclassified in terms of these new co-ordinates as

$$\begin{aligned}
 \dot{\tau}_{11} &= \tau_{12} \\
 &\cdot \\
 \dot{\tau}_{1\gamma_1} &= f_1(\boldsymbol{\tau}, \boldsymbol{\xi}) + g_1(\boldsymbol{\tau}, \boldsymbol{\xi})u_1 \\
 \dot{\tau}_{21} &= \tau_{22} \\
 &\cdot \\
 \dot{\tau}_{2\gamma_2} &= f_2(\boldsymbol{\tau}, \boldsymbol{\xi}) + g_2(\boldsymbol{\tau}, \boldsymbol{\xi})u_2 \\
 &\cdot \\
 &\cdot \\
 \dot{\tau}_{m1} &= \tau_{m2} \\
 &\cdot \\
 \dot{\tau}_{m\gamma_m} &= f_m(\boldsymbol{\tau}, \boldsymbol{\xi}) + g_m(\boldsymbol{\tau}, \boldsymbol{\xi})u_m \\
 \dot{\boldsymbol{\xi}} &= \varphi(\boldsymbol{\tau}, \boldsymbol{\xi}) \\
 y_1 &= \tau_{11} \\
 y_2 &= \tau_{21} \\
 &\cdot \\
 y_m &= \tau_{m1}
 \end{aligned} \tag{5.17}$$

where $f_1(\boldsymbol{\tau}, \boldsymbol{\xi})$ stands for $L_f^{\gamma_1} h_1(\mathbf{x})$ and $g_1(\boldsymbol{\tau}, \boldsymbol{\xi})$ stands for the first row of $\mathfrak{A}(\mathbf{x}, \boldsymbol{\theta})$ in the $(\boldsymbol{\tau}, \boldsymbol{\xi})$ co-ordinates. Besides, for $\mathbf{x} = 0$, equilibrium point of the system (5.1), the dynamics $\dot{\boldsymbol{\xi}} = \varphi(\mathbf{0}, \boldsymbol{\xi})$ is referred to as the zero dynamics, which is assumed to be asymptotically stable for this case. The asymptotic boundedness of zero dynamics can be easily established using *Proposition 2.1* of [6] for a MIMO system.

Furthermore, for the system given in (5.17), applying input (5.14) in the re-arranged form as

$$\begin{pmatrix} u_1 \\ u_2 \\ \cdot \\ u_m \end{pmatrix} = \mathfrak{A}(\boldsymbol{\tau}, \boldsymbol{\xi})^{-1} \left[-\mathfrak{B}(\boldsymbol{\tau}, \boldsymbol{\xi}) + \begin{pmatrix} \hat{v}_1 \\ \hat{v}_2 \\ \cdot \\ \hat{v}_m \end{pmatrix} \right] \tag{5.18}$$

will provide a system characterized by the following set of equations:

$$\begin{aligned}
 \dot{\tau}_{11} &= \tau_{12} \\
 &\cdot \\
 \dot{\tau}_{1\gamma_1} &= v_1 \\
 \dot{\tau}_{21} &= \tau_{22} \\
 &\cdot \\
 \dot{\tau}_{2\gamma_2} &= v_2 \\
 &\cdot \\
 &\cdot \\
 \dot{\tau}_{m1} &= \tau_{m2} \\
 &\cdot \\
 \dot{\tau}_{m\gamma_m} &= v_m \\
 y_i &= \tau_{i1}, \quad 1 \leq i \leq m
 \end{aligned} \tag{5.19}$$

The structure of the m set of equations given in (5.19) shows that noninteraction among the loops is achieved. As can be observed in Figure 5.1, the input v_1 is affecting only output y_1 through a chain of γ_1 integrators. Similarly the other set of inputs v_2, \dots, v_m is controlling only their respective outputs y_2, \dots, y_m [8].

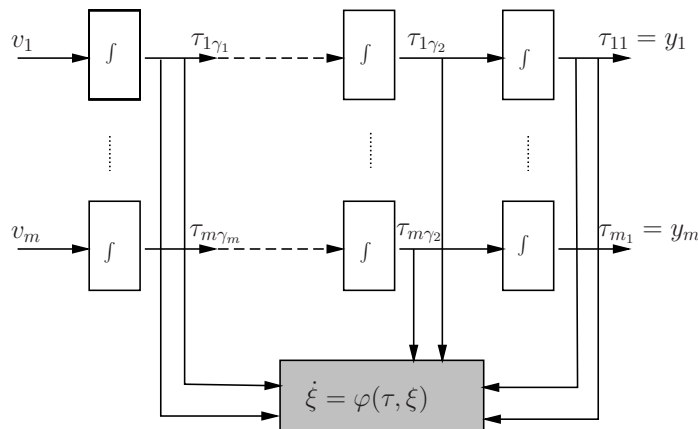


Figure 5.1: Noninteracting control

5.5 Introduction of Multiple Models

The previous sections are dedicated to adaptive control design of a class of nonlinear MIMO coupled system using single estimation model. In case of multiple models, the same estimator structure (5.4) is used for all the models but with N different parameter vector estimates $\hat{\boldsymbol{\theta}}_{f_j}, \hat{\boldsymbol{\theta}}_{g_j}, j = 1, \dots, N$, placed at different starting points inside the compact space $\mathcal{S}_f, \mathcal{S}_g$. Therefore, dynamics of N estimation models are given as

$$\dot{\hat{\mathbf{x}}}_j = \mathbf{A}(\hat{\mathbf{x}}_j - \mathbf{x}) + \boldsymbol{\omega}_f^T(\mathbf{x})\hat{\boldsymbol{\theta}}_{f_j} + \sum_{i=1}^m \boldsymbol{\omega}_{g_i}^T(\mathbf{x})\hat{\boldsymbol{\theta}}_{g_j}u_i \quad (5.20)$$

where $\hat{\mathbf{x}}_j$ denotes the state vector of the j -th estimation model. Following the earlier approach, the identifier error dynamics for each model is given as

$$\dot{\mathbf{e}}_{I_j} = \mathbf{A}\mathbf{e}_{I_j} + \boldsymbol{\omega}_f^T(\mathbf{x})\tilde{\boldsymbol{\theta}}_{f_j} + \sum_{i=1}^m \boldsymbol{\omega}_{g_i}^T(\mathbf{x})\tilde{\boldsymbol{\theta}}_{g_j}u_i \quad (5.21)$$

Similarly, the adaptive laws for the j -th model parameter vector $\hat{\boldsymbol{\theta}}_j = [\hat{\boldsymbol{\theta}}_{f_j}, \hat{\boldsymbol{\theta}}_{g_j}]^T$ can be found as

$$\begin{aligned} \dot{\tilde{\boldsymbol{\theta}}}_{f_j} &= \dot{\hat{\boldsymbol{\theta}}}_{f_j} = -\boldsymbol{\omega}_f^T(\mathbf{x})\mathbf{P}\mathbf{e}_{I_j} \\ \dot{\tilde{\boldsymbol{\theta}}}_{g_{i_j}} &= \dot{\hat{\boldsymbol{\theta}}}_{g_{i_j}} = -\boldsymbol{\omega}_{g_i}^T(\mathbf{x})u_i\mathbf{P}\mathbf{e}_{I_j} \end{aligned} \quad (5.22)$$

with system parameter vector $\boldsymbol{\theta}_f, \boldsymbol{\theta}_g$ and estimator model parameter vector $\hat{\boldsymbol{\theta}}_{f_j}, \hat{\boldsymbol{\theta}}_{g_j}$ both belonging to compact spaces \mathcal{S}_f and \mathcal{S}_g . The initial values of parameter estimates $\hat{\boldsymbol{\theta}}_j(t_0) = [\hat{\boldsymbol{\theta}}_{f_j}(t_0), \hat{\boldsymbol{\theta}}_{g_j}(t_0)]^T$ on parameter space $\mathcal{S}_f, \mathcal{S}_g$ are selected such that $\hat{\boldsymbol{\theta}}_j(t_0)$ covers the full parameter space [10].

5.6 Two Level Adaptation for Nonlinear MIMO Systems

In this section, the concept of second level adaptation introduced by Narendra et al. [20] for linear systems will be extended for a class of nonlinear MIMO coupled systems as discussed in Section 5.2. In methods reported earlier [9, 16], multiple models with switching selected one particular model at a time, based on the control error and changed the controller parameters accordingly. In the proposed case of multiple model based two level adaptation (MMTLA), there is no switching between models and all the models are used in the two levels. The regions of uncertainty of all the parameters are known and bounded. If the uncertainty region is big, initiation of a single estimation model farther from the actual value will lead to high transients and poor convergence. Therefore, different estimation models are initiated at different points within the bounded region. Adaptation of models at the first

level and their combination at the second level will enable the parameters to reach closer to their actual values with lesser transients and faster convergence. The combination of parameter models at the first level is done in such a manner that it follows the properties of convexity as defined in Section 3.3.3.

Following definition 3.1 in Section 3.3.3, the convex combination of first level models $\hat{\boldsymbol{\theta}}_{f_j}(t), \hat{\boldsymbol{\theta}}_{g_j}(t)$ with suitably chosen adaptive weights $w_j(t)$ gives rise to another single adaptive model termed as second level model $\boldsymbol{\theta}_s(t) = [\boldsymbol{\theta}_{s_f}(t), \boldsymbol{\theta}_{s_g}(t)]^T$ given as

$$\begin{aligned}\boldsymbol{\theta}_{s_f}(t) &= \sum_{j=1}^N w_j(t) \hat{\boldsymbol{\theta}}_{f_j}(t) \\ \boldsymbol{\theta}_{s_g}(t) &= \sum_{j=1}^N w_j(t) \hat{\boldsymbol{\theta}}_{g_j}(t)\end{aligned}\tag{5.23}$$

with the adaptive weights $w_j(t)$ satisfying the convexity conditions as $w_j(t) \geq 0$ and $\sum_{j=1}^N w_j(t) = 1$. The adaptive law for the adaptive weights $w_j(t)$ is provided in Section 3.3.3. Basically, the aim here is to assure that actual parameter vector $\boldsymbol{\theta}(t) = [\boldsymbol{\theta}_f(t), \boldsymbol{\theta}_g(t)]^T$ and second level parameter vector $\boldsymbol{\theta}_s(t) = [\boldsymbol{\theta}_{s_f}(t), \boldsymbol{\theta}_{s_g}(t)]^T$ lie in the convex region of first level parameter vectors $\hat{\boldsymbol{\theta}}_j = [\hat{\boldsymbol{\theta}}_{f_j}, \hat{\boldsymbol{\theta}}_{g_j}]^T$ for all $t \geq t_0$.

Therefore, following Theorem 3.3 and using the second level parameter vector $\boldsymbol{\theta}_s(t)$ with adaptive weights $w_j(t)$ at every instant, the new control input u_{s_i} can be obtained as

$$u_{s_i} = \mathfrak{A}_s(\mathbf{x}, \boldsymbol{\theta}_s)^{-1} [-\mathfrak{B}_s(\mathbf{x}, \boldsymbol{\theta}_{s_f}) + \hat{v}_i]\tag{5.24}$$

In (5.24) above, $\mathfrak{A}_s(\mathbf{x}, \boldsymbol{\theta}_s)$ is assumed to be bounded away from zero because of the fact that $\boldsymbol{\theta}_s$ always resides inside the convex hull of $\hat{\boldsymbol{\theta}}_j$ [6, 48]. Following Theorem 7.3.1 of [48], the parameters $\hat{\boldsymbol{\theta}}_j$ are kept in a certain range, such that, at every point inside their convex hull, $\mathfrak{A}_s(\mathbf{x}, \boldsymbol{\theta}_s)$ is bounded away from zero.

In this work, projection based adaptive laws [43, 44] are used to ensure the boundedness of estimated parameters to the predefined compact region $\mathcal{S}_\theta = [\mathcal{S}_f, \mathcal{S}_g]$. Therefore, applying projection, the system parameter estimate in (5.23) can be rewritten as

$$\boldsymbol{\theta}_s(t) = Proj_{\boldsymbol{\theta}_s(t) \in \mathcal{S}_\theta} \left\{ \sum_{j=1}^N w_j(t) \hat{\boldsymbol{\theta}}_j(t) \right\}.\tag{5.25}$$

Moreover, in adaptive control problems, the convergence of estimated parameters depends on the rich-

ness of its reference input with respect to the frequency content [7, 44]. For that purpose, persistence of excitation (PE) [7] of input signal is assumed to ensure the convergence of estimated parameters to their actual values.

5.6.1 System stability and tracking error convergence using two level adaptation

This section discussed the overall system stability with two level adaptation as well as convergence of control and parameter errors.

Representing $\mathfrak{B}_s(\mathbf{x}, \boldsymbol{\theta}_{s_f})$, $\mathfrak{A}_s(\mathbf{x}, \boldsymbol{\theta}_{s_f}, \boldsymbol{\theta}_{s_g})$ of (5.24) in terms of multilinear parameter elements [6, 10] as

$$\begin{aligned}\mathfrak{B}_s(\mathbf{x}, \boldsymbol{\theta}_{s_f}) &= \mathcal{P}_f^T \mathcal{F}(\mathbf{x}) \\ \mathfrak{A}_s(\mathbf{x}, \boldsymbol{\theta}_{s_f}, \boldsymbol{\theta}_{s_g}) &= \mathcal{P}_{gf}^T \mathcal{G}(\mathbf{x})\end{aligned}\quad (5.26)$$

with $\mathcal{P}_f^T = [\mathcal{P}_{f_1}, \dots, \mathcal{P}_{f_m}]$, $\mathcal{F}(\mathbf{x}) = [\mathcal{F}_1(\mathbf{x}), \dots, \mathcal{F}_m(\mathbf{x})]^T$ and $\mathcal{P}_{gf}^T = \begin{bmatrix} \mathcal{P}_{g1f1} & \cdot & \mathcal{P}_{gmf1} \\ \cdot & \cdot & \cdot \\ \mathcal{P}_{g1fm} & \cdot & \mathcal{P}_{gmfm} \end{bmatrix}$,

$\mathcal{G}(\mathbf{x}) = [\mathcal{G}_1(\mathbf{x}), \dots, \mathcal{G}_m(\mathbf{x})]^T$.

Consequently, rewriting control input u_{s_i} in (5.24) in terms of estimated values of multilinear parameter elements \mathcal{P}_{fs} , \mathcal{P}_{gfs} as

$$u_{s_i} = (\mathcal{P}_{gfs}^T \mathcal{G}(\mathbf{x}))^{-1} [-\mathcal{P}_{fs}^T \mathcal{F}(\mathbf{x}) + \hat{v}_i] \quad (5.27)$$

and writing (5.17) in terms of multilinear parameters for second level gives

$$\dot{\tau}_{i\gamma_i} = \mathcal{P}_{fi}^T \mathcal{F}_i(\mathbf{x}) + \mathcal{P}_{gifi}^T \mathcal{G}_i(\mathbf{x}) u_{s_i}. \quad (5.28)$$

Here, subscript i can be dropped for convenience and consequently (5.28) becomes,

$$\dot{\tau} = \mathcal{P}_f^T \mathcal{F}(\mathbf{x}) + \mathcal{P}_{gf}^T \mathcal{G}(\mathbf{x}) \mathbf{u}_s. \quad (5.29)$$

Again, rearranging terms in (5.29) as

$$\dot{\tau} = \mathcal{P}_f^T \mathcal{F}(\mathbf{x}) + \mathcal{P}_{gf}^T \mathcal{G}(\mathbf{x}) \mathbf{u}_s + [\mathcal{P}_{fs}^T \mathcal{F}(\mathbf{x}) + \mathcal{P}_{gfs}^T \mathcal{G}(\mathbf{x}) \mathbf{u}_s] - [\mathcal{P}_{fs}^T \mathcal{F}(\mathbf{x}) + \mathcal{P}_{gfs}^T \mathcal{G}(\mathbf{x}) \mathbf{u}_s] \quad (5.30)$$

and defining the multilinear parameter error vector as $\tilde{\mathcal{P}}_{fs} = \mathcal{P}_f - \mathcal{P}_{fs}$, $\tilde{\mathcal{P}}_{gfs} = \mathcal{P}_{gf} - \mathcal{P}_{gfs}$ yields

$$\dot{\tau} = \mathcal{P}_{fs}^T \mathcal{F}(\mathbf{x}) + \mathcal{P}_{gfs}^T \mathcal{G}(\mathbf{x}) u_s + \tilde{\mathcal{P}}_{fs}^T \mathcal{F}(\mathbf{x}) + \tilde{\mathcal{P}}_{gfs}^T \mathcal{G}(\mathbf{x}) u_s. \quad (5.31)$$

Thereafter, replacing \mathbf{u}_s in the second term of (5.31) from (5.27) yields

$$\dot{\tau} = \hat{v} + \tilde{\mathcal{P}}_{fs}^T \mathcal{F}(\mathbf{x}) + \tilde{\mathcal{P}}_{gfs}^T \mathcal{G}(\mathbf{x}) \mathbf{u}_s \quad (5.32)$$

Subsequently, defining the control error term as $e_i = y_i - y_{d_i}$ and using (5.17) gives the first control error term as

$$\begin{aligned} e_1 &= y_1 - y_{d_1} \\ \text{or, } e_1 &= \tau_{11} - y_{d_1} \\ \text{or, } \tau_{11} &= e_1 + y_{d_1}. \end{aligned} \quad (5.33)$$

Using (5.33), the complete control error is written as

$$\tau_{i\gamma_i} = e_i + r_i. \quad (5.34)$$

Using (5.34), the control error in vector form is given as

$$\boldsymbol{\tau} = \mathbf{e} + \mathbf{r} \quad (5.35)$$

with $\mathbf{r} = [r_1, r_2, \dots, r_\gamma] = [y_d, \dot{y}_d, \dots, y_d^{(\gamma-1)}]$. Further, taking first time differentiation in (5.35) yields

$$\begin{aligned} \dot{e}_1 &= e_2 \\ \dot{e}_2 &= e_3 \\ &\dots \\ \dot{e}_{\gamma-1} &= e_\gamma \\ \dot{e}_\gamma &= \dot{\tau} - \dot{r}_\gamma. \end{aligned} \quad (5.36)$$

Using (5.32) in (5.36) gives

$$\dot{\mathbf{e}} = \hat{v} + \tilde{\mathcal{P}}_{fs}^T \mathcal{F}(\mathbf{x}) + \tilde{\mathcal{P}}_{gfs}^T \mathcal{G}(\mathbf{x}) \mathbf{u}_s - \dot{r}_\gamma \quad (5.37)$$

Using (5.15), (5.37) can be rearranged as

$$\dot{\mathbf{e}} = \mathbf{A}\mathbf{e} + \tilde{\mathcal{P}}_{fs}^T \mathcal{F}(\mathbf{x}) + \tilde{\mathcal{P}}_{gfs}^T \mathcal{G}(\mathbf{x})\mathbf{u}_s \quad (5.38)$$

where $\mathbf{A} = \begin{bmatrix} 0 & 1 & 0 & \dots & 0 \\ 0 & 0 & 1 & \dots & 0 \\ \cdot & \cdot & \cdot & \cdot & \cdot \\ \cdot & \cdot & \cdot & \cdot & \cdot \\ 0 & \cdot & \cdot & \cdot & 1 \\ c_\gamma & c_{\gamma-1} & \cdot & \cdot & c_1 \end{bmatrix}$ is a Hurwitz matrix. Therefore, using (5.17), (5.35) and (5.38),

the complete closed loop error dynamics can be written as

$$\begin{aligned} \boldsymbol{\tau} &= \mathbf{e} + \mathbf{r} \\ \dot{\mathbf{e}} &= \mathbf{A}\mathbf{e} + \tilde{\mathcal{P}}_{fs}^T \mathcal{F}(\mathbf{x}) + \tilde{\mathcal{P}}_{gfs}^T \mathcal{G}(\mathbf{x})\mathbf{u}_s \\ \dot{\boldsymbol{\xi}} &= \varphi(\boldsymbol{\tau}, \boldsymbol{\xi}) \end{aligned} \quad (5.39)$$

Further, to assess the closed loop stability of the nonlinear coupled MIMO system (5.1) with relative degree γ_i and normal form as given in (5.17), following assumptions are made:

- (i) The zero dynamics $\varphi(0, \boldsymbol{\xi})$ is asymptotically stable and internal dynamics $\varphi(\boldsymbol{\tau}, \boldsymbol{\xi})$ is globally Lipschitz in $\boldsymbol{\tau}$ and $\boldsymbol{\xi}$. There exists an upper bound b_φ as such that

$$\|\varphi(\boldsymbol{\tau}, \boldsymbol{\xi}) - \varphi(0, \boldsymbol{\xi})\| \leq b_\varphi \|\boldsymbol{\tau}\|. \quad (5.40)$$

- (ii) The trajectory y_d to be tracked is bounded with bounded derivatives $\dot{y}_d, \dots, y_d^{(\gamma-1)}$. Defining b_d as an upper bound on y_d and its derivatives, it can be found that

$$\|\boldsymbol{\tau}\| \leq \|\mathbf{e}\| + b_d. \quad (5.41)$$

- (iii) The regressor vectors $\mathcal{F}(\mathbf{x}), \mathcal{G}(\mathbf{x})\mathbf{u}_s$ are bounded for bounded \mathbf{x} and every bounded control input \mathbf{u}_s with b_f, b_g as the upper bounds can be expressed as

$$\begin{aligned} \|\mathcal{F}(\mathbf{x})\| &\leq b_f \|\mathbf{x}\| \\ \|\mathcal{G}(\mathbf{x})\mathbf{u}_s\| &\leq b_g \|\mathbf{x}\|. \end{aligned} \quad (5.42)$$

(iv) Since \mathbf{x} is a local diffeomorphism of $\boldsymbol{\tau}$ and $\boldsymbol{\xi}$,

$$\|\mathbf{x}\| \leq b_0(\|\boldsymbol{\tau}\| + \|\boldsymbol{\xi}\|), \quad b_0 > 0 \quad (5.43)$$

Now that the zero dynamics is assumed to be asymptotically stable, there exists a Lyapunov function $V_\varphi(\boldsymbol{\xi})$ such that

$$\begin{aligned} c_1\|\boldsymbol{\xi}\|^2 &\leq V_\varphi(\boldsymbol{\xi}) \leq c_2\|\boldsymbol{\xi}\|^2 \\ \frac{\partial V_\varphi}{\partial \boldsymbol{\xi}}\varphi(0, \boldsymbol{\xi}) &\leq -c_3\|\boldsymbol{\xi}\|^2 \\ \left\| \frac{\partial V_\varphi(\boldsymbol{\xi})}{\partial \boldsymbol{\xi}} \right\| &\leq c_4\|\boldsymbol{\xi}\| \end{aligned} \quad (5.44)$$

where c_1, c_2, c_3, c_4 are positive constants. Similarly, a suitable Lyapunov function for closed loop error dynamics (5.39) is chosen as

$$V(\mathbf{e}, \boldsymbol{\xi}) = \mathbf{e}^T \mathbf{P} \mathbf{e} + \mu V_\varphi(\boldsymbol{\xi}) \quad (5.45)$$

where \mathbf{P} is the solution of Lyapunov equation $\mathbf{A}^T \mathbf{P} + \mathbf{P} \mathbf{A} = -\mathbf{I}$ and μ is a small positive constant.

Taking first time derivative of (5.45) yields

$$\dot{V}(\mathbf{e}, \boldsymbol{\xi}) = \dot{\mathbf{e}}^T \mathbf{P} \mathbf{e} + \mathbf{e}^T \mathbf{P} \dot{\mathbf{e}} + \mu \frac{\partial V_\varphi}{\partial \boldsymbol{\xi}} \varphi(\boldsymbol{\tau}, \boldsymbol{\xi}) \quad (5.46)$$

Using (5.39) gives

$$\begin{aligned} \dot{V}(\mathbf{e}, \boldsymbol{\xi}) &= -\mathbf{e}^T \mathbf{e} + 2\mathbf{e}^T \mathbf{P} [\tilde{\mathcal{P}}_{fs}^T \mathcal{F}(\mathbf{x}) + \tilde{\mathcal{P}}_{gfs}^T \mathcal{G}(\mathbf{x}) \mathbf{u}_s] + \mu \frac{\partial V_\varphi}{\partial \boldsymbol{\xi}} \varphi(0, \boldsymbol{\xi}) \\ &+ \left(\mu \frac{\partial V_\varphi}{\partial \boldsymbol{\xi}} \varphi(\boldsymbol{\tau}, \boldsymbol{\xi}) - \mu \frac{\partial V_\varphi}{\partial \boldsymbol{\xi}} \varphi(0, \boldsymbol{\xi}) \right) \end{aligned} \quad (5.47)$$

Using the assumptions (i) - (iv) yields

$$\dot{V}(\mathbf{e}, \boldsymbol{\xi}) \leq -\|\mathbf{e}\|^2 + \|\mathbf{e}\|(\|\mathbf{e}\| + \|\boldsymbol{\xi}\| + b_d)[b_{f_0}\|\tilde{\mathcal{P}}_{fs}\| + b_{g_0}\|\tilde{\mathcal{P}}_{gfs}\|] - \mu c_3\|\boldsymbol{\xi}\|^2 + \mu c_4 b_\varphi \|\boldsymbol{\xi}\|(\|\mathbf{e}\| + b_d) \quad (5.48)$$

with $b_{f_0} = b_f b_0$, $b_{g_0} = b_g b_0$. Again, rearranging the above equation provides

$$\begin{aligned} \dot{V}(\mathbf{e}, \boldsymbol{\xi}) &\leq [b_{f_0}\|\tilde{\mathcal{P}}_{fs}\| + b_{g_0}\|\tilde{\mathcal{P}}_{gfs}\| - 1]\|\mathbf{e}\|^2 - \mu c_3\|\boldsymbol{\xi}\|^2 + [b_{f_0}\|\tilde{\mathcal{P}}_{fs}\| + b_{g_0}\|\tilde{\mathcal{P}}_{gfs}\| \\ &+ \mu c_4 b_\varphi]\|\boldsymbol{\xi}\|\|\mathbf{e}\| + [b_{d_{f_0}}\|\tilde{\mathcal{P}}_{fs}\| + b_{d_{g_0}}\|\tilde{\mathcal{P}}_{gfs}\|]\|\mathbf{e}\| + \mu c_4 b_\varphi b_d \|\boldsymbol{\xi}\| \end{aligned} \quad (5.49)$$

with $b_{d_{f_0}} = b_d b_{f_0}$, $b_{d_{g_0}} = b_d b_{g_0}$. Moreover, defining $Z_1 = [b_{f_0}\|\tilde{\mathcal{P}}_{fs}\| + b_{g_0}\|\tilde{\mathcal{P}}_{gfs}\|]$, $Z_2 = [b_{d_{f_0}}\|\tilde{\mathcal{P}}_{fs}\| +$

$b_{d_{g_0}} \|\tilde{\mathcal{P}}_{gfs}\|$ gives

$$\dot{V}(\mathbf{e}, \boldsymbol{\xi}) \leq -\left(\|\mathbf{e}\| - \frac{Z_2}{2}\right)^2 - \left(\sqrt{\mu c_3} \|\boldsymbol{\xi}\| - \frac{\mu c_4 b_\varphi b_d}{2\sqrt{\mu c_3}}\right)^2 + \begin{bmatrix} \|\mathbf{e}\| \\ \|\boldsymbol{\xi}\| \end{bmatrix}^T \mathbf{Q} \begin{bmatrix} \|\mathbf{e}\| \\ \|\boldsymbol{\xi}\| \end{bmatrix} + \frac{Z_2^2}{4} - \frac{\mu}{4c_3} (c_4 b_\varphi b_d)^2 \quad (5.50)$$

where $\mathbf{Q} = \begin{bmatrix} Z_1 & \frac{Z_1 + \mu c_4 b_\varphi}{2} \\ \frac{Z_1 + \mu c_4 b_\varphi}{2} & -\mu c_3 \end{bmatrix}$. The third term in the right hand side of (5.50) will be negative if

\mathbf{Q} is a negative semidefinite matrix, which is possible if $2\mu c_3 \left(\sqrt{1 + \frac{b_\varphi}{c_3}} - 1\right) + \mu c_4 b_\varphi < Z_1 \leq 0$. Also, the last two terms in (5.50) will result in negativity if $Z_2 < \sqrt{\frac{\mu}{c_3}} c_4 b_\varphi b_d$. These conditions will ensure that $\dot{V} < 0$ for all $t > 0$. Since \dot{V} is negative definite, V is a decreasing function whose minimum value is zero. Also, V is positive definite, which implies it will be zero only when \mathbf{e} and $\boldsymbol{\xi}$ are both zero. Therefore, $\lim_{t \rightarrow \infty} \mathbf{e} = 0$ and $\lim_{t \rightarrow \infty} \boldsymbol{\xi} = 0$.

5.7 Simulation and Experimental Results

The proposed MMTLA controller is applied to a twin rotor MIMO system (TRMS) which is a benchmark example of highly nonlinear coupled MIMO system having unstable system dynamics and parametric uncertainty. Figure 5.2 shows the TRMS set-up [60] available in the laboratory. The TRMS model is interfaced to a Windows 7 PC with 4 GB RAM, installed with Matlab/simulink R2011a using advantech PCI card. Two encoders attached to the two rotors communicate the pitch and yaw angle measurements to the PC. The digital signal generated by the controller is converted to an analog signal comprising two voltages and are sent to the two motors attached to the rotors. A schematic description of the TRMS is provided in Figure 5.3 where it can be observed that the TRMS has two propellers attached at both ends of a beam pivoting on its base and driven by a DC motor. The two propellers are perpendicular to each other, designed such that these can rotate freely both in the horizontal and vertical planes. A counterbalance arm with a weight at its end is fixed to the horizontal beam. The main rotor causes the vertical movement known as the pitch motion and the tail rotor causes the horizontal movement called the yaw motion. In TRMS the angle of attack is fixed and the aerodynamic force is controlled by varying speed of the rotors. The dynamic cross-coupling in the TRMS is shown in Figure 5.4 [60], where α_v is the pitch angle, α_h is the yaw angle and u_v, u_h are input voltages to the main and tail rotors respectively.



Figure 5.2: TRMS laboratory model

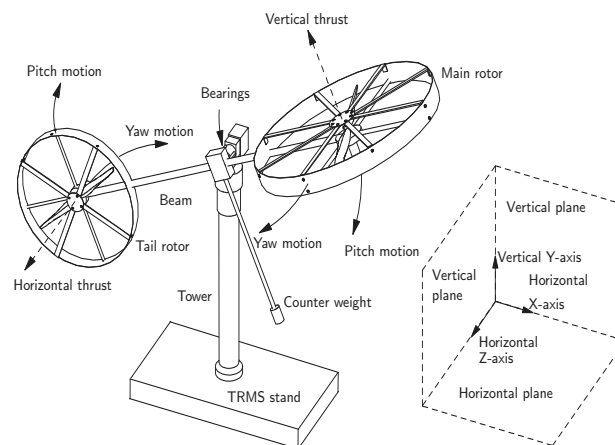


Figure 5.3: A schematic description of TRMS

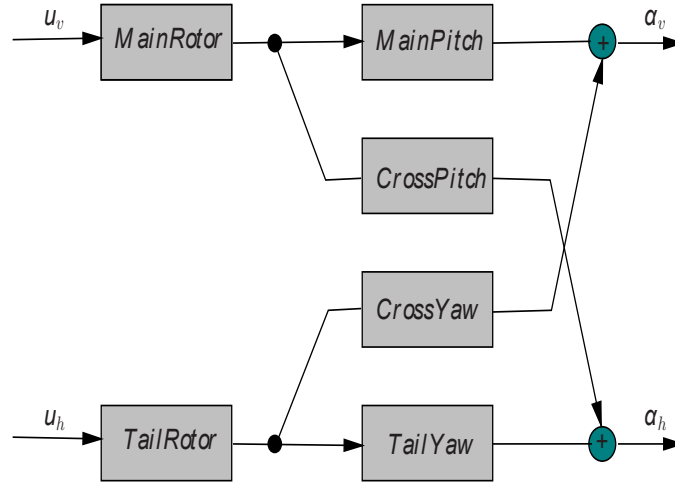


Figure 5.4: Cross coupled TRMS system

The dynamics of the TRMS in the state space form (Appendix A.6) can be written in terms of the unknown parameters as:

$$\begin{aligned}
 \dot{x}_1 &= x_2 \\
 \dot{x}_2 &= \theta_1 x_5^2 + \theta_2 x_5 - \theta_3 \sin x_1 - \theta_4 x_2 + \theta_5 x_4^2 \sin(2x_2) \\
 &\quad - \theta_6 x_4 x_5^2 \cos(x_1) - \theta_7 x_4 x_5 \cos(x_1) \\
 \dot{x}_3 &= x_4 \\
 \dot{x}_4 &= \theta_8 x_6^2 + \theta_9 x_6 - \theta_{10} x_4 - \theta_{11} x_5^2 - \theta_{12} x_5 \\
 \dot{x}_5 &= -\theta_{13} x_5 + \theta_{14} u_v \\
 \dot{x}_6 &= -\theta_{15} x_6 + \theta_{16} u_h \\
 y_1 &= x_1, \quad y_2 = x_3
 \end{aligned} \tag{5.51}$$

where x_1 denotes the pitch angle, x_2 denotes the pitch angular velocity, x_3 represents the yaw angle, x_4 represents the yaw angular velocity, x_5 denotes the momentum of the main motor and x_6 denotes the momentum of the tail motor. Similarly, y_1, y_2 denote the outputs. The vector of unknown parameters $\theta = [\theta_f, \theta_g]^T$ is given by $\theta_f = [\theta_1, \dots, \theta_{13}, \theta_{15}]^T$, $\theta_g = [\theta_{14}, \theta_{16}]^T$.

The above unknown parameters are given in terms of the TRMS physical parameters by

$$\begin{aligned}
 \theta_1 &= a_1/l_1; \quad \theta_2 = b_1/l_1; \quad \theta_3 = M_g/l_1; \quad \theta_4 = B_{1\alpha_v}/l_1; \quad \theta_5 = 0.0326/2l_1; \quad \theta_6 = k_{gy}a_1/l_1; \\
 \theta_7 &= k_{gy}b_1/l_1; \quad \theta_8 = a_2/l_2; \quad \theta_9 = b_2/l_2; \quad \theta_{10} = B_{1\alpha_h}/l_2; \quad \theta_{11} = -1.75k_c a_1/l_2; \\
 \theta_{12} &= -1.75k_c b_1/l_2; \quad \theta_{13} = T_{10}/T_{11}; \quad \theta_{14} = k_m/T_{11}; \quad \theta_{15} = T_{20}/T_{21}; \quad \theta_{16} = k_t/T_{21}
 \end{aligned} \tag{5.52}$$

The above physical parameters belonging to the TRMS laboratory set-up used for simulation and experimental studies are described in Table 5.1 [60] below.

Table 5.1: Physical parameters of the TRMS

Symb.	Description	Value	Unit
l_1	Moment of inertia of vertical rotor	0.068	$\text{kg}\cdot\text{m}^2$
l_2	Moment of inertia of horizontal rotor	0.02	$\text{kg}\cdot\text{m}^2$
a_1	Static characteristic parameter	0.0135	-
b_1	Static characteristic parameter	0.0294	-
a_2	Static characteristic parameter	0.02	-
b_2	Static characteristic parameter	0.09	-
M_g	Gravity momentum	0.32	N-m
$B_{1\alpha_v}$	Friction momentum function parameter	0.006	N-m-s/rad
$B_{1\alpha_h}$	Friction momentum function parameter	0.1	N-m-s/rad
k_{gy}	Gyroscopic momentum parameter	0.0155	s/rad
k_m	Main rotor gain	1.1	-
k_t	Tail rotor gain	0.8	-
T_{11}	Main rotor denominator parameter	1.1	-
T_{10}	Main rotor denominator parameter	1	-
T_{21}	Tail rotor denominator parameter	1	-
T_{20}	Tail rotor denominator parameter	1	-
T_p	Cross reaction momentum parameter	2	-
T_0	Cross reaction momentum parameter	3.5	-
k_c	Cross reaction momentum gain	-0.2	-

Among the 6 states, only pitch angle x_1 and yaw angle x_3 are available for measurement. Therefore, an Extended Kalman Filter (EKF) [75, 76] (A.4) is used to estimate all the states of the system. The parameters used in the EKF are the variances $Q = 1/3$, $R = 0.1/3$ and the error covariance matrix Γ is an unit matrix of 6×6 dimension as required. The initial condition of the TRMS is considered as $\mathbf{x}(0) = [0, 0, 0, 0, 0, 0]^T$. Consequently, the initial states of identification and observer models are also set to zero. Further, the initial values of the unknown parameters for the single model case are chosen as $\hat{\theta} = [3, 3, 8, 2, 3, 2, 2, 3, 8, 8, -2, -2, 3, 3, 3, 3]^T$. For the multiple model case, 4 models are chosen with initial parameters as given below:

$$\begin{aligned}
 \text{Model 1} &= [-1, -1, 3, -1, -1, -1, -1, -1, 3, 3, -2, -2, -1, -1, -1, -1] \\
 \text{Model 2} &= [1, 1, 4, 0, 1, 0, 0, 1, 4, 4, -1, -1, 1, 1, 1, 1] \\
 \text{Model 3} &= [2, 2, 7, 1, 2, 1, 1, 2, 7, 7, 0, 0, 2, 2, 2, 2] \\
 \text{Model 4} &= [3, 3, 8, 2, 3, 2, 2, 3, 8, 8, 1, 1, 3, 3, 3, 3]
 \end{aligned} \tag{5.53}$$

Here the number of models is searched heuristically. The number of models based on the discussion in Section 3.3.1 is $N = 2^p$. In the TRMS model, the number of unknown parameters is $p = 16$,

which is a high number. However, it is found that it becomes computationally prohibitive to experiment for more than 8 number of models. Therefore, the experiments are started with 8 number of models. It is observed that for number of models 4 and higher, similar results are obtained. Therefore, number of models is selected as 4. Initial values of all the four weights are selected as $w_j(0) = [0.25, 0.25, 0.25, 0.25]$. Also, for the two-input two-output TRMS system the relative degrees are found to be $\gamma_1 = 3, \gamma_2 = 3$. Therefore, the constants used in (5.15) for both inputs v_i , $i = 1, 2$ are chosen as $c_{1i} = [30, 45, 60]$, $c_{2i} = [15, 30, 15]$. The matrix \mathbf{A} in (5.4) for both inputs is chosen as $\mathbf{A} = [-3, 0, 0; 0, -8, 0; 0, 0, -3]$. The actual control input voltages for main and tail DC motors are maintained within the permitted range of $[-2.5, 2.5]$ volts.

5.7.1 Case 1: Step input tracking

The TRMS is made to follow the desired outputs $y_{d1} = 0.5$ and $y_{d2} = 1$ for pitch and yaw angles respectively. The initial values of pitch and yaw angles are set at the TRMS equilibrium state $[0, 0]$. Figures 5.5-5.9 compare simulation and experimental results obtained by using the proposed MMTLA controller with a single model based adaptive control method.

Tables 5.2 and 5.3 compare the transient and steady state performances and also show the input and output performances for pitch angle tracking and yaw angle tracking respectively. The definitions of performance specifications can be found in A.5. It is observed from Tables 5.2 and 5.3 that in

Table 5.2: Comparison between single model and MMTLA: Pitch control for step input

Simulation								
Adaptation Mechanism	Performance Specifications							
	M_p	M_u	t_s	e_{ss}	TV	CE	ISE	IAE
single model	12.02 %	0 %	3.33 s	0	3.13×10^3	455.15	149.03	724.718
MMTLA Control	9.91 %	0 %	3.04 s	0	915.017	412.83	148.6	669.71

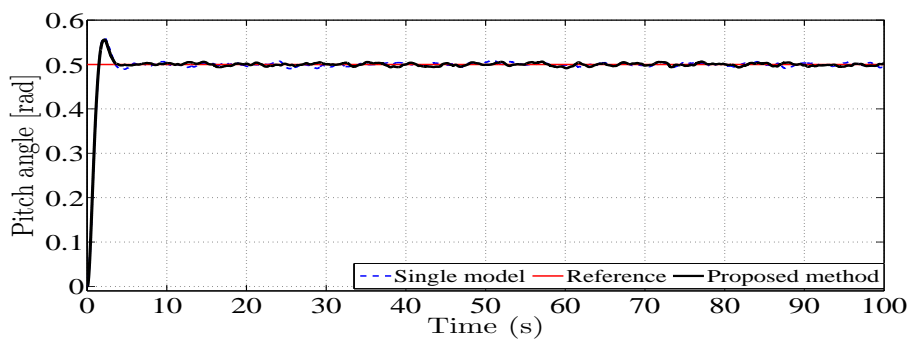
Experimental								
Adaptation Mechanism	Performance Specifications							
	M_p	M_u	t_s	e_{ss}	TV	CE	ISE	IAE
single model	35.6 %	7.9 %	-	0.0983	164.5	480.67	1.49×10^3	1.12×10^4
MMTLA Control	35.6 %	6.12 %	20.0 s	0.0246	677.4	435.89	197.68	3.7×10^3

M_p : Peak overshoot, M_u : Peak undershoot

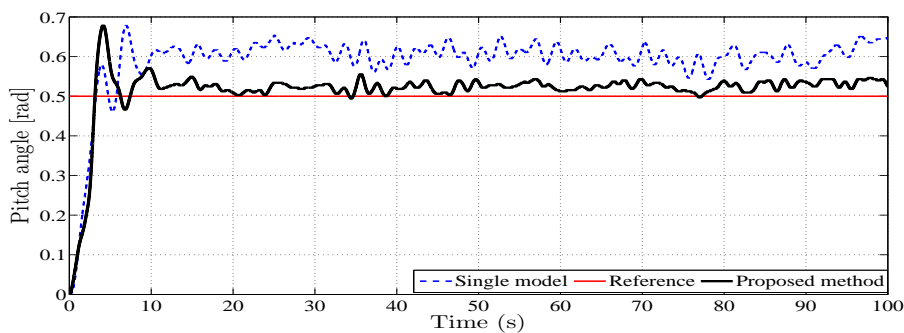
t_s : Settling time, e_{ss} : Steady state error

TV : Total variation, CE : Control energy

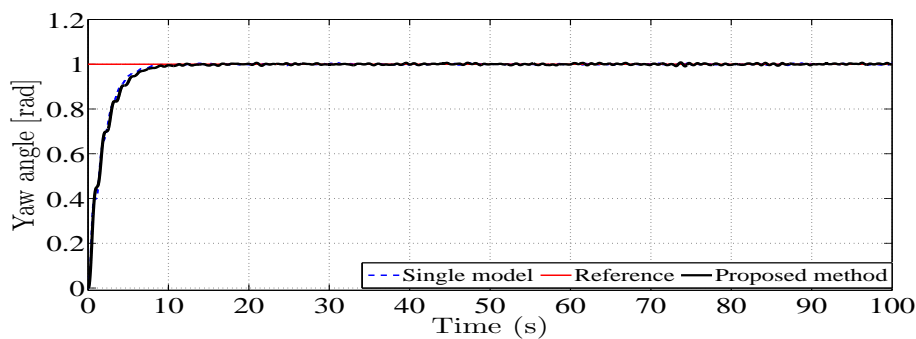
ISE : Integral square error, IAE : Integral absolute error



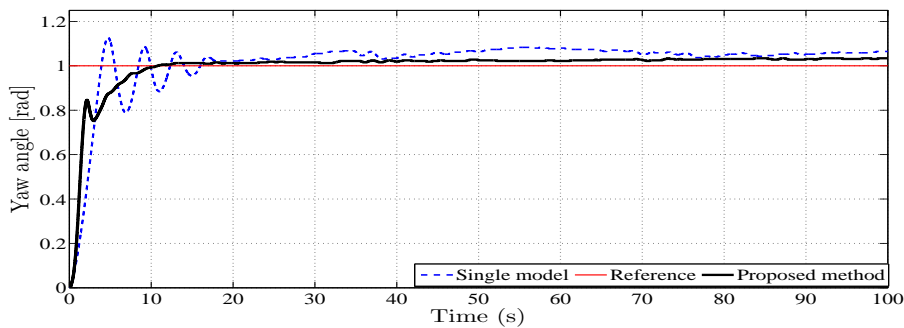
(a) Simulation: Pitch angle tracking



(b) Experimental: Pitch angle tracking

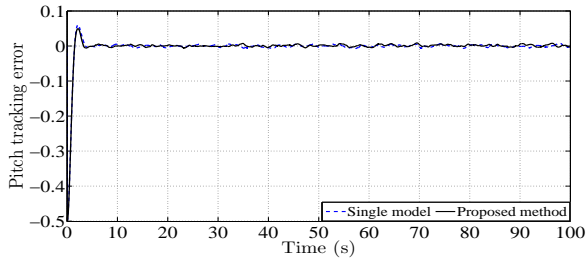


(c) Simulation: Yaw angle tracking

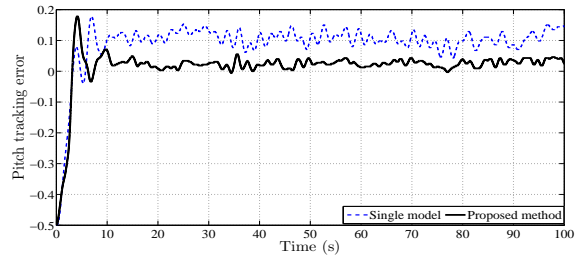


(d) Experimental: Yaw angle tracking

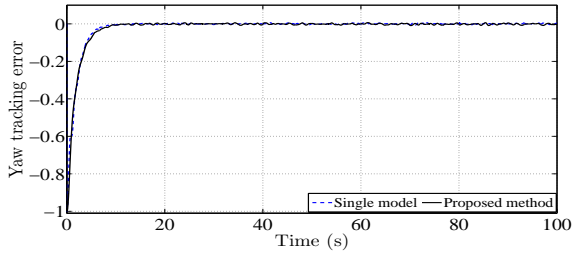
Figure 5.5: Trajectory tracking for Step input



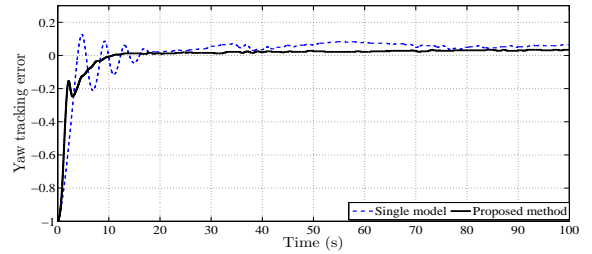
(a) Simulation: Pitch tracking error



(b) Experimental: Pitch tracking error

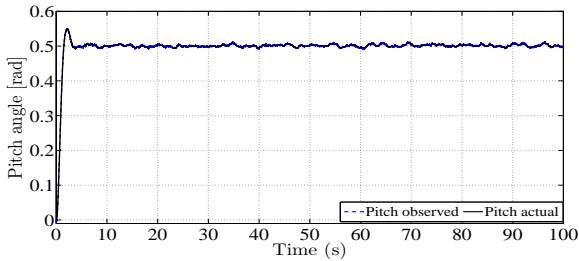


(c) Simulation: Yaw tracking error

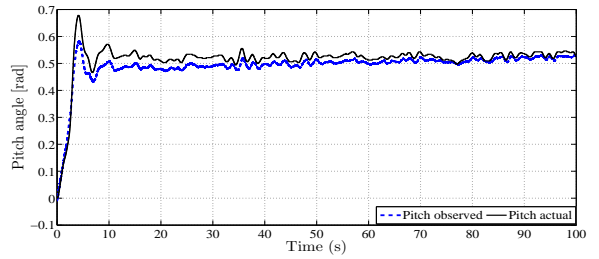


(d) Experimental: Yaw tracking error

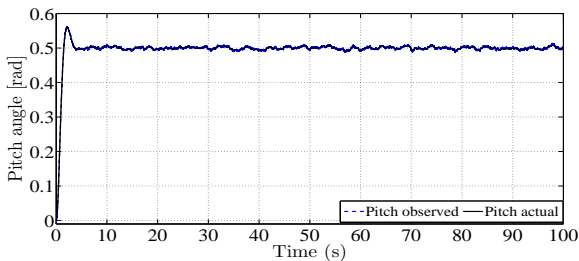
Figure 5.6: Tracking error for step input



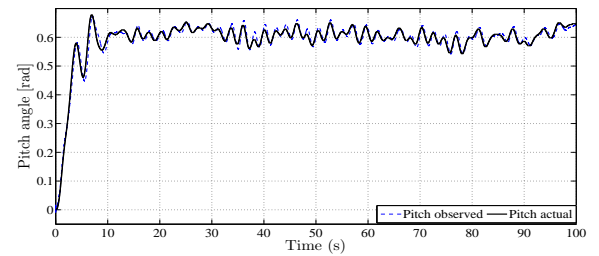
(a) Simulation: Pitch response for single model



(b) Experimental: Pitch response for single model



(c) Simulation: Pitch response for proposed method



(d) Experimental: Pitch response for proposed method

Figure 5.7: Observed vs actual pitch angle for step input

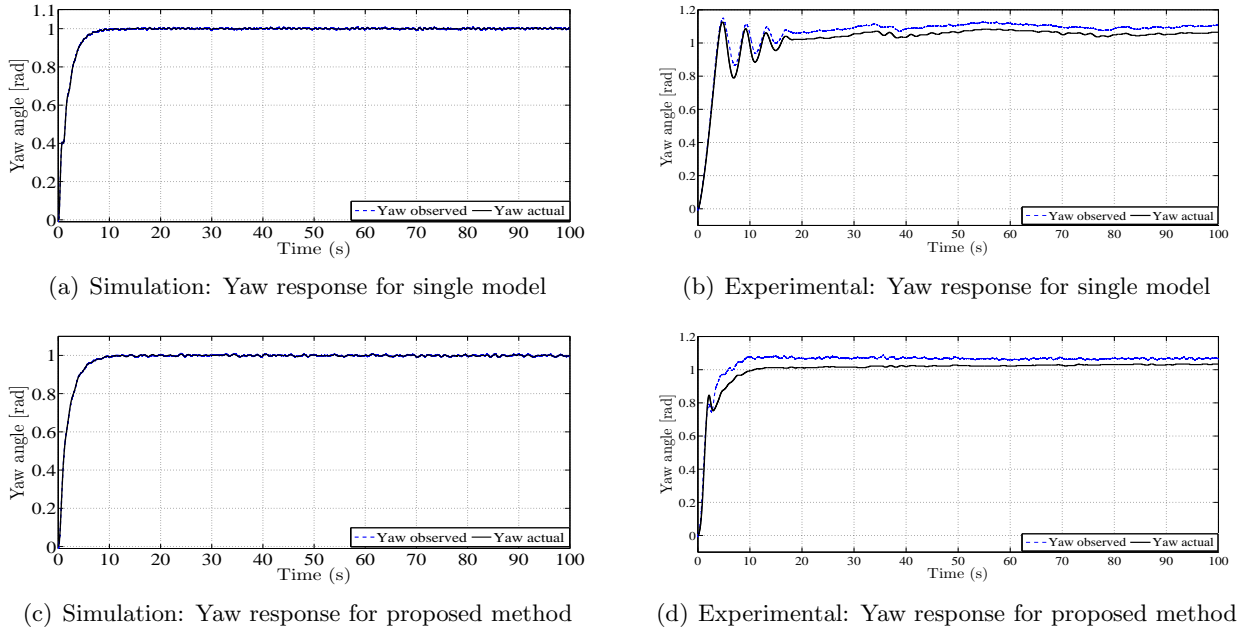


Figure 5.8: Observed vs actual yaw angle for step input

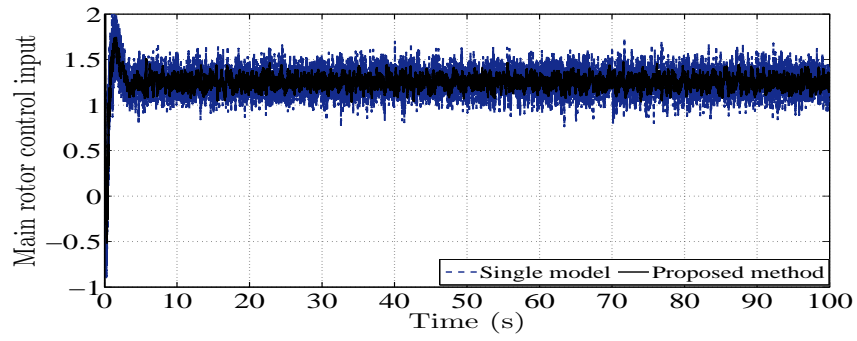
Table 5.3: Comparison between single model and MMTLA: Yaw control for step input

Simulation								
Adaptation Mechanism	Performance Specifications							
	M_p	M_u	t_s	e_{ss}	TV	CE	ISE	IAE
single model	0.68 %	0 %	7.7 s	0	2.42×10^3	340.468	986.6	2.1×10^3
MMTLA Control	0.63 %	0 %	6.74 s	0	811.39	286.72	912.02	1.93×10^3

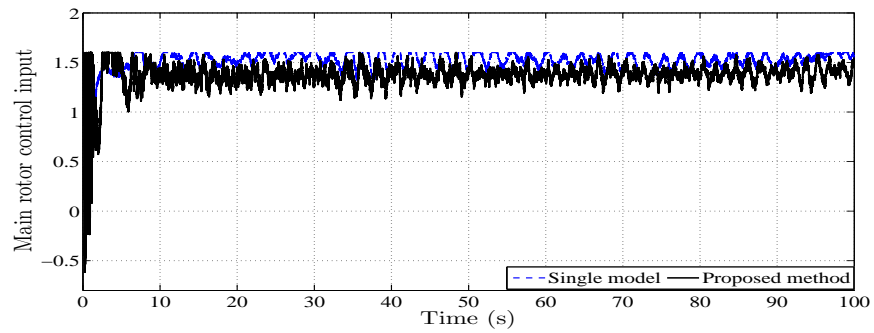
Experimental								
Adaptation Mechanism	Performance Specifications							
	M_p	M_u	t_s	e_{ss}	TV	CE	ISE	IAE
single model	12.59 %	20.85 %	20.0 s	0.0523	199.4	153.76	2.013×10^3	7.7×10^3
MMTLA Control	0 %	0 %	12.9 s	0.0216	441.6	147.42	1.2×10^3	4.19×10^3

M_p : Peak overshoot, M_u : Peak undershoot
 t_s : Settling time, e_{ss} : Steady state error
 TV : Total variation, CE : Control energy
 ISE : Integral square error, IAE : Integral absolute error

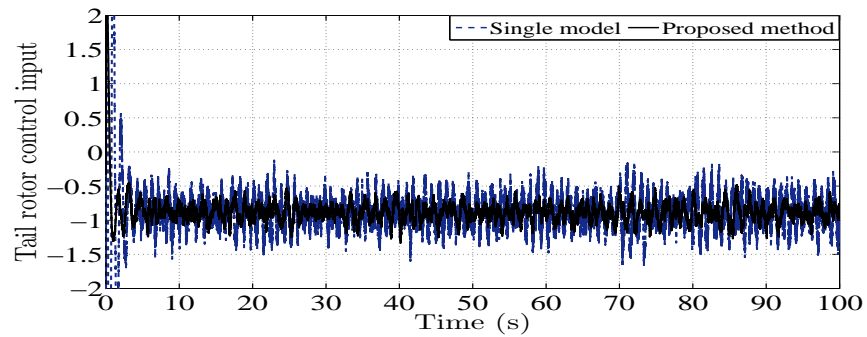
both simulation and experimental studies, the MMTLA control method outperforms the single model based adaptive control method in both transient and steady state performances at the expense of lesser control energy. Moreover, the output tracking performance in the case of MMTLA controller is superior than the single model based adaptive control method as indicated by ISE and IAE values. A



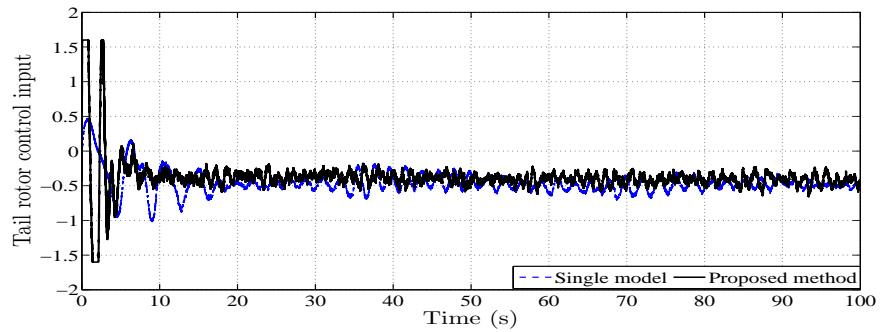
(a) Simulation: Main rotor control input (volts)



(b) Experimental: Main rotor control input (volts)



(c) Simulation: Tail rotor control input (volts)



(d) Experimental: Tail rotor control input (volts)

Figure 5.9: Control input for step trajectory tracking

higher total variation (TV) value in the experimental case suggests increased chattering in the control inputs and this is expected in the real time experiment scenario because of unwanted disturbances like air gust, voltage fluctuation etc.

5.7.2 Case 2: Sinusoidal input tracking

Next, the TRMS output is made to follow a sinusoidal trajectory with amplitude 0.3 rad for pitch and 0.5 rad for yaw and time period of 40 s in each case. The pitch and yaw angle tracking results are shown in Figures 5.10-5.12 and summarized in Tables 5.4 and 5.5. It can be observed in Figures

Table 5.4: Comparison between single model and MMTLA: Pitch control for sinusoidal input

Simulation							
Adaptation Mechanism	Performance Specifications						
	M_p	M_u	TV	CE	RMSE	ISE	IAE
single model	0 %	93.80 %	2.17×10^3	195.08	0.0267	71.07	2.37×10^3
MMTLA Control	0 %	90.79 %	1.26×10^3	192.1	0.02	70.6	2.35×10^3

Experimental							
Adaptation Mechanism	Performance Specifications						
	M_p	M_u	TV	CE	RMSE	ISE	IAE
single model	80.1 %	161.27 %	2.3×10^3	243.6	0.0551	304.1	3.39×10^3
MMTLA Control	55.7 %	72.85 %	3.09×10^3	250.9	0.0371	137.3	2.83×10^3

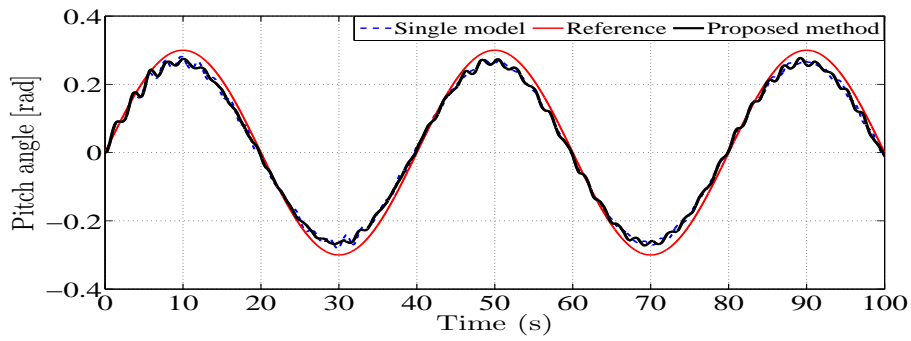
M_p : Peak overshoot, M_u : Peak undershoot

TV : Total variation, CE : Control energy

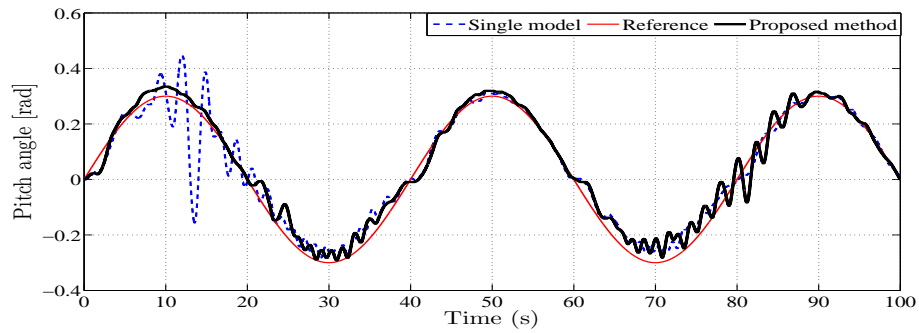
RMSE : Root mean square error

ISE : Integral square error, IAE : Integral absolute error

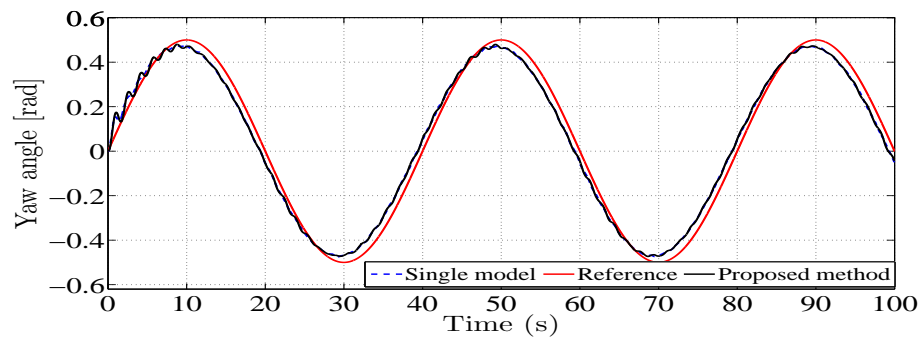
5.10-5.12 that in the case of single model based adaptive control, high transients occur every time the trajectory of the output signal crosses a peak, but for the proposed MMTLA method these transients are significantly reduced. Tables 5.4 and 5.5 confirm superiority of the MMTLA control method over the single model based adaptive control method in transient performance. Also, the output tracking performance in the case of MMTLA control method is better. The MMTLA controller achieves superior transient and output performances than the single model adaptive control method at the expense of almost the same control energy. Moreover, the smoothness of the control signal in the MMTLA controller is comparable with the single model adaptive control method.



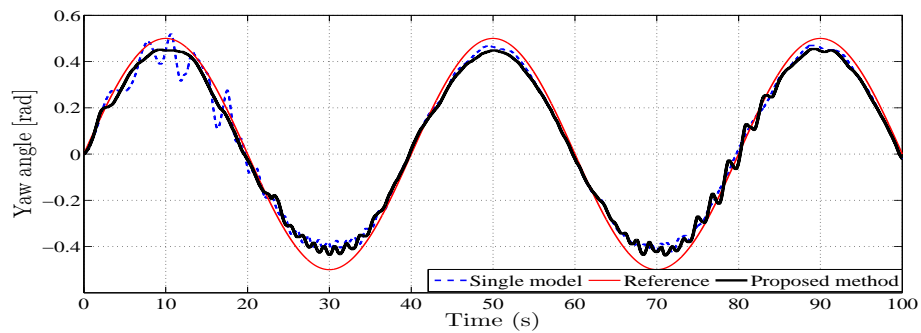
(a) Simulation: Pitch tracking



(b) Experimental: Pitch tracking



(c) Simulation: Yaw tracking



(d) Experimental: Yaw tracking

Figure 5.10: Trajectory tracking for sinusoidal input

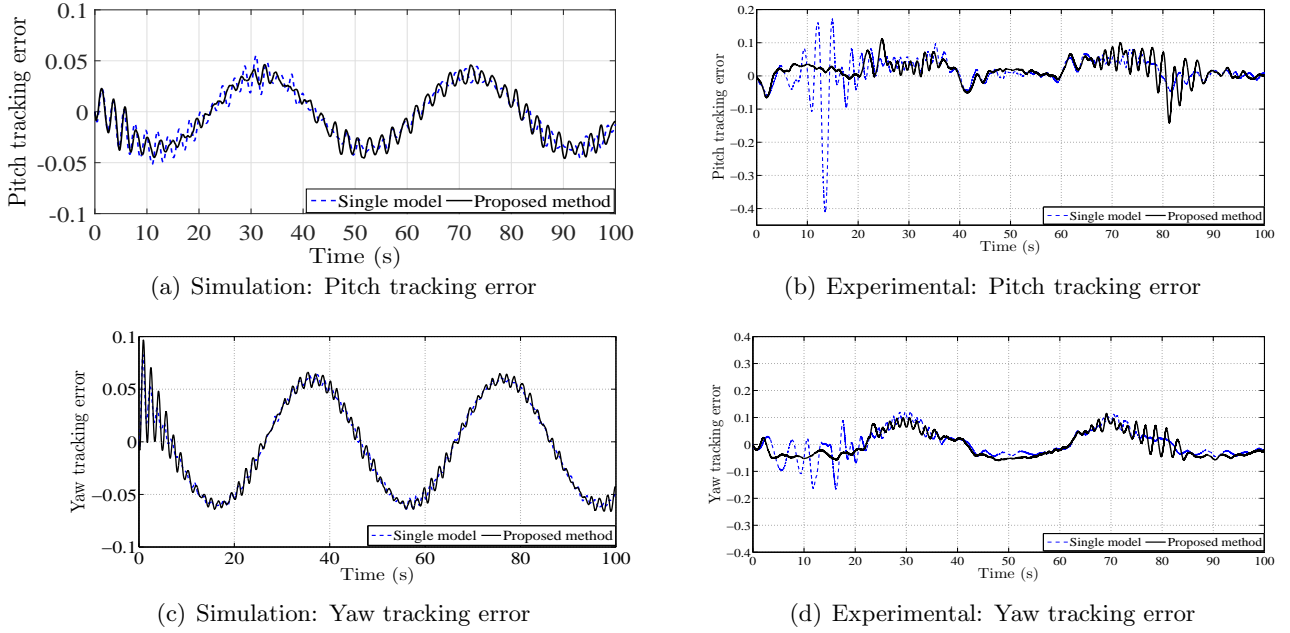


Figure 5.11: Trajectory tracking error for sinusoidal input

Table 5.5: Comparison between single model and MMTLA: Yaw control for sinusoidal input

Simulation							
Adaptation Mechanism	Performance Specifications						
	M_p	M_u	TV	CE	RMSE	ISE	IAE
single model	-	95.21 %	2.17×10^3	122.56	0.043	185.09	3.83×10^3
MMTLA Control	-	94.6 %	543.8	113.35	0.042	179.5	3.79×10^3

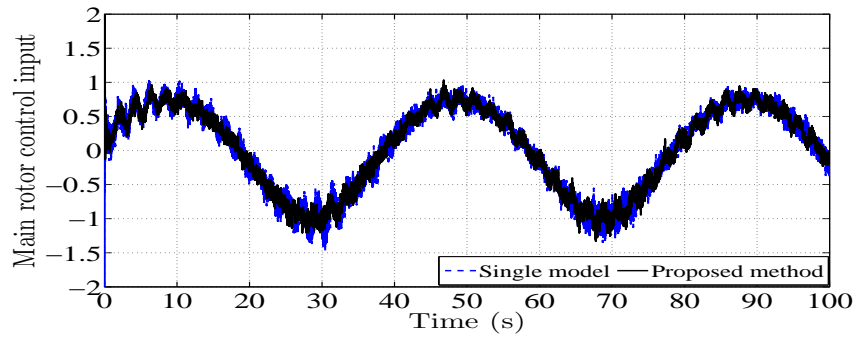
Experimental							
Adaptation Mechanism	Performance Specifications						
	M_p	M_u	TV	CE	RMSE	ISE	IAE
single model	24.5 %	60.08 %	1.16×10^3	211.77	0.0509	259.316	4.08×10^3
MMTLA Control	19.9 %	21.07 %	1.01×10^3	180.98	0.0459	210.325	4.14×10^3

M_p : Peak overshoot, M_u : Peak undershoot

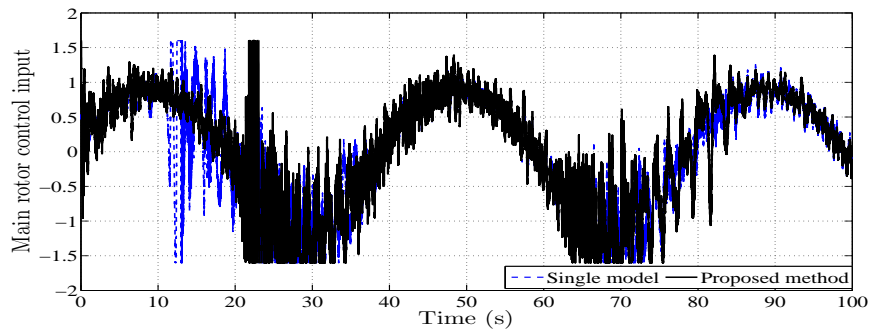
TV : Total variation, CE : Control energy

RMSE : Root mean square error

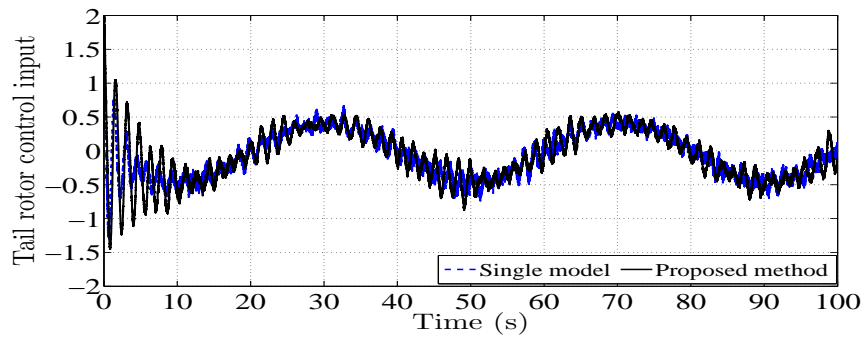
ISE : Integral square error, IAE : Integral absolute error



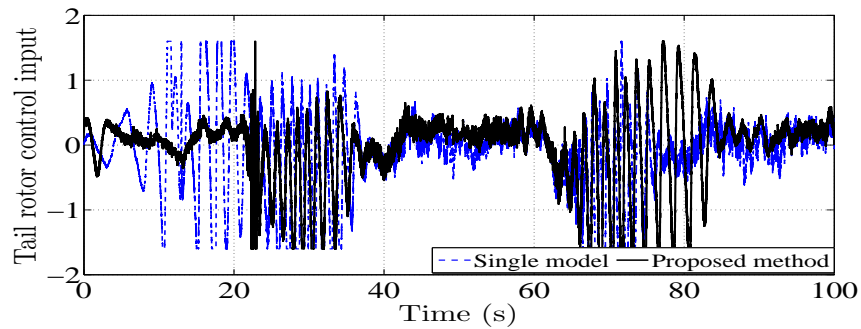
(a) Simulation: Main rotor control input (volts)



(b) Experimental: Main rotor control input (volts)



(c) Simulation: Tail rotor control input (volts)



(d) Experimental: Tail rotor control input (volts)

Figure 5.12: Control input for sinusoidal trajectory tracking

5.7.3 Case 3: Square input tracking

Finally, tracking responses of the TRMS for a square reference input is investigated. The input square wave has amplitude 0.3 rad for pitch and 0.5 rad for yaw and a time period of 50 s for each case. Figures 5.13 - 5.15 compare trajectory tracking results for the MMTLA controller with the single model based adaptive controller. Tables 5.6 and 5.7 tabulate these tracking results for pitch and yaw angle tracking respectively. As can be observed from Figure 5.13, the pitch responds better at sig-

Table 5.6: Comparison between single model and MMTLA: Pitch control for square input

Simulation					
Adaptation Mechanism	Performance Specifications				
	TV	CE	RMSE	ISE	IAE
single model	225.49	327.94	0.127	1.61×10^3	5.1×10^3
MMTLA Control	166.3	316.9	0.125	1.56×10^3	5.03×10^3

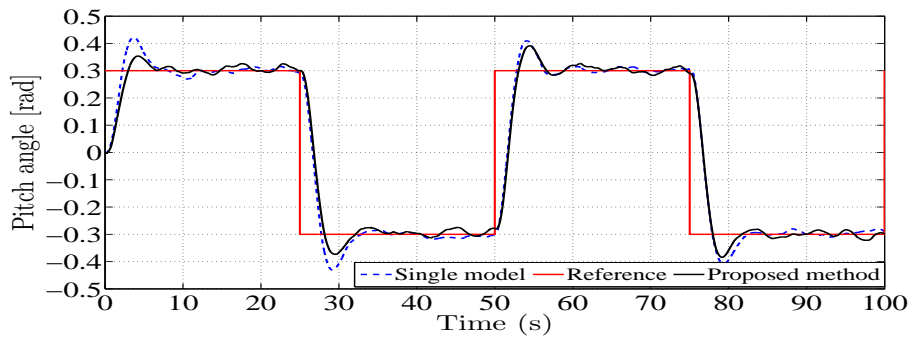
Experimental					
Adaptation Mechanism	Performance Specifications				
	TV	CE	RMSE	ISE	IAE
single model	1.72×10^3	270.3	0.1598	2.55×10^3	1.11×10^4
MMTLA Control	2.6×10^3	274.02	0.1654	2.73×10^3	1.16×10^4

TV : Total variation, *CE* : Control energy

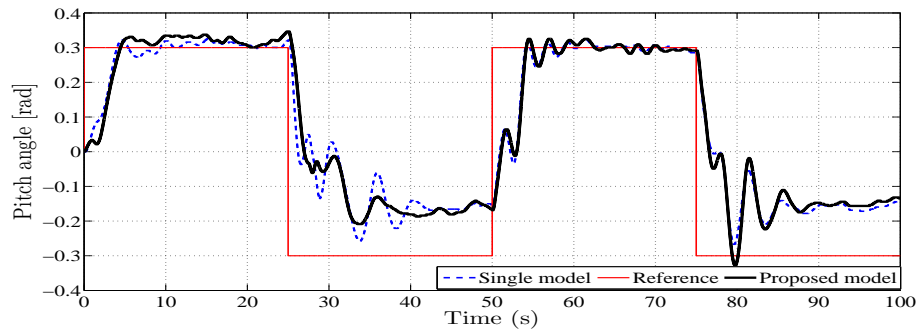
RMSE : Root mean square error

ISE : Integral square error, *IAE* : Integral absolute error

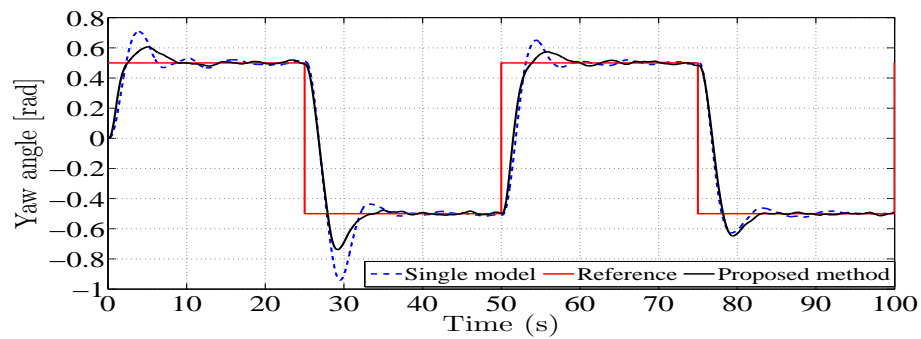
nal rise, whereas it gives a sluggish response at signal fall. Further, while the behavior of pitch angle tracking with the proposed MMTLA control method are almost similar with those by the single model cases, the yaw angle tracking performance in the proposed MMTLA method is considerably better. From Tables 5.6 and 5.7 it is evident that output tracking performance by the MMTLA method is better than the single model case at the expense of comparable control energy.



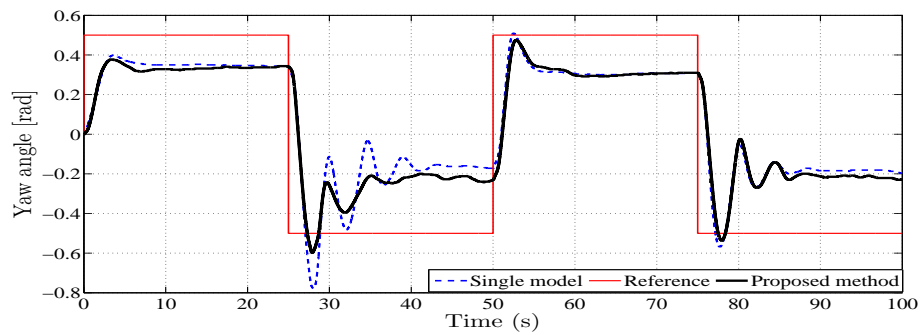
(a) Simulation: Pitch tracking



(b) Experimental: Pitch tracking



(c) Simulation: Yaw tracking



(d) Experimental: Yaw tracking

Figure 5.13: Trajectory tracking for square input

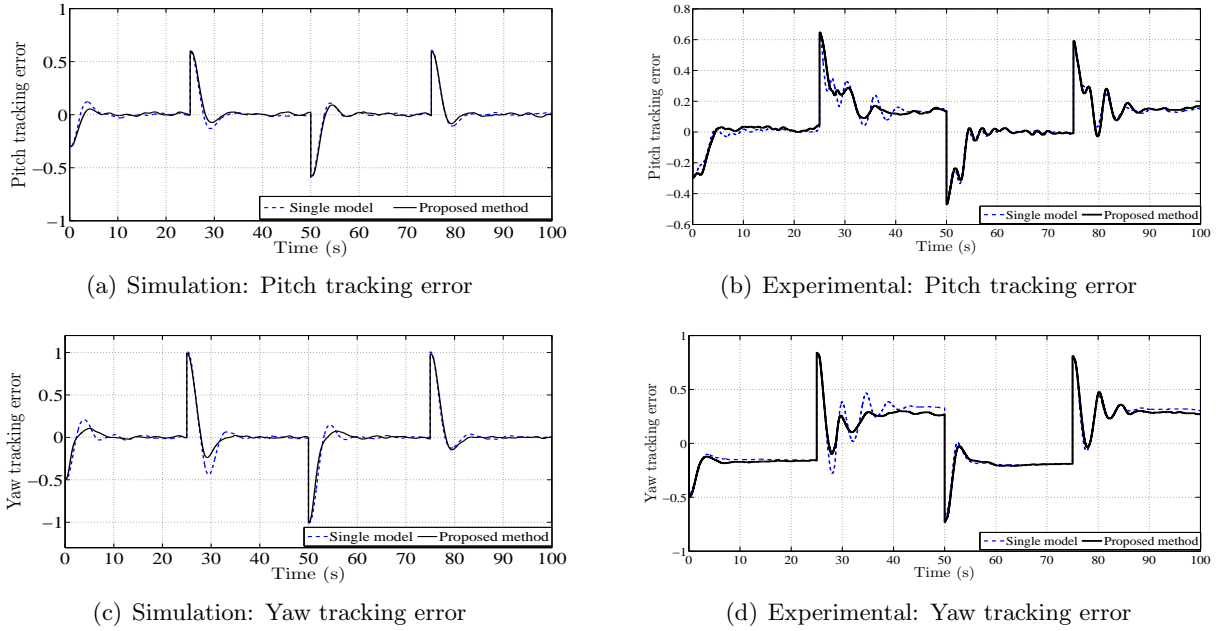


Figure 5.14: Trajectory tracking error for square input

Table 5.7: Comparison between single model and MMTLA: Yaw control for square input

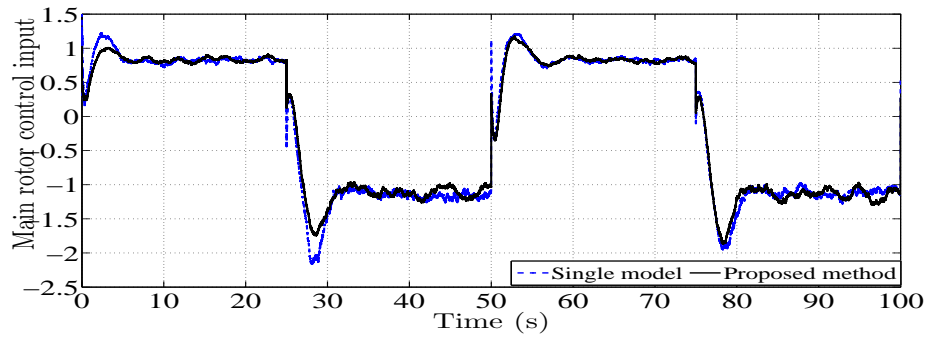
Simulation					
Adaptation Mechanism	Performance Specifications				
	TV	CE	RMSE	ISE	IAE
single model	112.25	172.12	0.221	4.9×10^3	9.3×10^3
MMTLA Control	75.0	170.1	0.206	4.27×10^3	7.79×10^3

Experimental					
Adaptation Mechanism	Performance Specifications				
	TV	CE	RMSE	ISE	IAE
single model	485.7	131.69	0.2792	7.8×10^3	2.5×10^4
MMTLA Control	876.9	128.63	0.2655	7.05×10^3	2.36×10^4

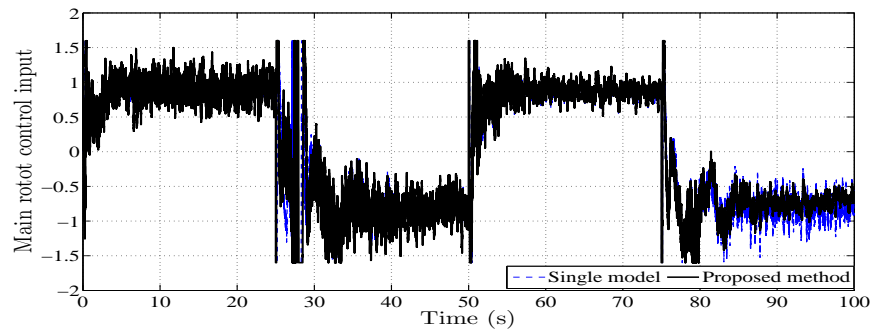
TV : Total variation, *CE* : Control energy

RMSE : Root mean square error

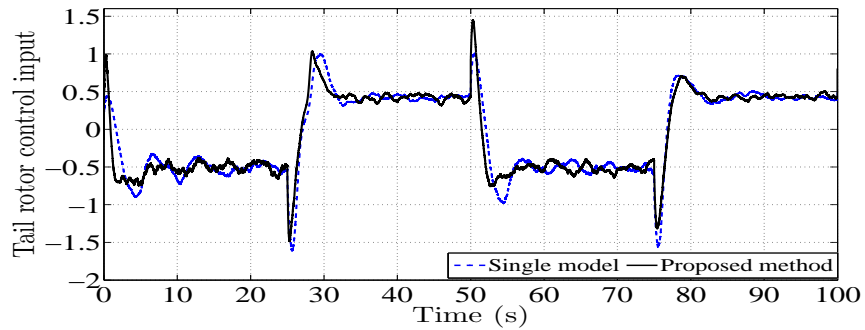
ISE : Integral square error, *IAE* : Integral absolute error



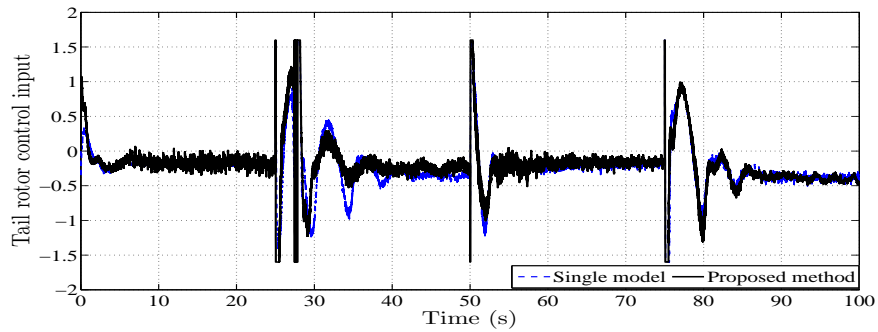
(a) Simulation: Main rotor control input (volts)



(b) Experimental: Main rotor control input (volts)



(c) Simulation: Tail rotor control input (volts)



(d) Experimental: Tail rotor control input (volts)

Figure 5.15: Control input for square trajectory tracking

5.8 Summary

An adaptive controller using multiple model based two level adaptation (MMTLA) strategy is proposed for nonlinear coupled MIMO systems. A feedback linearization technique is used to design the control input, while also decoupling the system. Multiple estimation models are used to tune the unknown parameters. The adaptive weights at the second level combine all the parameter vectors of the first level to provide a single parameter vector to be used in the controller. A twin rotor MIMO system (TRMS) is used for conducting simulation and experimental studies to investigate the performance of the proposed MMTLA control method. Step and sinusoidal reference inputs are applied to assess the tracking performance of the proposed control method. A square reference input is used to investigate the controller's performance in the case of sudden input change. The control energy used by the controller is computed in all these applications to evaluate the input performance. Simulation and experimental results for pitch and yaw angle tracking show improvement in transient and steady state performances using the proposed multiple model with two level adaptation (MMTLA) method compared to the existing single model based adaptive control method. Superior tracking response, improved transients and smoother control effort with reduction in energy establish efficacy of the proposed method. Results of real time experiments conducted on the TRMS support theoretical propositions of the proposed MMTLA control method.

6

Adaptive Controller Design for Nonlinear MIMO Model Following Control Systems Using Multiple Model Based Two Level Adaptation Technique

Contents

6.1	Introduction	100
6.2	System Model	101
6.3	Estimation Model Architecture	101
6.4	Model Following Controller Architecture	102
6.5	Controller Design Using MMTLA Method	104
6.6	Simulation Results	105
6.7	Summary	110

6.1 Introduction

A good number of methods exist in literature to design controllers for nonlinear multi-input multi-output (MIMO) coupled systems [62,66,67]. However, most of these methods are based on decoupling techniques [62,66–68]. In [62], the MIMO coupled system is divided into horizontal and vertical subsystems and the coupling is treated as the uncertainty between subsystems. Few other techniques using decoupling method include sliding mode controller [66], backstepping controller [67], T-S fuzzy model based controller [68]. In [77], a nonlinear model predictive control based on successive linearization of nonlinear helicopter model is presented. In designing controllers for nonlinear multi-input multi-output (MIMO) coupled systems, the commonly utilized practice is to use the feedback linearization technique to design the control input which also decouples the nonlinear system [8]. However, if the decoupling matrix happens to be singular, the common static state feedback is not be able to decouple the system. To deal with this type of system, a nonlinear adaptive model following control design using nonlinear structure algorithm is presented in [25, 78]. In this case a dynamic state feedback controller is designed which also decouples the system.

This chapter investigates the application of multiple models with two level adaptation (MMTLA) for adaptive control of a class of nonlinear MIMO systems with cross-couplings which cannot be decoupled using static state feedback because of singularity of the decoupling matrix. A dynamic state feedback controller is designed here to decouple the system. The MMTLA method is used and unknown parameters present in the model are estimated using an observer based estimation model [5,45]. Adaptive tuning laws for the unknown parameters are derived using Lyapunov stability criterion.

Simulation studies are conducted on a 3-degrees-of-freedom (DOF) laboratory helicopter [79,80] is a classic example of above mentioned class of nonlinear MIMO system with inter-axis cross-coupling and singular decoupling matrix. The proposed MMTLA method is compared with a single model based adaptive controller.

6.2 System Model

This work considers a class of nonlinear multi-input multi-output (MIMO) system [6]

$$\begin{aligned}\dot{\mathbf{x}} &= f(\mathbf{x}, \boldsymbol{\theta}) + \sum_{i=1}^m g_i(\mathbf{x}, \boldsymbol{\theta}) u_i \\ y_i &= h_i(\mathbf{x}), \quad i = 1, \dots, m\end{aligned}\tag{6.1}$$

where $\mathbf{x} \in \mathbb{R}^n$, $u_i, y_i : \mathbb{R}^+ \rightarrow \mathbb{R}$, and $f(\mathbf{x}, \boldsymbol{\theta})$, $g_i(\mathbf{x}, \boldsymbol{\theta})$, $h_i(\mathbf{x})$ are smooth functions. Besides, $\boldsymbol{\theta} \in \mathcal{S}_\theta$ is the unknown parameter vector with a compact set \mathcal{S}_θ . Moreover, the system (6.1) is assumed to satisfy the following properties:

- (i) Functions $f(\mathbf{x}, \boldsymbol{\theta})$ and $g_i(\mathbf{x}, \boldsymbol{\theta})$ can be characterized as

$$\begin{aligned}f(\mathbf{x}, \boldsymbol{\theta}) &= \boldsymbol{\omega}_f^T(\mathbf{x}) \boldsymbol{\theta}_f \\ g_i(\mathbf{x}, \boldsymbol{\theta}) &= \boldsymbol{\omega}_{g_i}^T(\mathbf{x}) \boldsymbol{\theta}_g\end{aligned}\tag{6.2}$$

where $\boldsymbol{\omega}_f(\mathbf{x})$ and $\boldsymbol{\omega}_{g_i}(\mathbf{x})$ are known functions.

- (ii) The system has constant relative degree γ_i [6], i.e.

$$L_{g_i(\mathbf{x}, \boldsymbol{\theta})} L_{f(\mathbf{x}, \boldsymbol{\theta})}^{i-1} h_i(\mathbf{x}) = 0, \quad i = 1, 2, \dots, (\gamma_i - 1) \text{ and } L_{g_i(\mathbf{x}, \boldsymbol{\theta})} L_{f(\mathbf{x}, \boldsymbol{\theta})}^{\gamma_i-1} h_i(\mathbf{x}) \neq 0, \quad \forall \mathbf{x} \in \mathbb{R}^n, \boldsymbol{\theta} \in \mathcal{S}_\theta.$$

- (iii) The system (6.1) has zero dynamics with asymptotically stable equilibrium point [6].

6.3 Estimation Model Architecture

In this Section, an estimation model is designed for the system under consideration. The adaptive laws for tuning of unknown parameter vector $\boldsymbol{\theta}$ is derived using Lyapunov technique. Using (6.2), the system (6.1) can be rewritten as

$$\dot{\mathbf{x}} = \boldsymbol{\omega}_f^T(\mathbf{x}) \boldsymbol{\theta}_f + \sum_{i=1}^m \boldsymbol{\omega}_{g_i}^T(\mathbf{x}) \boldsymbol{\theta}_g u_i\tag{6.3}$$

An observer based estimation model [5, 45] for the system (6.3) defined as

$$\dot{\hat{\mathbf{x}}} = \mathbf{A}(\hat{\mathbf{x}} - \mathbf{x}) + \boldsymbol{\omega}_f^T(\mathbf{x}) \hat{\boldsymbol{\theta}}_f + \sum_{i=1}^m \boldsymbol{\omega}_{g_i}^T(\mathbf{x}) \hat{\boldsymbol{\theta}}_g u_i\tag{6.4}$$

Subtracting (6.3) from (6.4) gives the estimation error dynamics for system (6.3) as

$$\dot{\mathbf{e}}_I = \mathbf{A} \mathbf{e}_I + \boldsymbol{\omega}_f^T(\mathbf{x}) \tilde{\boldsymbol{\theta}}_f + \sum_{i=1}^m \boldsymbol{\omega}_{g_i}^T(\mathbf{x}) \tilde{\boldsymbol{\theta}}_g u_i\tag{6.5}$$

with $\mathbf{e}_I = \hat{\mathbf{x}} - \mathbf{x}$, $\tilde{\boldsymbol{\theta}} = \hat{\boldsymbol{\theta}} - \boldsymbol{\theta}$. Here, the matrix $\mathbf{A} \in \mathbb{R}^{n \times n}$ is considered as stable. A suitable Lyapunov function is chosen as $V(\mathbf{e}_I, \tilde{\boldsymbol{\theta}}_f, \tilde{\boldsymbol{\theta}}_{g_i}) = \mathbf{e}_I^T \mathbf{P} \mathbf{e}_I + \tilde{\boldsymbol{\theta}}_f^T \tilde{\boldsymbol{\theta}}_f + \tilde{\boldsymbol{\theta}}_{g_i}^T \tilde{\boldsymbol{\theta}}_{g_i}$ where \mathbf{P} is the positive definite matrix solution of the Lyapunov equation $\mathbf{A}^T \mathbf{P} + \mathbf{P} \mathbf{A} = -\mathbf{Q}$ and $\mathbf{Q} = \mathbf{Q}^T > 0$. Considering adaptive laws for the parameter estimates as

$$\begin{aligned}\dot{\tilde{\boldsymbol{\theta}}}_f &= \dot{\hat{\boldsymbol{\theta}}}_f = -\boldsymbol{\omega}_f^T(\mathbf{x}) \mathbf{P} \mathbf{e}_I \\ \dot{\tilde{\boldsymbol{\theta}}}_{g_i} &= \dot{\hat{\boldsymbol{\theta}}}_{g_i} = -\boldsymbol{\omega}_{g_i}^T(\mathbf{x}) u_i \mathbf{P} \mathbf{e}_I\end{aligned}\tag{6.6}$$

and following *Theorem 2.1* in [45], it can be guaranteed that $\mathbf{e}_I \rightarrow 0$ as $t \rightarrow \infty$. Besides, regressor vectors $\boldsymbol{\omega}_f(\mathbf{x}), \boldsymbol{\omega}_{g_i}(\mathbf{x})$ which are rich in frequency contents [7] (A.1) will lead to asymptotic convergence of $\tilde{\boldsymbol{\theta}} = [\tilde{\boldsymbol{\theta}}_f, \tilde{\boldsymbol{\theta}}_g]^T$ to zero [6, 45].

6.4 Model Following Controller Architecture

The dynamic state feedback controller design using which the output of a nonlinear system follows that of a nonlinear reference model is presented in details in [78]. In this section, a nonlinear model following control [78] is described for the nonlinear MIMO coupled system (6.1). The outputs y_i are differentiated γ_i times with respect to time, such that at least one of the inputs appear in $y_i^{(\gamma_i)}$ [6], i.e.

$$y_i^{(\gamma_i)} = L_{f(\mathbf{x}, \boldsymbol{\theta})}^{\gamma_j} h_i(\mathbf{x}) + \sum_{i=1}^m L_{g_i}(L_{f(\mathbf{x}, \boldsymbol{\theta})}^{\gamma_i-1} h_i(\mathbf{x})) u_i\tag{6.7}$$

with at least one of the $L_{g_i}(L_{f(\mathbf{x}, \boldsymbol{\theta})}^{\gamma_i-1} h_i(\mathbf{x})) \neq 0, \forall \mathbf{x} \in \mathbb{R}^n, \boldsymbol{\theta} \in \mathcal{S}_\theta$. Further, $m \times 1$ vector $\mathfrak{B}(\mathbf{x}, \boldsymbol{\theta})$ and $m \times m$ matrix $\mathfrak{A}(\mathbf{x}, \boldsymbol{\theta})$ are defined as

$$\mathfrak{B}(\mathbf{x}, \boldsymbol{\theta}) = \begin{bmatrix} L_{f(\mathbf{x}, \boldsymbol{\theta})}^{\gamma_1} h_1(\mathbf{x}) \\ \cdot \\ \cdot \\ \cdot \\ L_{f(\mathbf{x}, \boldsymbol{\theta})}^{\gamma_p} h_m(\mathbf{x}) \end{bmatrix}, \quad (6.8)$$

$$\mathfrak{A}(\mathbf{x}, \boldsymbol{\theta}) = \begin{bmatrix} L_{g_1(\mathbf{x}, \boldsymbol{\theta})}(L_{f(\mathbf{x}, \boldsymbol{\theta})}^{\gamma_1-1} h_1(\mathbf{x})) & \cdot & \cdot & L_{g_m(\mathbf{x}, \boldsymbol{\theta})}(L_{f(\mathbf{x}, \boldsymbol{\theta})}^{\gamma_1-1} h_1(\mathbf{x})) \\ \cdot & & & \cdot \\ \cdot & & & \cdot \\ \cdot & & & \cdot \\ L_{g_1(\mathbf{x}, \boldsymbol{\theta})}(L_{f(\mathbf{x}, \boldsymbol{\theta})}^{\gamma_m-1} h_m(\mathbf{x})) & \cdot & \cdot & L_{g_m(\mathbf{x}, \boldsymbol{\theta})}(L_{f(\mathbf{x}, \boldsymbol{\theta})}^{\gamma_m-1} h_m(\mathbf{x})) \end{bmatrix}$$

Now (6.7) can be written as

$$\mathbf{y} = \mathfrak{B}(\mathbf{x}, \boldsymbol{\theta}) + \mathfrak{A}(\mathbf{x}, \boldsymbol{\theta})\mathbf{u} \quad (6.9)$$

where \mathbf{y} and \mathbf{u} are m -dimensional column vectors. The matrix $\mathfrak{A}(\mathbf{x}, \boldsymbol{\theta})$ in (6.8) is the decoupling matrix. If $\mathfrak{A}(\mathbf{x}, \boldsymbol{\theta})$ is nonsingular, the design of feedback controller using static state feedback is straightforward [8, 48]. However, in cases where the decoupling matrix $\mathfrak{A}(\mathbf{x}, \boldsymbol{\theta})$ is singular, static state feedback technique cannot be applied. Consequently, such a system is not decouplable by static state feedback. The well known nonlinear structure algorithm [25, 78] is used here to design the model following control for the nonlinear coupled MIMO system (6.1). The reference model is chosen as

$$\begin{aligned} \dot{\mathbf{x}}_M &= f_M(\mathbf{x}_M, \boldsymbol{\theta}) + \sum_{i=1}^m g_{Mi}(\mathbf{x}_M, \boldsymbol{\theta}) u_{Mi} \\ y_{Mi} &= h_{Mi}(\mathbf{x}_M), \quad i = 1, \dots, m \end{aligned} \quad (6.10)$$

Now, using (6.1) and (6.10), the error between the output of the reference model and the system output is found as

$$\mathbf{e}_i = h_{Mi}(\mathbf{x}_M) - h_i(\mathbf{x}), \quad i = 1, \dots, m \quad (6.11)$$

The nonlinear structure algorithm [78] states that, elimination of one of the inputs and differentiation of the error equation (6.11) is repeated until a nonsingular decoupling matrix appears. Following the

steps of nonlinear model following control [78], the compensator used to control the system (6.1) is considered in dynamic state feedback form as

$$\mathbf{u} = \alpha(\mathbf{x}, \boldsymbol{\theta}) + \beta(\mathbf{x}, \boldsymbol{\theta})\mathbf{u}_M. \quad (6.12)$$

Replacing unknown values of parameter $\boldsymbol{\theta}$ with their estimates $\hat{\boldsymbol{\theta}}$ provides

$$\mathbf{u} = \alpha(\mathbf{x}, \hat{\boldsymbol{\theta}}) + \beta(\mathbf{x}, \hat{\boldsymbol{\theta}})\mathbf{u}_M \quad (6.13)$$

where $\alpha(\mathbf{x}, \hat{\boldsymbol{\theta}})$, $\beta(\mathbf{x}, \hat{\boldsymbol{\theta}})$ can be found using *Theorem 3.1* in [78]. Theorem 3.1 in [78] discusses the conditions for existence of α and β such that (6.10) is a model following control system.

6.5 Controller Design Using MMTLA Method

Multiple estimation models $M_j(j = 1, \dots, N)$ and two level adaptation method are used next. In case of multiple models, the same estimator structure (6.4) is used for all the models but with N different parameter vector estimates $\hat{\boldsymbol{\theta}}_j$ placed at different starting points inside the compact space \mathcal{S}_θ .

The initial values of parameter estimates $\hat{\boldsymbol{\theta}}_j$ are chosen such that these cover the entire compact space \mathcal{S}_θ . Consequently, the observer based estimation model (6.4) for N different parameter estimates can be given as

$$\dot{\hat{\mathbf{x}}}_j = \mathbf{A}(\hat{\mathbf{x}}_j - \mathbf{x}) + \boldsymbol{\omega}_f^T(\mathbf{x})\hat{\boldsymbol{\theta}}_{f_j} + \sum_{i=1}^m \boldsymbol{\omega}_{g_i}^T(\mathbf{x})\hat{\boldsymbol{\theta}}_{g_j} u_i \quad (6.14)$$

which provides the identifier error dynamics for each model as

$$\dot{\mathbf{e}}_{I_j} = \mathbf{A}\mathbf{e}_{I_j} + \boldsymbol{\omega}_f^T(\mathbf{x})\tilde{\boldsymbol{\theta}}_{f_j} + \sum_{i=1}^m \boldsymbol{\omega}_{g_i}^T(\mathbf{x})\tilde{\boldsymbol{\theta}}_{g_j} u_i \quad (6.15)$$

The adaptive tuning laws for the j -th model parameter vector $\hat{\boldsymbol{\theta}}_j = [\hat{\boldsymbol{\theta}}_{f_j}, \hat{\boldsymbol{\theta}}_{g_j}]^T$ can be found as

$$\begin{aligned} \dot{\tilde{\boldsymbol{\theta}}}_{f_j} &= \dot{\hat{\boldsymbol{\theta}}}_{f_j} = -\boldsymbol{\omega}_f^T(\mathbf{x})\mathbf{P}\mathbf{e}_{I_j} \\ \dot{\tilde{\boldsymbol{\theta}}}_{g_{i_j}} &= \dot{\hat{\boldsymbol{\theta}}}_{g_{i_j}} = -\boldsymbol{\omega}_{g_i}^T(\mathbf{x})u_i\mathbf{P}\mathbf{e}_{I_j} \end{aligned} \quad (6.16)$$

where $\boldsymbol{\theta}, \hat{\boldsymbol{\theta}}_j \in \mathcal{S}_\theta$.

Now, the MMTLA method discussed in Section 3.3.3 is applied to the nonlinear MIMO coupled system described in Section 6.2.

The parameter vector $\boldsymbol{\theta}_s(t)$ of the second level model is a convex combination of the first level models $\hat{\boldsymbol{\theta}}_j(t)$, given by

$$\boldsymbol{\theta}_s(t) = \sum_{j=1}^N w_j(t) \hat{\boldsymbol{\theta}}_j(t) \quad (6.17)$$

with the adaptive weights $w_j(t)$ satisfying the convexity conditions as, $w_j \geq 0$ and $\sum_{j=1}^N w_j(t) = 1$. The adaptive tuning law for the adaptive weights $w_j(t)$ is provided in Section 3.3.3. Consequently, using the combination of $\boldsymbol{\theta}_s$ with adaptive weights $w_j(t)$ at every instant, the new control input is found as

$$\mathbf{u}_s = \alpha_s(\mathbf{x}, \boldsymbol{\theta}_s) + \beta_s(\mathbf{x}, \boldsymbol{\theta}_s) u_{Mi} \quad (6.18)$$

where $\alpha_s(\mathbf{x}, \boldsymbol{\theta}_s)$, $\beta_s(\mathbf{x}, \boldsymbol{\theta}_s)$ are similar to $\alpha(\mathbf{x}, \hat{\boldsymbol{\theta}})$, $\beta(\mathbf{x}, \hat{\boldsymbol{\theta}})$ after incorporating the second level parameters $\boldsymbol{\theta}_s$.

The Lyapunov stability analysis after second level and control error convergence for this Chapter can be directly assessed following the analysis provided in Section 5.6.1.

6.6 Simulation Results

A 3 degrees of freedom (DOF) helicopter model [25, 80] is a good example of a nonlinear MIMO system with inter-axes cross-coupling and having a singular decoupling matrix. Hence, simulation studies are conducted on a 3-DOF helicopter model shown in Figure 6.1 [25] and results are compared with a single model based adaptive control method. As observed in Figure 6.1, the 3-DOF helicopter has a front rotor and a rear rotor. The three degrees of freedom are the elevation ε , pitch Θ and travel ϕ . The aim here is to control elevation and travel angles using the voltages generated by two DC motors attached to the propellers. The dynamical equation of helicopter model in state space form is given as [80]:

$$\begin{aligned} \dot{x}_1 &= x_2 \\ \dot{x}_2 &= \theta_1 \cos x_1 + \theta_2 \sin x_1 + \theta_3 x_2 + \theta_4 \cos x_3 u_1 \\ \dot{x}_3 &= x_4 \\ \dot{x}_4 &= \theta_5 \cos x_3 + \theta_6 \sin x_3 + \theta_7 x_4 + \theta_8 u_2 \\ \dot{x}_5 &= x_6 \\ \dot{x}_6 &= \theta_9 x_6 + \theta_{10} \sin x_3 u_1 \\ y_1 &= x_1, \quad y_2 = x_5 \end{aligned} \quad (6.19)$$

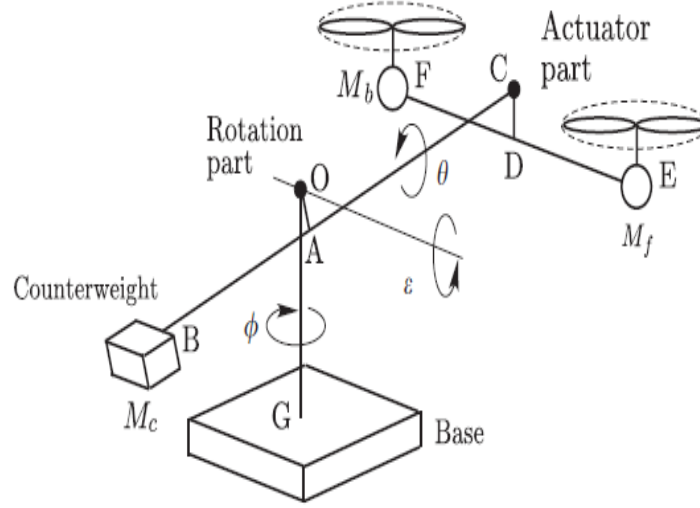


Figure 6.1: 3-DOF laboratory helicopter model

where x_1 denotes the elevation angle, x_2 denotes the elevation angular velocity, x_3 represents the pitch angle, x_4 denotes the pitch angular velocity, x_5 represents the travel angle, x_6 denotes the travel angular velocity and y_1, y_2 are the outputs. Similarly, $u_1 = V_f + V_b$, $u_2 = V_f - V_b$ denotes the control inputs to the main rotor and tail rotor respectively. Here, V_f, V_b are the voltages applied to the front and rear motors respectively. The unknown parameter vector $\theta = [\theta_f, \theta_g]^T$ is given by $\theta_f = [\theta_1, \theta_2, \theta_3, \theta_5, \theta_6, \theta_7, \theta_9]^T$, $\theta_g = [\theta_4, \theta_8, \theta_{10}]^T$. The system (6.19) has constant relative degrees $\gamma_1 = 2$ and $\gamma_2 = 2$. In (6.19), the unknown parameters comprise of

$$\begin{aligned}
 \theta_1 &= [-(M_f + M_b)gL_a + M_cgL_c]/J_\epsilon \\
 \theta_2 &= -[(M_f + M_b)gL_a \tan \delta_a + M_cgL_c \tan \delta_c]/J_\epsilon \\
 \theta_3 &= -\eta_\epsilon/J_\epsilon \\
 \theta_4 &= K_m L_a/J_\epsilon \\
 \theta_5 &= -(M_f + M_b)gL_h/J_\Theta \\
 \theta_6 &= -(M_f + M_b)gL_h \tan \delta_h/J_\Theta \\
 \theta_7 &= -\eta_p/J_\Theta \\
 \theta_8 &= K_m L_h/J_\Theta \\
 \theta_9 &= -\eta_t/J_\phi \\
 \theta_{10} &= -K_m L_a/J_\phi
 \end{aligned} \tag{6.20}$$

where $\delta_a = \tan^{-1}\{(L_d + L_e)/L_a\}$, $\delta_c = \tan^{-1}(L_d/L_c)$ and $\delta_h = \tan^{-1}(L_e/L_h)$. The nominal values of above physical constants belonging to 3-DOF helicopter model shown in Figure 6.1 are provided in Table 6.1 [80]. The two reference inputs u_{M1} , u_{M2} are chosen as square waves having amplitudes 0.3,

Table 6.1: Physical parameters of the 3 DOF helicopter model

Symb.	Description	Value	Unit
J_ε	Moment of inertia about elevation	0.086	kg-m ²
J_Θ	Moment of inertia about pitch	0.044	kg-m ²
J_ϕ	Moment of inertia about travel	0.82	kg-m ²
η_ε	Coefficient of viscous friction abt elevation	0.001	kg-m ² /s
η_Θ	Coefficient of viscous friction abt pitch	0.001	kg-m ² /s
η_ϕ	Coefficient of viscous friction abt travel	0.005	kg-m ² /s
L_a	Distance AC in (6.1)	0.62	m
L_c	Distance AB in (6.1)	0.44	m
L_d	Distance OA in (6.1)	0.05	m
L_e	Distance CD in (6.1)	0.02	m
L_h	Distance DE=DF in (6.1)	0.177	m
M_f	Mass of front section	0.69	kg
M_b	Mass of rear section	0.69	kg
M_c	Mass of counterbalance	1.67	kg
K_m	Force constant	0.5	N/V
g	Gravity constant	9.81	m/s ²

0.8 respectively, with time period of 50 sec in each case. Further, the initial values of the unknown parameter vector θ for the single model case are chosen as

$\hat{\theta} = [-2.5, -3.0, -0.5, 0.1, -0.8, -8.0, -0.8, 1.5, -0.8, -0.8]^T$. For the multiple model case, $N = 4$ number of models are chosen as

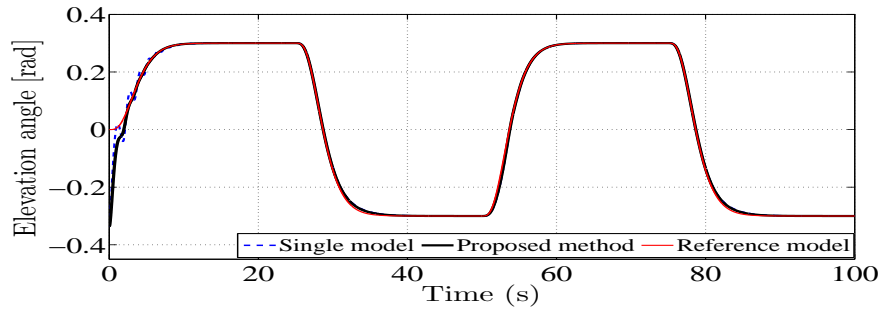
$$\begin{aligned}
 \text{Model 1} &= [-2.5, -3.0, -0.5, 0.1, -0.8, -8.0, -0.8, 1.5, -0.8, -0.8] \\
 \text{Model 2} &= [-2.0, -2.4, -0.3, 0.3, -0.4, -7.0, -0.6, 1.7, -0.5, -0.6] \\
 \text{Model 3} &= [-1.4, -1.8, -0.1, 0.4, 0.1, -6.0, -0.3, 2.0, -0.2, -0.4] \\
 \text{Model 4} &= [-0.8, -1.2, 0, 0.6, 0.5, -5.2, 0, 2.2, 0, -0.2]
 \end{aligned} \tag{6.21}$$

As in Chapter 5, here also the number of models is searched heuristically. The simulations are started with 16 number of models. It is found that simulation results with 4 number of models do not vary for number of models greater than 4. Therefore, number of models is selected as 4. The observer gain

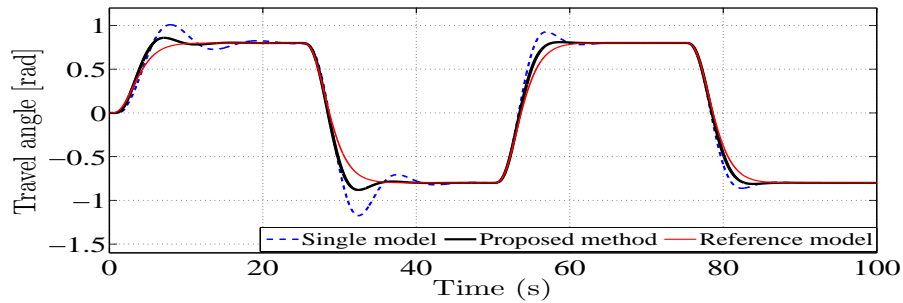
matrix is chosen as

$$A = \begin{bmatrix} -1 & 0 & 0 & 0 & 0 & 0 \\ 0 & -2 & 0 & 0 & 0 & 0 \\ 0 & 0 & -1 & 0 & 0 & 0 \\ 0 & 0 & 0 & -2 & 0 & 0 \\ 0 & 0 & 0 & 0 & -1 & 0 \\ 0 & 0 & 0 & 0 & 0 & -2 \end{bmatrix} \quad (6.22)$$

for both single and multiple models. Simulation results obtained using the proposed method with $N = 4$ number of models are compared with those obtained by using only single model as shown in Figures 6.2 - Figure 6.4. Tables 6.2 summarize the transient and steady state performances for



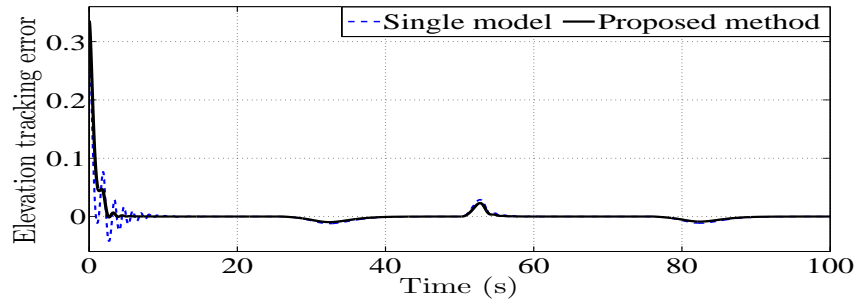
(a) Elevation angle tracking reference trajectory



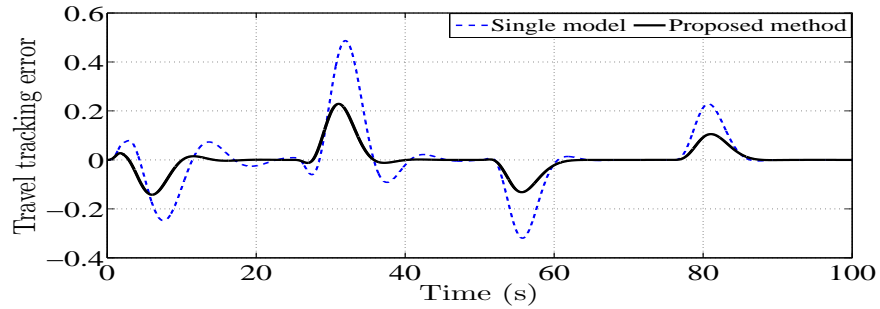
(b) Travel angle tracking reference trajectory

Figure 6.2: Reference trajectory tracking

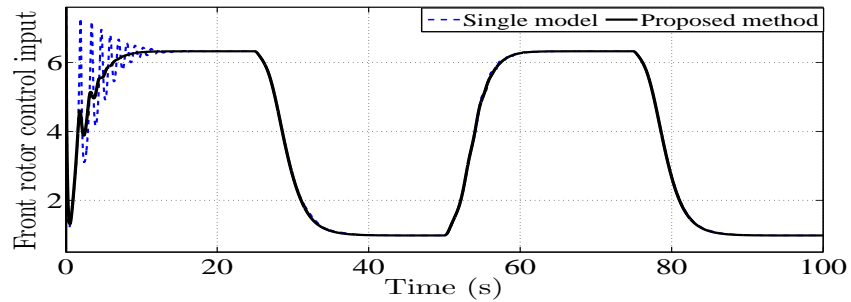
elevation and travel angles. Moreover, the input performances in terms of total variation (TV) and control energy (CE) and the output performance in terms of root mean square error (RMSE) are provided in the tables for comparative analysis of a single adaptation model against the proposed method with $N = 4$ models and two level adaptation. The definitions of performance specifications



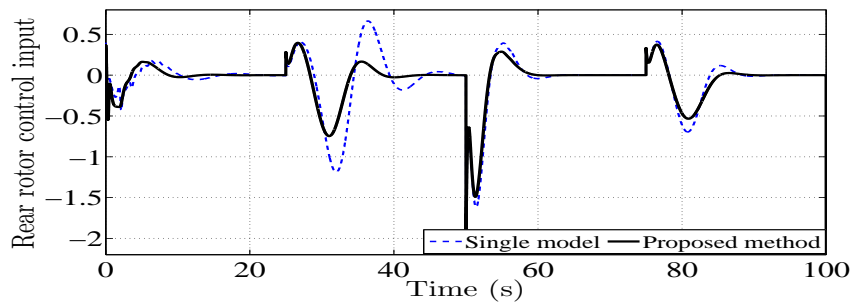
(a) Elevation angle tracking error



(b) Travel angle tracking error

Figure 6.3: Tracking error

(a) Front rotor control input



(b) Rear rotor control input

Figure 6.4: Control input

can be found in A.5. From Table 6.2 it is observed that the overshoots in case of elevation control are eliminated completely using the proposed method. Also, there is significant improvement in overshoot for travel angle control. Similarly, the improvements in settling time is visible in both the cases. Also, while there is mild improvement in smoothness of the control signal for travel angle, it is quite significant for elevation control. The reduction in control energy for both elevation and travel control is an added advantage of the proposed method. RMSE in output tracking is comparable in both the methods indicating similar performance. Besides, parameter estimates converge to the actual values for all the persistently exciting input signals.

Table 6.2: Comparison between single model and MMTLA

Elevation angle tracking

Adaptation Mechanism	Performance Specifications						
	M_p	M_u	t_s	e_{ss}	TV	CE	RMSE
single model	25.56 %	13.4 %	9.84 s	0	104.31	1424.7	0.0195
MMTLA Control	0 %	0 %	4.64 s	0	38.17	1415	0.0225

Travel angle tracking

Adaptation Mechanism	Performance Specifications						
	M_p	M_u	t_s	e_{ss}	TV	CE	RMSE
single model	9.8 %	30.9 %	23.0 s	0	18.37	106.7	0.1232
MMTLA Control	3.4 %	17.78 %	15.5 s	0	16.47	83.02	0.0576

M_p : Peak overshoot, M_u : Peak undershoot

t_s : Settling time, e_{ss} : Steady state error

TV : Total variation, CE : Control energy

RMSE : Root mean square error

6.7 Summary

A multiple model with two level adaptation technique is proposed for a class of nonlinear MIMO coupled system which cannot be decoupled using traditional static state feedback control technique because of the singularity in the decoupling matrix. An adaptive model following control, using nonlinear structure algorithm with dynamic state feedback is designed. An observer based estimation model with Lyapunov technique is used to find the adaptive laws for online estimation of unknown parameters of the system. The MMTLA technique is introduced for the system under consideration. The same observer based estimation model is now equipped with multiple parameter models with

different initial values covering the full compact space. A combination of multiple models at first level provides the single virtual parameter model termed as second level adaptation model. Better tracking response, improved settling time and smoother as well as lesser control effort establish efficacy of the proposed method.

7

Conclusions and Scope for Future Work

Contents

7.1	Conclusions	113
7.2	Scope for Future Work	114

7.1 Conclusions

In this thesis, an adaptive controller using multiple model based two level adaptation technique is developed for nonlinear uncertain systems.

At first, a multiple model based two level adaptation (MMTLA) control technique is proposed for a SISO nonlinear system with linear parameterization. The control input is found by using feedback linearization method. The adaptive laws for unknown parameters at the first level are computed using Lyapunov stability criterion. Thereafter, multiple estimation models having identical structures and adaptive nature are built. The initial parameters of the estimation models are chosen to span the entire compact parameter space. The multiple estimation models at the first level are combined using adaptive weights to get a single virtual adaptive model referred to as the second level model. The adaptive tuning laws for weights at the second level are found using the identifier error. Overall closed loop stability of the system and tracking error convergence with MMTLA are derived using Lyapunov stability analysis. Simulation results establish that the proposed MMTLA control method outperforms existing switching based multiple model adaptive control method. A notable feature of the proposed MMTLA control method is that it requires significantly lesser number of identification models than that of existing multiple model based techniques at no cost on the overall performance. Moreover, the proposed MMTLA method offers quick parameter convergence.

An adaptive controller design using MMTLA method for SISO nonlinear systems having nonlinear parameterization is proposed next. The controller design follows similar design methodology as used for linearly parameterized SISO systems. Simulation results confirm improvement in transient, input and output performances with the MMTLA controller compared to an existing adaptive control technique. The MMTLA control technique is best suited for systems where parametric errors are large and convergence of first level models is slow.

An adaptive controller using MMTLA technique is proposed next for nonlinear coupled MIMO systems. Feedback linearization technique is used to design a static state feedback control input which also decouples the system. The design of multiple estimation models follows similar design method as used for nonlinear SISO systems. The model states are estimated using an Extended Kalman Filter (EKF). A twin rotor MIMO system (TRMS) which is a benchmark example of highly nonlinear uncertain coupled MIMO system is considered for testing the proposed controller. Simulation and experimental studies are conducted on the TRMS applying different types of reference inputs like

step, sinusoidal and square signals to evaluate the performance of the proposed MMTLA approach. Superior tracking response, improved transients and smoother control effort with reduction in control energy establish efficacy of the proposed method. Results of real time experiments conducted on the TRMS support theoretical propositions of the proposed MMTLA control method. The input reference signal is considered to be persistently exciting which ensures convergence in tuning.

The MMTLA control technique is investigated next for the challenging problem of controlling a class of nonlinear MIMO model following control systems. A model following method using feedback linearization technique with dynamic state feedback and nonlinear structure algorithm are used to tackle the singularity arising in the decoupling matrix. After designing the control input, the proposed MMTLA method is applied to control a 3-degrees-of-freedom (DOF) laboratory helicopter model which is an appropriate example of MIMO coupled nonlinear systems having singular decoupling matrix. An Extended Kalman Filter (EKF) is used to find the system states. Simulation studies confirm that the proposed MMTLA method outperforms existing switching based multiple model adaptive control methods but using lesser number of models.

Considerable improvement in transient and steady state performances is noticed by using the proposed multiple model based two level adaptive control scheme compared to existing single model based adaptive control methods. Moreover, smoother as well as lesser control effort establish efficacy of the proposed method. Further, parameter convergence of the proposed MMTLA method is reasonably fast which makes it appropriate for practical applications requiring online tuning. Requirement of lesser number of models is another advantage of using two level adaptation. Therefore, sufficient number of multiple adaptive models is evenly distributed to cover the complete range of parameter space. Simulation results show that if the positions of selected models are not optimal, the control effort needed is high.

7.2 Scope for Future Work

Future possible directions of research based on the MMTLA method developed in this thesis are outlined below:

- In the proposed MMTLA technique the parameters which are far away from their actual values have little contribution in the second level model. An intelligent system can be built such that the models whose contribution is lesser than a prescribed threshold can automatically get removed.

This intelligent system should be able to add/delete the new models online.

- Autonomous vehicles having huge number of uncertain parameters and expected to perform in dynamic environment may use this technique for longitudinal and lateral course correction during adaptive cruise control.
- The proposed technique may find application in electronic stability program (ESP) and antilock braking system (ABS).
- **Longitudinal speed control of autonomous vehicle at different speed ranges:** In autonomous vehicles, a driver controller is used to control the speed of vehicles. The driver controller takes feedback from different sensors present in modern vehicles [81]. Any Level 2 autonomous vehicle (or a vehicle with basic advanced driver assistance system (ADAS) features) is expected to perform some basic manoeuvres involving speed control [82]. Few basic manoeuvres are *cruise control*, *automatic lane change*, *automatic overtaking*, *automatic parking*, *remote parking*. In all these applications, the speed to be controlled is different, varying from very low speed for remote parking to high speed for cruise control. The scope of a single conventional controller to operate in this wide range may be limited. The proposed multiple models with two level adaptive (MMTLA) control would be a potential choice for the above discussed applications.
- **Adaptive vehicle navigation:** Many companies and research laboratories like google, tesla, uber, intel, nuTonomy and many others [83] are ready with their own versions of autonomous cars. The current challenging topic in autonomous vehicles is the complete testing of vehicles for their full life cycle, which is around 11 billion miles [84]. The solution to this challenge is simulation of critical scenarios, which can exponentially reduce the testing time for deployment of autonomous vehicles on the road. The research in this area requires adaptive vehicle navigation in a real-time traffic scenario [85] [86]. The proposed MMTLA technique is a promising candidate for adaptive vehicle navigation to improve navigation performance.



Appendix

Contents

A.1	Definitions	117
A.2	Cezayirli et al.'s method	117
A.3	Ge et al.'s method	118
A.4	Extended Kalman Filter (EKF)	118
A.5	Performance Specifications	119
A.6	Momentum equation for TRMS	120

A.1 Definitions

- (i) **Sufficiently rich condition:** As discussed in Chapter 8 of [7], the stability and convergence of adaptive controllers require the signals in the system to be sufficiently rich so that the estimated parameters converge to the true parameters.
- (ii) **Certainty equivalence principle:** As mentioned in Chapter 8 of [7], the controller parameters are computed from the estimates of the system parameters as if they were the true system parameters. This idea is often called the certainty equivalence principle.

A.2 Cezayirli et al.'s method

In Cezayirli et al.'s method [9] [10], an indirect adaptive controller for a class of SISO nonlinear systems is designed using multiple fixed identification models and switching. The system under consideration is given as [10]

$$\begin{aligned}\dot{\mathbf{x}}(t) &= f(\mathbf{x}(t), \boldsymbol{\theta}(t)) + g(\mathbf{x}(t), \boldsymbol{\theta}(t))u(t) \\ y(t) &= h(\mathbf{x}(t))\end{aligned}\tag{A.2.1}$$

where $\mathbf{x}(t) : \mathbb{R}^+ \rightarrow \mathbb{R}^n$ is the state vector, which is assumed to be fully available for measurement. Next, $f, g : \mathbb{R}^n \rightarrow \mathbb{R}^n$ are sufficiently smooth vector fields and $h : \mathbb{R}^n \rightarrow \mathbb{R}$ is a scalar valued function. Further, $\boldsymbol{\theta}(t) = [\theta_1, \theta_2, \dots, \theta_p]^T \in \mathcal{S}$ is the unknown parameter vector, where p is the number of unknown parameters and $\mathcal{S} \subset \mathbb{R}^p$ is a compact set. Finally, $u(t) : \mathbb{R}^+ \rightarrow \mathbb{R}$ is the control input and $y(t) : \mathbb{R}^+ \rightarrow \mathbb{R}$ represents the output.

Thereafter, N fixed identification model for the system (A.2.1) is designed as

$$\dot{\hat{\mathbf{x}}}_j = \mathbf{A}(\hat{\mathbf{x}}_j - \mathbf{x}) + \boldsymbol{\omega}^T(\mathbf{x}, u)\hat{\boldsymbol{\theta}}_j, \quad j = 1, \dots, N\tag{A.2.2}$$

with the control input given as

$$u = \frac{1}{\hat{\boldsymbol{\mathcal{P}}}^T \mathcal{G}(\mathbf{x})} (-\hat{\boldsymbol{\mathcal{P}}}^T \mathcal{F}(\mathbf{x}) + \hat{v})\tag{A.2.3}$$

The cost function for the switching between fixed models given as

$$J_j(t) = \tilde{\mathbf{x}}_j^T(t) G \tilde{\mathbf{x}}_j(t), \quad j = 1, \dots, N\tag{A.2.4}$$

where $G \in \mathbb{R}^{n \times n}$ is a positive-definite weight matrix. The switching logic based on the cost function (A.2.4) is given as

$$j^*(t) = \{j(t) : (J_0(t) - \min J_j(t)) \geq \kappa > 0\}, \quad j = 1, \dots, N, \quad t \in [T_i, T_{i+1}) \quad (\text{A.2.5})$$

where j^* gives the index for the chosen identification model.

A.3 Ge et al.'s method

In [12], Ge et al. designed an adaptive controller for nonlinear systems having nonlinear parameterization. A nonlinearly parameterized nonlinear system is considered as [12]

$$\begin{aligned} \dot{x}_i &= x_{i+1}, \quad i = 1, \dots, n-1 \\ \dot{x}_n &= \frac{1}{\beta(\mathbf{x})} [f(\mathbf{x}) + g(\mathbf{x})u] \\ y &= x_1 \end{aligned} \quad (\text{A.3.1})$$

where the state vector $\mathbf{x} : \mathbb{R}^+ \rightarrow \mathbb{R}^n$ is measurable. Moreover, $u : \mathbb{R}^+ \rightarrow \mathbb{R}$ is the control input and $y : \mathbb{R}^+ \rightarrow \mathbb{R}$ represents the output. Further, $f(\mathbf{x}), \beta(\mathbf{x}) : \mathbb{R}^n \rightarrow \mathbb{R}^n$ are sufficiently smooth vector fields and $g(\mathbf{x}) : \mathbb{R}^n \rightarrow \mathbb{R}^n$ is a known continuous function. Control input for the system (A.3.1) is derived as

$$u = \frac{1}{g(\mathbf{x})} \left[-\frac{k\varepsilon_s}{\alpha(\mathbf{x})} - \hat{\boldsymbol{\theta}}^T w(\mathbf{z}) - h(\mathbf{z}) \right] \quad (\text{A.3.2})$$

with adaptive tuning law for the estimate of unknown parameter $\boldsymbol{\theta}$ given as

$$\dot{\hat{\boldsymbol{\theta}}} = \Gamma w(\mathbf{z}) \alpha(\mathbf{x}) \varepsilon_s \quad (\text{A.3.3})$$

where $k, \varepsilon_s, \alpha(\mathbf{x}), z, w(\mathbf{z}), h(\mathbf{z})$ and Γ can be found in [12].

A.4 Extended Kalman Filter (EKF)

For the state estimation of nonlinear systems, the Kalman filter estimate is based on the linearized system and the new filter is called Extended Kalman Filter (EKF) [76]. The nonlinear system dynamics

are

$$\begin{aligned}\dot{\mathbf{x}} &= f(\mathbf{x}, u, w) \\ y &= h(\mathbf{x}, v)\end{aligned}\tag{A.4.1}$$

where $\mathbf{x}(t)$ is the state vector and f, h are nonlinear functions [76]. Here $w \sim \mathcal{N}(0, Q)$ and $v \sim \mathcal{N}(0, R)$ are normally distributed state and measurement noises respectively, with Q, R the corresponding covariance matrices. The linearized dynamics for (A.4.1) can be given as

$$\begin{aligned}F &= \left. \frac{\partial f(\mathbf{x})}{\partial \mathbf{x}} \right|_{\mathbf{x}=\hat{\mathbf{x}}} \\ N &= \left. \frac{\partial f(\mathbf{x})}{\partial w} \right|_{\mathbf{x}=\hat{\mathbf{x}}} \\ H &= \left. \frac{\partial h(\mathbf{x})}{\partial \mathbf{x}} \right|_{\mathbf{x}=\hat{\mathbf{x}}} \\ M &= \left. \frac{\partial h(\mathbf{x})}{\partial v} \right|_{\mathbf{x}=\hat{\mathbf{x}}}\end{aligned}\tag{A.4.2}$$

The Extended Kalman Filter update equations are given as

$$\begin{aligned}\dot{\hat{\mathbf{x}}} &= f(\hat{\mathbf{x}}, u, w) + K[y - h(\hat{\mathbf{x}}, v)] \\ K &= \Gamma H^T R_c^{-1} \\ \dot{\Gamma} &= F\Gamma + \Gamma F^T + Q_c - \Gamma H^T R_c^{-1} H\Gamma\end{aligned}\tag{A.4.3}$$

where K is the Kalman gain matrix and Γ is the error covariance matrix. The matrices $Q_c = NQN^T$ and $R_c = MRM^T$ are used.

A.5 Performance Specifications

The performance indices like peak overshoot (M_p), peak undershoot (M_u), settling time (t_s) represent the transient performance and e_{ss} represents the steady state performance of the controlled system. The control energy (CE) given by $\|u\|_2$ denotes the input performance. The root mean square error (RMSE), integral square error (ISE) and integral absolute error (IAE) denoting the output tracking performance and are given as

$$RMSE = \sqrt{\frac{\sum_{l=1}^{n_s} e_i^2(l)}{n_s}}\tag{A.5.1}$$

$$\begin{aligned}
 ISE &= \sum_{l=1}^{n_s} e_i^2(l) \\
 IAE &= \sum_{l=1}^{n_s} |e_i(l)|
 \end{aligned} \tag{A.5.2}$$

where e_i is the control error with $i = 1$ for SISO system and $i = 2, \dots, m$ for MIMO system. Further, n_s is the number of samples used.

Lastly, total variation (TV) characterizes smoothness of the control signal and input usage and is given as

$$TV = \sum_{l=1}^{n_s} |u_i(l+1) - u_i(l)| \tag{A.5.3}$$

where $u_i(1), u_i(2), \dots, u_i(n_s)$ is the discretized sequence of the input signal. A low value of TV indicates smoothness of the control input.

A.6 Momentum equation for TRMS

The momentum equation for the vertical movement of the TRMS is given as [60]:

$$l_1 \ddot{\alpha}_v = M_1 - M_{FG} - M_{B\alpha_v} - M_G \tag{A.6.1}$$

where

$$M_1 = a_1 \mathfrak{S}_1^2 + b_1 \mathfrak{S}_1 \quad \text{denotes nonlinear static characteristic}$$

$$M_{FG} = M_g \sin \alpha_v \quad \text{denotes gravity momentum}$$

$$M_{B\alpha_v} = B_{1\alpha_v} \dot{\alpha}_v - \frac{0.0326}{2} \sin 2\alpha_v \dot{\alpha}_h^2 \quad \text{represents friction forces momentum}$$

$$M_G = k_{gy} M_1 \dot{\alpha}_h \cos \alpha_v \quad \text{represents gyroscopic momentum}$$

The relation between the main motor input voltage u_v and the momentum \mathfrak{S}_1 can be approximated by a first order transfer function given as

$$\mathfrak{S}_1 = \frac{k_m}{T_{11}s + T_{10}} u_v \tag{A.6.2}$$

Similarly, the momentum equation for the horizontal movement is given as:

$$l_2 \ddot{\alpha}_h = M_2 - M_{B\alpha_h} - M_R \tag{A.6.3}$$

where

$$M_2 = a_2 \mathfrak{S}_2^2 + b_2 \mathfrak{S}_2 \quad \text{denotes nonlinear static characteristic}$$

$$M_{B\alpha_h} = B_{1\alpha_h} \dot{\alpha}_h \quad \text{represents friction forces momentum}$$

and M_R is the cross reaction momentum approximated by

$$M_R = \frac{k_c(T_o s + 1)}{(T_p s + 1)} M_1 \quad (\text{A.6.4})$$

Further, the relation of tail motor momentum \mathfrak{S}_2 with its input voltage u_h can be given as

$$\mathfrak{S}_2 = \frac{k_t}{T_{21}s + T_{20}} u_h \quad (\text{A.6.5})$$

Therefore, the dynamics of the TRMS in the state space form can be derived as [60]:

$$\begin{aligned} \dot{x}_1 &= x_2 \\ \dot{x}_2 &= \frac{a_1}{l_1} x_5^2 + \frac{b_1}{l_1} x_5 - \frac{M_g}{l_1} \sin x_1 - \frac{B_{1\alpha_v}}{l_1} x_2 + \frac{0.0326}{2l_1} x_4^2 \sin(2x_2) \\ &\quad - \frac{k_{gy} a_1}{l_1} x_4 x_5^2 \cos(x_1) - \frac{k_{gy} b_1}{l_1} x_4 x_5 \cos(x_1) \\ \dot{x}_3 &= x_4 \\ \dot{x}_4 &= \frac{a_2}{l_2} x_6^2 + \frac{b_2}{l_2} x_6 - \frac{B_{1\alpha_h}}{l_2} x_4 + \frac{1.75k_c a_1}{l_2} x_5^2 + \frac{1.75k_c b_1}{l_2} x_5 \\ \dot{x}_5 &= -\frac{T_{10}}{T_{11}} x_5 + \frac{k_m}{T_{11}} u_v \\ \dot{x}_6 &= -\frac{T_{20}}{T_{21}} x_6 + \frac{k_t}{T_{21}} u_h \\ y_1 &= x_1, \quad y_2 = x_3 \end{aligned} \quad (\text{A.6.6})$$

where x_1 denotes the pitch angle, x_2 denotes the pitch angular velocity, x_3 represents the yaw angle, x_4 represents the yaw angular velocity, x_5 denotes the momentum of the main motor and x_6 denotes the momentum of the tail motor. Further, y_1, y_2 denote the outputs.

References

- [1] J. D. Boskovic, “Adaptive control of a class of nonlinearly parameterized plants,” *IEEE Transactions on Automatic Control*, vol. 43, no. 7, pp. 930–934, Jul 1998.
- [2] A. N. Ouda, “A robust adaptive control approach to missile autopilot design,” *International Journal of Dynamics and Control*, pp. 1–33, Sep 2017.
- [3] K. J. Åström and B. Wittenmark, *Adaptive Control*, 2nd ed. Boston, MA, USA: Addison-Wesley Longman Publishing Co., Inc., 1994.
- [4] M. Krstic, I. Kanellakopoulos, and P. V. Kokotovic, *Nonlinear and Adaptive Control Design (Adaptive and Learning Systems for Signal Processing, Communications and Control Series)*. Wiley-Interscience, 1995.
- [5] K. S. Narendra and A. M. Annaswamy, *Stable Adaptive Systems*. Mineola, New York, USA: Dover Publications, 2005.
- [6] S. Sastry and A. Isidori, “Adaptive control of linearizable systems,” *IEEE Transactions on Automatic Control*, vol. 34, no. 11, pp. 1123–1131, 1989.
- [7] J.-J. E. Slotine and W. Li, *Applied nonlinear control*. Englewood Cliffs, New Jersey, USA: Prentice Hall, 1991.
- [8] A. Isidori, *Nonlinear Control Systems*, 3rd ed. Secaucus, New Jersey, USA: Springer-Verlag New York, Inc., 1995.
- [9] A. Cezayirli and M. K. Ciliz, “Transient performance enhancement of direct adaptive control of nonlinear systems using multiple models and switching,” *IET Control Theory Applications*, vol. 1, no. 6, pp. 1711–1725, Nov 2007.
- [10] —, “Indirect adaptive control of non-linear systems using multiple identification models and switching,” *International Journal of Control*, vol. 81, no. 9, pp. 1434–1450, 2008.
- [11] D. Cartes and L. Wu, “Experimental evaluation of adaptive three-tank level control,” *ISA Transactions*, vol. 44, no. 2, pp. 283 – 293, 2005.
- [12] S. S. Ge, C. C. Hang, and T. Zhang, “A direct adaptive controller for dynamic systems with a class of nonlinear parameterizations,” *Automatica*, vol. 35, no. 4, pp. 741 – 747, 1999.
- [13] T.-Z. Wu and Y.-T. Juang, “Adaptive fuzzy sliding-mode controller of uncertain nonlinear systems,” *ISA Transactions*, vol. 47, no. 3, pp. 279 – 285, 2008.
- [14] X. Ye, “Nonlinear adaptive control using multiple identification models,” *Systems & Control Letters*, vol. 57, no. 7, pp. 578 – 584, 2008.
- [15] M. Athans, K.-P. Dunn, C. Greene, W. Lee, N. Sandell, I. Segall, and A. Willsky, “The stochastic control of the f-8c aircraft using the multiple model adaptive control (mmac) method,” in *IEEE Conference on Decision and Control including the 14th Symposium on Adaptive Processes*, 1975, pp. 217–228.
- [16] K. S. Narendra and J. Balakrishnan, “Improving transient response of adaptive control systems using multiple models and switching,” *IEEE Transactions on Automatic Control*, vol. 39, no. 9, pp. 1861–1866, 1994.
- [17] K. S. Narendra, J. Balakrishnan, and M. K. Ciliz, “Adaptation and learning using multiple models, switching, and tuning,” *IEEE Control Systems*, vol. 15, no. 3, pp. 37 –51, June 1995.

-
- [18] K. S. Narendra and J. Balakrishnan, "Adaptive control using multiple models," *IEEE Transactions on Automatic Control*, vol. 42, no. 2, pp. 171–187, Feb 1997.
- [19] K. S. Narendra and Z. Han, "The changing face of adaptive control: The use of multiple models," *Annual Reviews in Control*, vol. 35, no. 1, pp. 1 – 12, 2011.
- [20] Z. Han and K. S. Narendra, "New concepts in adaptive control using multiple models," *IEEE Transactions on Automatic Control*, vol. 57, no. 1, pp. 78 –89, Jan 2012.
- [21] M. Kuipers and P. Ioannou, "Multiple model adaptive control with mixing," *IEEE Transactions on Automatic Control*, vol. 55, no. 8, pp. 1822 –1836, Aug 2010.
- [22] A. Cezayirli and M. K. Ciliz, "Increased transient performance for the adaptive control of feedback linearizable systems using multiple models," *International Journal of Control*, vol. 79, no. 10, pp. 1205–1215, 2006.
- [23] J. D. Boskovic and R. K. Mehra, "A multiple model-based reconfigurable flight control system design," in *Proceedings of the 37th IEEE Conference on Decision and Control*, vol. 4, Dec 1998, pp. 4503 –4508.
- [24] W. Chen and B. Anderson, "A combined multiple model adaptive control scheme and its application to nonlinear systems with nonlinear parameterization," *IEEE Transactions on Automatic Control*, vol. 57, no. 7, pp. 1778 –1782, 2012.
- [25] M. Ishitobi, M. Nishi, and K. Nakasaki, "Nonlinear adaptive model following control for a 3-dof tandem-rotor model helicopter," *Control Engineering Practice*, vol. 18, no. 8, pp. 936 – 943, 2010.
- [26] M. Chemachema and S. Zeghlache, "Output feedback linearization based controller for a helicopter-like twin rotor mimo system," *Journal of Intelligent & Robotic Systems*, vol. 80, no. 1, pp. 181 –190, 2015.
- [27] A. Cristofaro, T. A. Johansen, and A. P. Aguiar, "Icing detection and identification for unmanned aerial vehicles: Multiple model adaptive estimation," in *2015 European Control Conference (ECC)*, July 2015, pp. 1651–1656.
- [28] —, "Icing detection and identification for unmanned aerial vehicles using adaptive nested multiple models," *International Journal of Adaptive Control and Signal Processing*, vol. 31, no. 11, pp. 1584–1607, 2017.
- [29] X. Tao, N. Li, and S. Li, "Multiple model predictive control for large envelope flight of hypersonic vehicle systems," *Information Sciences*, vol. 328, no. Supplement C, pp. 115 – 126, 2016.
- [30] C. Tan, G. Tao, H. Yang, and F. Xu, "A multiple-model adaptive control scheme for multivariable systems with uncertain actuation signs," in *2017 American Control Conference (ACC)*, May 2017, pp. 1121–1126.
- [31] C. Tan, G. Tao, R. Qi, and H. Yang, "A direct mrac based multivariable multiple-model switching control scheme," *Automatica*, vol. 84, pp. 190 – 198, 2017.
- [32] T. Zhang, S. Ge, C. Hang, and T. Chai, "Adaptive control of first-order systems with nonlinear parameterization," *IEEE Transactions on Automatic Control*, vol. 45, no. 8, pp. 1512–1516, Aug 2000.
- [33] W. Lin and C. Qian, "Adaptive control of nonlinearly parameterized systems: the smooth feedback case," *Automatic Control, IEEE Transactions on*, vol. 47, no. 8, pp. 1249–1266, Aug 2002.
- [34] I. Tyukin, D. Prokhorov, and C. van Leeuwen, "Adaptation and parameter estimation in systems with unstable target dynamics and nonlinear parametrization," *IEEE Transactions on Automatic Control*, vol. 52, no. 9, pp. 1543–1559, Sep 2007.
- [35] N. Hung, H. Tuan, T. Narikiyo, and P. Apkarian, "Adaptive control for nonlinearly parameterized uncertainties in robot manipulators," *IEEE Transactions on Control Systems Technology*, vol. 16, no. 3, pp. 458–468, May 2008.
- [36] C. Guan and S. Pan, "Adaptive sliding mode control of electro-hydraulic system with nonlinear unknown parameters," *Control Engineering Practice*, vol. 16, no. 11, pp. 1275 – 1284, 2008.
- [37] M. Farza, M. M'Saad, T. Maatoug, and M. Kamoun, "Adaptive observers for nonlinearly parameterized class of nonlinear systems," *Automatica*, vol. 45, no. 10, pp. 2292 – 2299, 2009.
-

-
- [38] K. J. Åström and T. Hägglund, “The future of pid control,” *Control Engineering Practice*, vol. 9, no. 11, pp. 1163 – 1175, 2001.
- [39] A. Cezayirli and M. K. Ciliz, “Multiple model based adaptive control of a dc motor under load changes,” in *Proceedings of the IEEE International Conference on Mechatronics, ICM’04*, June 2004, pp. 328 – 333.
- [40] H. Khalil, *Nonlinear System*. Englewood Cliffs, NJ, USA: Prentice Hall, 1996.
- [41] S. Boyd and S. Sastry, “Necessary and sufficient conditions for parameter convergence in adaptive control,” *Automatica*, vol. 22, no. 6, pp. 629 – 639, 1986.
- [42] C. Cao, A. M. Annaswamy, and A. Kojic, “Parameter convergence in nonlinearly parameterized systems,” *IEEE Transactions on Automatic Control*, vol. 48, no. 3, pp. 397–412, Mar 2003.
- [43] G. C. Goodwin and K. S. Sin, *Adaptive Filtering Prediction and Control*. New York, USA: Dover Publications, Inc., 2009.
- [44] N. Hovakimyan and C. Cao, *L1 Adaptive Control Theory: Guaranteed Robustness with Fast Adaptation*. Philadelphia, PA, USA: Society for Industrial and Applied Mathematics, 2010.
- [45] A. Teel, R. Kadiyala, P. Kokotovic, and S. Sastry, “Indirect techniques for adaptive input output linearization of nonlinear systems,” in *American Control Conference*, May 1990, pp. 79–80.
- [46] G. Campion, G. Bastin *et al.*, “Indirect adaptive state feedback control of linearly parametrized non-linear systems.” *Int. J. Adaptive Control Signal Process.*, vol. 4, no. 5, pp. 345–358, 1990.
- [47] I. Kanellakopoulos, P. Kokotovic, and A. Morse, “Systematic design of adaptive controllers for feedback linearizable systems,” *IEEE Transactions on Automatic Control*, vol. 36, no. 11, pp. 1241–1253, 1991.
- [48] S. Sastry and M. Bodson, *Adaptive Control: Stability, Convergence and Robustness*. Englewood Cliffs, NJ: Prentice Hall, 1989.
- [49] D. Dawson, J. Carroll, and M. Schneider, “Integrator backstepping control of a brush dc motor turning a robotic load,” *IEEE Transactions on Control Systems Technology*, vol. 2, no. 3, pp. 233–244, Sep 1994.
- [50] A. Yadav and P. Gaur, “Ai-based adaptive control and design of autopilot system for nonlinear uav,” *Sadhana*, vol. 39, no. 4, pp. 765–783, 2014.
- [51] M. Shahi and A. Mazinan, “Automated adaptive sliding mode control scheme for a class of real complicated systems,” *Sadhana*, vol. 40, no. 1, pp. 51–74, 2015.
- [52] A.-P. Loh, A. Annaswamy, and F. Skantze, “Adaptation in the presence of a general nonlinear parameterization: an error model approach,” *IEEE Transactions on Automatic Control*, vol. 44, no. 9, pp. 1634–1652, Sep 1999.
- [53] S. Li, L. Yang, Z. Gao, and K. Li, “Stabilization strategies of a general nonlinear car-following model with varying reaction-time delay of the drivers,” *ISA Transactions*, vol. 53, pp. 1739–1745, 2014.
- [54] P. Rosa and C. Silvestre, “Multiple-model adaptive control using set-valued observers,” *International Journal of Robust and Nonlinear Control*, vol. 24, no. 16, pp. 2490–2511, 2014.
- [55] J. Xie, D. Yang, and J. Zhao, “Multiple model adaptive control for switched linear systems: A two-layer switching strategy,” *International Journal of Robust and Nonlinear Control*, 2017. [Online]. Available: <http://dx.doi.org/10.1002/rnc.4015>
- [56] J. Chen, W. Chen, and J. Sun, “Smooth controller design for non-linear systems using multiple fixed models,” *IET Control Theory Applications*, vol. 11, no. 9, pp. 1467–1473, 2017.
- [57] W.-S. Lin and C.-S. Chen, “Robust adaptive sliding mode control using fuzzy modelling for a class of uncertain mimo nonlinear systems,” *IEE Proceedings - Control Theory and Applications*, vol. 149, pp. 193–202(9), May 2002.
- [58] M. Deng and S. Bi, “Operator-based robust nonlinear control system design for mimo nonlinear plants with unknown coupling effects,” *International Journal of Control*, vol. 83, no. 9, pp. 1939–1946, 2010.
- [59] H. Lee, “Robust adaptive fuzzy control by backstepping for a class of mimo nonlinear systems,” *IEEE Transactions on Fuzzy Systems*, vol. 19, no. 2, pp. 265–275, April 2011.
-

-
- [60] TRMS, *Twin Rotor MIMO System Control Experiments 33-949S*, 33rd ed., Feedback Instruments Ltd., Crowborough, U.K., 1997.
- [61] L. Sandino, M. Bejar, and A. Ollero, "A survey on methods for elaborated modeling of the mechanics of a small-size helicopter. analysis and comparison," *Journal of Intelligent & Robotic Systems*, vol. 72, no. 2, pp. 219–238, 2013.
- [62] C.-W. Tao, J.-S. Taur, Y.-H. Chang, and C.-W. Chang, "A novel fuzzy-sliding and fuzzy-integral-sliding controller for the twin-rotor multi-input multi-output system," *IEEE Transactions on Fuzzy Systems*, no. 5, pp. 893–905, Oct 2010.
- [63] J.-H. Yang and W.-C. Hsu, "Adaptive backstepping control for electrically driven unmanned helicopter," *Control Engineering Practice*, vol. 17, no. 8, pp. 903 – 913, 2009.
- [64] J. Pradhan and A. Ghosh, "Design and implementation of decoupled compensation for a twin rotor multiple-input and multiple-output system," *Control Theory Applications, IET*, vol. 7, no. 2, pp. 282–289, Jan 2013.
- [65] S. Mondal and C. Mahanta, "Second order sliding mode controller for twin rotor mimo system," in *India Conference (INDICON), 2011 Annual IEEE*, Dec 2011, pp. 1–5.
- [66] D. Saroj, I. Kar, and V. Pandey, "Sliding mode controller design for twin rotor mimo system with a nonlinear state observer," in *Automation, Computing, Communication, Control and Compressed Sensing (iMac4s), 2013 International Multi-Conference on*, March 2013, pp. 668–673.
- [67] P. Sodhi and I. Kar, "Adaptive backstepping control for a twin rotor mimo system," in *Advances in Control and Optimization of Dynamical Systems (ACODS)*, March 2014, pp. 740–747.
- [68] D. Saroj and I. Kar, "T-s fuzzy model based controller and observer design for a twin rotor mimo system," in *IEEE International Conference on Fuzzy Systems (FUZZ)*, July 2013, pp. 1–8.
- [69] A. Rahideh and M. Shaheed, "Constrained output feedback model predictive control for nonlinear systems," *Control Engineering Practice*, vol. 20, no. 4, pp. 431 – 443, 2012.
- [70] H. Liu, G. Lu, and Y. Zhong, "Robust lqr attitude control of a 3-dof laboratory helicopter for aggressive maneuvers," *IEEE Transactions on Industrial Electronics*, vol. 60, no. 10, pp. 4627–4636, 2013.
- [71] H. Liu, J. Xi, and Y. Zhong, "Robust hierarchical control of a laboratory helicopter," *Journal of the Franklin Institute*, vol. 351, no. 1, pp. 259 – 276, 2014.
- [72] H. Liu, Y. Yu, and Y. Zhong, "Robust trajectory tracking control for a laboratory helicopter," *Nonlinear Dynamics*, vol. 77, no. 3, pp. 621–634, 2014.
- [73] Y. Yu, G. Lu, C. Sun, and H. Liu, "Robust backstepping decentralized tracking control for a 3-dof helicopter," *Nonlinear Dynamics*, vol. 82, no. 1-2, pp. 947–960, 2015.
- [74] M. Chen, P. Shi, and C.-C. Lim, "Adaptive neural fault-tolerant control of a 3-dof model helicopter system," *IEEE Transactions on Systems, Man, and Cybernetics: Systems*, 2015.
- [75] S. S. Haykin, *Kalman Filtering and Neural Networks*. New York, USA: John Wiley & Sons, Inc., 2001.
- [76] S. Beyhan, Z. Lendek, M. Alci, and R. Babuska, "Takagi-sugeno fuzzy observer and extended-kalman filter for adaptive payload estimation," in *Control Conference (ASCC), 2013 9th Asian*, June 2013, pp. 1–6.
- [77] Y. Zhai, M. Nounou, H. Nounou, and Y. Al-Hamidi, "Model predictive control of a 3-dof helicopter system using successive linearization," *International Journal of Engineering, Science and Technology*, vol. 2, no. 10, 2010.
- [78] Y. Isurugi, *Model Following Control for Nonlinear Systems*, ser. Rapports de recherche. Institut National de Recherche en Informatique et en Automatique, 1990.
- [79] Quanser, *Quanser 3-DOF Helicopter reference manual, Document number 644, Revision 2.1*, Quanser Consulting, Canada, 1998.
- [80] J. Apkarian, *3-DOF Helicopter experiment manual for Matlab/simulink users*, Quanser Consulting, Canada, 1998.
-

-
- [81] S. Kumar. (2017) Global advanced driver assistance systems. MILTECH PR Distribution. Warsaw, Poland. [Online]. Available: <http://www.military-technologies.net/2017/08/05/global-advanced-driver-assistance-systems>
- [82] N. news. (2013) Nissan leaf with highly advanced driver assist system gets first license plate for public road testing in japan. Nissan global. Yokohama, Japan. [Online]. Available: http://www.nissan-global.com/EN/NEWS/2013/_STORY/130926-04-e.html
- [83] W. Group. (2017) autonomous-vehicles. Condé Nast Publications. San Francisco, California, USA. [Online]. Available: <https://www.wired.com/tag/autonomous-vehicles/>
- [84] S. carney. (2017) New way to test self-driving cars could cut 99.9 percent of validation costs. Phys.org. NewYork, USA. [Online]. Available: <https://phys.org/news/2017-05-self-driving-cars-percent-validation.html>
- [85] L. Kishonti. (2017) Game engine-based simulation set to outshine real-world testing for self-driving. D2 Emerge. NewYork, USA. [Online]. Available: <https://sdtimes.com/game-engine-based-simulation-outshine-testing-self-driving/>
- [86] L. Xiao and H. K. Lo, “Adaptive vehicle navigation with en route stochastic traffic information,” *IEEE Transactions on Intelligent Transportation Systems*, vol. 15, no. 5, pp. 1900–1912, Oct 2014.